AD_____

Award Number: DAMD17-03-C-0012

TITLE: Generation of Recombinant Human AChE OP-Scavengers with Extended Circulatory Longevity

PRINCIPAL INVESTIGATOR: Avigdor Shafferman Ph.D.

CONTRACTING ORGANIZATION: Israel Institute for Biological Research
Ness-Ziona 74100

REPORT DATE: November 2006

TYPE OF REPORT: Final

PREPARED FOR: U.S. Army Medical Research and Materiel Command
Fort Detrick, Maryland 21702-5012

REPORT DOCUMENTATION PAGE

Form Approved
OMB No. 0704-0188

1. REPORT DATE *(DD-MM-YYYY)*	2. REPORT TYPE	3. DATES COVERED *(From - To)*
01/11/06	Final	03 Mar 03 – 02 Oct 06

4. TITLE AND SUBTITLE
Generation of Recombinant Human AChE OP-Scavengers with Extended Circulatory Longevity

5a. CONTRACT NUMBER

5b. GRANT NUMBER
DAMD17-03-C-0012

5c. PROGRAM ELEMENT NUMBER

6. AUTHOR(S)
Avigdor Shafferman Ph.D.

E-Mail: avigdor@iibr.gov.il

5d. PROJECT NUMBER

5e. TASK NUMBER

5f. WORK UNIT NUMBER

7. PERFORMING ORGANIZATION NAME(S) AND ADDRESS(ES)
Israel Institute for Biological Research
Ness-Ziona 7410

8. PERFORMING ORGANIZATION REPORT NUMBER

9. SPONSORING / MONITORING AGENCY NAME(S) AND ADDRESS(ES)
U.S. Army Medical Research and Materiel Command
Fort Detrick, Maryland 21702-5012

10. SPONSOR/MONITOR'S ACRONYM(S)

11. SPONSOR/MONITOR'S REPORT NUMBER(S)

12. DISTRIBUTION / AVAILABILITY STATEMENT
Approved for Public Release; Distribution Unlimited

13. SUPPLEMENTARY NOTES

14. ABSTRACT
We demonstrate that chemical conjugation of polyethylene glycol (PEG) moieties to recombinant human acetylcholinesterase (rHuAChE) gives rise to OP bioscavenger species which reside for very long periods of time in the circulation of mice, regardless of their post-translation-modification state, and that circulatory elimination of AChE via specific amino acid-related epitopes can also be efficiently overcome by enzyme PEGylation. Taken together, these findings indicate that the circulatory residence is dictated primarily by the PEG appendage. In line with these findings, we examined the possibility to express human AChE in microorganism-based production systems which do not support animal-cell-related enzyme processing, utilizing a specialized designed synthetic human AChE gene. Although the gene product was rapidly degraded in Bacillus brevis cells, the Pichia pastoris yeast cell system was shown to support production and secretion of bioactive rHuAChE. In a series of studies we demonstrate that selective removal of human AChE lysine residues, which serve as target sites for PEG-conjugation, can generate an enzyme, which upon PEGylation, displays a high degree of homogeneity, extended circulatory longevity and reduced immunogenicity. In structure-function studies of AChE, we compared the reactivities of enantiomers of VX and their noncharged isosters, as well as ecothiophate, in conjunction with a battery of AChE mutants. These studies allowed us to define two subsites, located in the active site and peripheral anionic subsites, which confer enzyme stereoselectivity to CW agents such as VX.

15. SUBJECT TERMS
Chemical Defense

16. SECURITY CLASSIFICATION OF:			17. LIMITATION OF ABSTRACT	18. NUMBER OF PAGES	19a. NAME OF RESPONSIBLE PERSON
a. REPORT	b. ABSTRACT	c. THIS PAGE			USAMRMC
U	U	U	UU	144	19b. TELEPHONE NUMBER *(include area code)*

Table of Contents

I. GENERAL INTRODUCTION

The primary role of acetylcholinesterase (acetylcholine acetylhydrolase 3.1.1.7, AChE) is the termination of impulse transmission in cholinergic synapses by rapid hydrolysis of the neurotransmitter acetylcholine (ACh). The enzyme has been the subject of intense research due to its focal position in several fields of interest. Modification in the levels of human brain AChE have been reported in various disorders such as Down's syndrome (Yates *et al.*, 1980) and Alzheimer's disease (Coyle *et al.,* 1983). Several cholinesterase inhibitors have proven to be of value as medicinal agents and are used for the treatment of glaucoma or myasthenia gravis (Taylor, 1990). Some organophosphorus (OP) inhibitors of ChEs such as malathion and diazinon, act as efficient insecticides and have been widely used in combating medfly and other agricultural pests. Other OP compounds, such as the nerve agent sarin and soman, inhibit AChE irreversibly by rapid phosphorylation of the serine residue in the enzyme active site. The acute toxicity of these nerve agents is elicited in motor and respiratory failure following inhibition of AChE in the peripheral and central nervous system. The high reactivity of ChEs towards OP-agents led to propose these biomolecules as exogenous scavengers for sequestration of toxic OP-agents before they reach their physiological target (Wolfe *et al.*, 1987; Raveh; *et al.*, 1989; Broomfield *et al.*, 1991; Doctor *et al.*, 1992). The AChEs react irreversibly and on a molar basis with the OP agents and therefore, the amounts of AChE required for treatment are high. This limitation could be overcome provided that the OP-enzyme conjugates could be efficiently reactivated before the excess OP has reached its physiological target. This goal is difficult to attain especially in cases where the OP-AChE conjugates undergo catalytic post-inhibitory processes termed aging. In native AChEs the spontaneous reactivation, through displacement of the phosphyl moiety from the active site, is usually very slow and unable to compete with the aging process, yet efficient enzyme reactivation can be achieved by various oxime nucleophiles. Our goal is therefore to generate enzymes based on the HuAChE template, the OP-adducts of which are more readily reactivated and are resistant to aging, yet still retain their high reactivity towards the OP agents. To meet this challenge, we as well as others initiated studies designed for better understanding of the functional architecture of the AChE active center. These include X-ray crystallography (Sussman *et al.*, 1991; Harel *et al.*, 1996; Raves *et al.*, 1997; Kryger *et al.*, 1998; Millard *et al.*, 1999a; Bourne *et al.*, 1999; Kryger *et al.*, 2000); site directed mutagenesis and molecular modeling together with kinetic studies of the

AChE muteins with substrates and reversible inhibitors (Ordentlich *et al.*, 1993; Barak *et al.*, 1994; Shafferman *et al.*, 1992a, 1992b; Vellom *et al.*, 1993; Radic *et al.*, 1992, 1993; Shafferman *et al.*, 1995; Ordentlich *et al.*, 1996; Ariel *et al.*, 1998; Ordentlich *et al.*, 1998a). The functional role of the various active center subsites identified this way include: a) the esteratic site containing the catalytic triad Ser203, His447 and Glu334; b) the "oxyanion hole" consisting of residues Gly121, Gly122 and Ala204; c) the "anionic subsite" or the choline binding subsite -Trp86; d) the hydrophobic site for the alkoxy leaving group of the substrate containing an "aromatic patch" that includes residues Trp86, Tyr337 and Phe338; e) the acyl pocket - Phe295 and Phe297 and f) the peripheral anionic subsite (PAS) including residues Tyr72, Asp74, Tyr124, Trp286 and Tyr341. Recently, we have examined the specific involvement of all these elements of the active center functional architecture, in determining reactivity and specificity of human AChE (HuAChE) towards different OP-inhibitors. We have also demonstrated the ability to generate novel enzymes that are more efficient in OP scavenging through the combined effects of improved activity toward the OP-agents together with higher resistance to the aging process (Ordentlich *et al.*, 1996; Shafferman *et al.*, 1996). Such studies, by us and others (see review in Taylor and Radic, 1994; Hosea *et al.*, 1995; Millard *et al.*, 1995; Hosea *et al.*, 1996; Lockridge *et al.*, 1997), reveal the structural and mechanistic determinants of AChE activity that are essential for the design of true OP hydrolytic activity into the AChE mold. Information regarding the potential diversity of aging mechanisms is essential for further elucidation of the role of AChE active center in these processes, as part of the development of effective treatment for human intoxication by organophosphorus agents, like certain insecticides and nerve agents.

Exploitation of the bioscavenging potential of the recombinant bioengineered mutant derivatives of AChE depends on large-scale production systems (Fischer *et al.*, 1993; Kronman *et al.*, 1992). However pharmacokinetic studies (Kronman *et al.*, 1992; Mendelson *et al.*, 1998) have shown that recombinant enzymes generated by these systems, relying on either bacterial or mammalian cells, are retained in the circulation of experimental animals for much shorter periods of time than native fetal bovine serum acetylcholinesterase (FBS-AChE) or human serum butyrylcholinesterase (BChE). Therefore, deciphering the mechanisms involved in clearance of cholinesterases from the bloodstream is of importance for the development of enzyme-based bioscavengers for treatment of organophosphorus poisoning. Our previous studies (Kronman *et al.*, 1995) have shown that the structures of the appended glycans of rHuAChE, and in particular the distal termini of these glycan

projections, constitute a major factor in determining the circulatory duration of rHuAChE. This was exemplified by establishing the major role of N-glycan sialylation in determining the circulatory lifetime of rHuAChE. As a continuation of these studies, we have demonstrated (Chitlaru *et al.*, 1998) that production of rHuAChE with highly sialylated glycans (achieved by genetic modification of rHuAChE producer cell lines to coexpress a sialyltransferase gene) resulted in the generation of high levels of rHuAChE, which exhibited increased circulatory retention. However, the highly sialylated enzyme was still eliminated from the circulation more rapidly than native serum-derived cholinesterases, suggesting that factors other than glycan sialylation also play a role in determining the circulatory fate of AChE.

To allow a comprehensive appreciation of the structural basis for the circulatory residence of AChE, we conducted a series of studies (Kronman *et al.*, 2000; Chitlaru *et al.*, 2001) in which the post-translation-related differences between serum-derived native bovine AChE and its recombinant HEK-293-expressed counterpart were determined by MALDI-TOF analyses of N-glycans and sucrose-gradient analyses of enzyme subunit assembly status. These studies, together with extensive pharmacokinetic profiling of various AChE forms in mice, allowed us to demonstrate that sialic acid occupancy and enzyme oligomerization determine both together the circulatory residence of bovine AChE in an hierarchical manner. Thus, molecular species in which both glycan sialylation and enzyme subunit assembly were optimized, are characterized by exceedingly long circulatory life-time values which are comparable to that exhibited by native serum derived BoAChE. Further studies displayed that the circulatory longevity of the human form of AChE in mice is regulated by the same set and pattern of rules (Chitlaru *et al.*, 2001). Increasing the number of appended N-glycans to human AChE was also shown to contribute to the circulatory performance of the enzyme (Chitlaru *et al.*, 2002). Extensive pharmacokinetic analyses of an array of enzyme species differing in their state of sialylation, subunit assembly and number of appended N-glycans, demonstrated that the effect of N-glycan addition on the pharmacokinetics of AChE is fully manifested only in the case of efficiently sialylated tetrameric forms of the enzyme. Thus, N-glycan loading operates as a third component together with sialylation and tetramerization, within a hierarchical set of rules governing the circulatory lifetime of AChE in mice. Whether additional traits of the enzyme also play a part in determining its circulatory fate, and whether the same set of post-translation-related factors preside over the circulatory residence of AChE in other animal systems as well, remain to be resolved.

In parallel, studies carried out in our laboratory (Cohen *et al.*, 2001) allowed us to determine a set of conditions for the generation of chemically modified recombinant AChE exhibiting full preservation of its catalytic abilities, and which resides in the circulation of mice for unprecedented periods of time (Mean residence time = 2100 min.), surpassing that of native serum-derived enzymes such the fetal bovine serum AChE (FBS-AChE).

The finding that AChE circulatory residence may be extended both by either post-translation modification or by PEG-conjugation, raises a question concerning the interrelationship between the effect of PEGylation and the enzyme processing, with regard to the overall effect on the pharmacokinetic performance of the enzyme. This line of studies should have practical implications on determining the source for large-scale recombinant AChE production for its subsequent transformation into a long-lived therapeutic product by PEGylation. The finding that enzyme processing and PEG-conjugation operate in an additive manner, resulting in the generation of enzyme forms exhibiting higher levels of circulatory residence, would necessitate enzyme-processing optimization prior to its subjection to PEG-appendage. On the other hand, if PEG-conjugation will prove to be equally effective regardless of the post-translation processing state of the AChE enzyme, cost-effective production systems (e.g. bacterial, or other microorganisms) may be utilized for the large-scale production of recombinant human AChE.

Although PEG-conjugation of AChE leads to the generation of a circulatory long-lived species, the practical use of PEGylated AChE as an OP-bioscavenger would require that the enzyme product exhibit a high degree of homogeneity. This may demand the removal of some of the lysine residues that serve as targets for PEGylation, to allow production of uniformly PEGylated enzyme. To this end, a series of studies aimed to determine the effect of lysine removal on enzyme functionality, pharmacokinetic performance and structural homogeneity following PEGylation should be performed.

The present report covers the progress in all these research areas. The following section (section II) deals with the regulation of AChE retention in the circulation by post-translational processing and species-specific amino acid epitopes. In this section, we also included for the sake of completeness, pertinent data regarding AChE circulatory residence in rhesus macaques that were derived from a series of experiments funded by sources other than the USAMRMC contract, since they may have a major impact on the present project. Section III focuses on the interrelationship between PEG-conjugation and the post-translation modifications of proteins with regard to the overall pharamacokinetic performance of the

protein. Section IV describes the generation and characterization of various hypolysine rHuAChEs with regard to their enzymatic activity, stability and pharmacokinetic performance upon PEGylation. This is followed (Section V) by antigenic and immunogenic characterization of non-modified and PEGylated wild type or hypolysine rHuAChEs. In section VI we describe our efforts to establish a microorganism-based system for cost-effective production of rHuAChE at high levels. Finally, in section VII we summarize our findings regarding the stereoselectivity of HuAChE toward the enantiomers of VX, through comparisons with their noncharged isosteres, as well as with the symmetrical diethyl phosphates echothiophate and its noncharged analogue. Each of these sections includes a brief background introduction, methods and a result and discussion subsection. A summary of the main findings of the research concludes this report (Section VIII).

II. REGULATION OF ACETYLCHOLINESTERASE CIRCULATORY RESIDENCE BY POST-TRANSLATIONAL PROCESSING AND SPECIES-SPECIFIC AMINO ACID EPITOPES

INTRODUCTION

Acetylcholinesterase plays a pivotal role in the cholinergic system where it functions in the rapid termination of nerve impulse transmission. AChE, unlike the related butyrylcholinesterase which is abundant in the serum of adult primates, is preferentially found in insoluble, cell-associated forms (Massoulie *et al.*, 1999). Previous studies suggest that exogenous cholinesterase can serve as an effective therapeutic agent in the prophylaxis and treatment of organophosphate (OP) poisoning. Indeed the successful exploitation of the scavenging potential of administered cholinesterase has been demonstrated in rodents and in non-human primates (Wolfe *et al.*, 1987; Broomfield *et al.*, 1991; Maxwell *et al.*, 1992; Raveh *et al.*, 1993). The use of human AChE as an efficient therapeutic bioscavenger has been advanced by the development of recombinant production systems (Kronman *et al.*, 1992; Lazar *et al.*, 1993) and the introduction of catalytically favorable mutations (Millard *et al.*, 1995; Ordentlich *et al.*, 1996; Shafferman *et al.*, 1996; Hosea *et al.*, 1996).

In addition to their high reactivity towards OP toxic agents, native serum-derived cholinesterases (serum butyrylcholinesterase or AChE from fetal bovine serum) were found to be retained in the circulation of experimental animals for extended periods of time, exhibiting mean residence times (MRTs) of more than 1000 minutes (Kronman *et al.*, 1995; Saxena *et al.*, 1997; Mendelson *et al.*, 1998; Saxena *et al.*, 1998). In contrast, recombinant human or bovine AChEs produced in stably transfected cell lines of the human embryonic kidney 293 (HEK-293) cell line, were eliminated from the bloodstream of experimental animals within much shorter periods of time (MRTs = 60-100 min).

Using the previously defined sets of recombinant human and bovine AChE molecular arrays (Kronman *et al.*, 2000; Chitlaru *et al.*, 2002) as well as a similar set of newly-cloned and expressed rhesus AChE, we now reveal that specific amino-acid domains promote the elimination of soluble primate AChEs from the circulation of rhesus monkeys but not of mice, thereby mitigating the positive contribution of post-translation-related processing to circulatory retention. This specific process for removal of homologous AChE molecules by macaques may however be countermanded by the effective masking of these domains, for example by chemical conjugation of polyethylene glycol (PEG) moieties, resulting in the

generation of primate AChEs exhibiting extraordinarily long-term circulatory residence in monkeys.

METHODS

Cell culture techniques, enzyme production and purification of rAChEs

Generation of HEK-293 cell lines stably expressing high levels of rHuAChE, and rBoAChE was described previously (Kronman *et al.*, 2000; Chitlaru *et al.*, 2001). Generation of a HEK-293 cell line stably expressing high levels of rRhAChE was performed in the same manner, by transfecting the cells with the pRhAChE-nc vector (see below), followed by G418 selection to form rRhAChE stable producer cells. The generation of *in-vivo* highly sialylated rHuAChE (wild type and tetraglycosylated mutant), rBoAChE and rRhAChE was achieved by stably expressing the human (wild type or D61N mutant), bovine and rhesus acetylcholinesterase genes, in the genetically modified 293ST 2D6 cells that express high levels of heterologous 2,6-sialyltransferase followed by G418 selection to form rAChE stable producer cells, as described previously (Chitlaru *et al.*, 1998). The method for purification of the secreted rHuAChE and rBoAChE enzymes was described previously (Kronman *et al.*, 1995) and served also for the purification of secreted rRhAChE.

DNA sequencing

The coding sequence of the rhesus AChE gene was determined through PCR amplification of rhesus genomic adult female lymphocyte DNA fragments. Five amplified overlapping DNA fragments were generated, using primers based on the human AChE sequence (see Fig. 2A). Sequence determination (ABI prism rhodamine kit using the ABI310 Genetic Analyzer, Applied Biosystems) was based on two independent clone isolates for each amplified DNA fragment. Sequences of exons 2 to 6 of the rhesus AChE gene were deposited in the Genebank database under accession numbers AY372522 to AY372526.

Generation of the RhAChE cDNA

To generate the recombinant rhesus AChE gene, the human AChE gene cloned in the pBluescript vector (Stratagene, USA) was subjected to site-directed mutagenesis to replace human-specific codons with those coding for rhesus amino acids. Using the QuikChange site-directed mutagenesis kit (Stratagene, USA), each of the codons ATG, CAC and GCA, corresponding to amino acids Met42, His284 and Ala467 of the human AChE gene was replaced individually with the codons ACA, AAT and ACG, respectively, to code for Thr42, Asn284 and Thr467. The fragments *Eco*RV-*Bst*EII containing the rhesus codon coding for Thr42, *Bst*EII-*Sbf*I containing the rhesus codon coding for Asn284, and *Sbf*I-*Not*I containing

the rhesus codon coding for Thr467, were excised from the corresponding mutated pBluescript vectors and used to replace the parallel fragments in the pAChE-nc expression vector (Kronman *et al.*, 1992), to generate the pRhAChE-nc vector. The AChE coding region within pRhAChE-nc was verified by DNA sequencing as described above.

Enzyme activity

AChE activities of purified AChE preparations were measured according to Ellman *et al.* (1961). Assays were performed in the presence of 0.5 mM acetylthiocholine, 50 mM sodium phosphate buffer pH 8.0, 0.1 mg/ml BSA and 0.3 mM 5,5'-dithiobis-(2-nitrobenzoic acid). The assay was carried out at 27^0C and monitored by a Thermomax microplate reader (Molecular Devices).

To allow measurement of residual AChE activity in rhesus macaque serum samples, endogenous butyrylcholinesterase (BChE) background activity was reduced by pretreatment of the samples with the BChE-specific inhibitor, tetraisopropylpyrophosphoramide (iso-OMPA). This was achieved by preincubating the serum samples in the presence of 50 mM sodium phosphate buffer pH 8.0/0.1 mg/ml BSA/ 0.3 mM 5,5'-dithiobis-(2-nitrobenzoic acid) and 4 x 10^{-5} M iso-OMPA for 10 minutes at room temperature before adding the substrate, acetylthiocholine (final conc. =0.5 mM). Under these conditions, >98% of the endogenous BChE activity was inhibited without affecting AChE activity.

Removal of sialic acid from rAChE

Recombinant HuAChE, BoAChE and RhAChE (15-30 nmol enzyme) in PBS were incubated for 16h with 0.2-0.4U of agarose-bound sialidase at room temperature. Sialidase was removed by Eppendorf centrifugation. Desialylated enzyme was dialyzed against PBS to remove free sialic acid.

***In-vitro* tetramerization of rAChE**

Synthesis and quality control of human ColQ- PRAD peptide CLLTPPPPPLFPPPFFRG were described previously (Kronman *et al.*, 2000). Preparative tetramerization for the generation of milligram amounts of tetrameric rHuAChE (wild type or D61N mutant), rBoAChE and rRhAChE for pharmacokinetic studies was performed by incubating 70 nmol of highly sialylated rAChE with 140 nmol PRAD synthetic peptide for 12-16h at room temperature, in the presence of 5mM phosphate buffer pH 8.0 in a final volume of 2ml. Prior to administration to monkeys, the various *in-vitro* tetramerized rAChEs were dialyzed

extensively against PBS. Complete conversion of the enzymes into tetrameric forms was verified by sucrose-gradient density analysis, as described previously (Kronman *et al.*, 2000).

MALDI-TOF analysis of glycans

N-glycans of rAChEs (~100 μg protein) were purified, 2-aminobenzamide labeled (Bigge *et al.*, 1995) and converted into their neutral methylated forms by methyl iodide esterification, as described previously (Kronman *et al.*, 2000). Mass spectra of 2-aminobenzamide-labeled esterified rAChE glycans were acquired on a Micromass TofSpec 2E reflectron time-of-flight (TOF) mass spectrometer. Samples of 1 μl of glycan samples diluted 1:10 in water were mixed with an equal volume of freshly prepared 2,5-dihydroxybenzoic acid (10mg/ml in 70% acetonitrile) and loaded onto the mass spectrometer target. Dried spots were recrystallized by adding 0.5 μl ethanol and allowed to dry again. Glycans were observed as $[M+Na]^+$ ions. 1 μl of peptide mixture (renin substrate, ACTH fragment 18-39, and angiotensin, 10 pMole/μl all from Sigma), which served as a three-point external calibrant for mass assignment of the ions, was mixed with freshly prepared α-cyano-4-hydroxycinnamic acid (10 mg/ml in 49.5% acetonitrile; 49.5% ethanol; 0.001% TFA), loaded on the mass spectrometer target and allowed to dry. All oligosaccharides were analyzed at 20 kV with a single-stage reflectron in the positive-ion mode. Between 100 and 200 scans were averaged for each of the spectra shown.

Conjugation of polyethylene glycol to AChE

Attachment of PEG chains to primary amines in rHuAChE was performed using succinimidyl propionate activated methoxy PEG (SPA-PEG; Shearwater polymers, Inc.), as described previously (Laub and Gallo, 1996). Briefly, purified rHuAChE or rRhAChE (5mM) were incubated with PEG-20000 at a ratio of 50:1 $[PEG]_0/[AChE\ primary\ amines]_0$ in 50mM phosphate buffer pH 8.0 for 2 hours at room temperature. The chemically modified products were dialyzed extensively against phosphate buffer saline (PBS) and analyzed on 6% SDS-PAGE gels.

Animal procedures

Female rhesus macaques (*Macaca mulatta*, 2.7-3.0 kg) were obtained from Covance, USA. Animals were quarantined upon arrival and screened for evidence of disease. The animals were individually housed in stainless-steel cages in animal rooms that were maintained at 20-22^{0}C and relative humidity of 50±10% on a 12-hr light-dark cycle. The monkeys were fed

commercial certified Primate Chow (Koffolk, Inc., Tel-Aviv, Israel) and provided with tap water *ad libitum.* Male outbred ICR mice (Charles River Laboratories, UK) were maintained at 20-22^{0}C and relative humidity of 50±10% on a 12-hr light-dark cycle, fed with commercial rodent chow (Koffolk, Inc., Tel-Aviv, Israel) and provided with tap water *ad libitum.* Treatment of animals was in accordance with regulations outlined in the USDA Animal Welfare Act and the conditions specified in *The Guide for Care and Use of Laboratory Animals* (National Institute of Health, 1996). All pharmacokinetic studies (see below) in monkeys and mice were approved by the local ethical committee on animal experiments.

Clearance experiments and analysis of pharmacokinetic profiles in mice and rhesus macaques

Following extensive dialysis against PBS (pH 7.4), 1000 units of the various rAChEs (165 μg and 330 μg and 165 μg for the human, bovine and rhesus forms, respectively) were injected i.v. to 3 rhesus macaques, (injection volumes <1ml/kg). Samples (0.25 ml) of blood were collected at various periods of time in Microtainer tubes (Becton, Dickinson and Co., USA), centrifuged for 1 minute at 10,000 rpm in an Eppendorf microfuge and stored at -20^{0}C until AChE activity in serum samples was determined. Enzymatic activity was determined following iso-OMPA-mediated BChE inhibition, as described above. AChE activity values in samples removed 2 minutes after injection were referred to as input activities and were used for the calculation of residual activity throughout the experiment. AChE values were corrected for background activity determined in blood samples withdrawn 1h before performing the experiment. Exogenously administered AChE was at least 20-fold higher than background endogenous iso-OMPA-resistant ChE activity. To avoid the possible generation of anti-ChE antibodies, which might affect the circulatory retention times of the injected proteins, in all cases each of the monkeys were administered only once with ChE.

Clearance experiments in mice (3 to 6 mice per enzyme sample) were carried out essentially as described previously (Kronman *et al.*, 1995). Mice were injected i.v. with the various rRhAChE preparations (100 units/mouse in 0.2 ml PBS). Residual AChE activity in blood samples was measured and all values were corrected for background hydrolytic activity in the blood (using samples withdrawn 1 hour before performing the experiment). AChE activity values in samples removed 1 minute after injection were assigned a value of 100% and used for calculation of residual activity. Background cholinesterase levels in blood of pre-administered mice were less than 2 units/ml.

The clearance patterns of the various enzyme preparations were usually biphasic and fitted to a bi-exponential elimination pharmacokinetic model ($C_t=Ae^{-k\alpha t}+Be^{-k\beta t}$) as described previously (Kronman *et al.*, 2000; Chitlaru *et al.*, 2001). This model enables determination of the parameters A and B which represent the fractions of the material removed from the circulation in the first-fast and second-slow elimination phases respectively, and $T_{1/2}\alpha$ and $T_{1/2}\beta$ which represent the circulatory half-life values of the enzyme in the fast and slow phases. The pharmacokinetic parameter MRT (mean residence time, which reflects the average length of time the administered molecules are retained in the organism) was independently obtained by analyzing the clearance data according to a noncompartmental pharmacokinetic model using the WinNonlin computer program (Laub and Gallo, 1996).

Clearance experiments of native and radiolabeled RhBChE in rhesus macaques

Serum BChE collected from rhesus macaques was purified on procainamide columns as described previously (Kronman *et al.*, 1995). Purified native BChE was radiolabeled by incubating the enzyme (7.2 nmole) with a tritiated organophosphorus compound, [^{3}H]-diisopropyl phosphorofluoridate (DFP) (60μCi, 8.4Ci/mmol; Amersham Biosience). Excess radioactive material was removed by passing the labeling mixture on a G-50 column. The labeled enzyme was administered to 3 rhesus macaques, blood samples were removed at various time periods and residual labeled BChE in blood samples was measured by radioactivity counting of trichloroacetic acid (TCA) precipitates in a liquid scintillation counter. Radioactivity values in samples removed 2 minutes after injection were assigned a value of 100% and used for residual-enzyme calculation.

To determine the pharmacokinetic profile of non-labeled rhesus serum BChE, ~10,000U of the enzyme was administered to a single monkey. Residual BChE enzymatic activity in blood samples removed at various periods of time was determined as described above, using butyrylthiocholine as the substrate.

RESULTS AND DISCUSSION

Pharmacokinetics of recombinant BoAChE forms obey the same hierarchical rules in rhesus macaques and mice

The effect of post-translation processing on the circulatory retention of heterologous AChE in non-human primates was addressed by monitoring the pharmacokinetic profiles of an array of differently processed recombinant bovine AChEs in rhesus macaques. The contribution of sialic acid contents to the circulatory retention of the recombinant enzyme forms was evaluated by comparing the clearance profiles of enzymatically desialylated enzyme, partially sialylated enzyme produced by HEK-293 producer cells, and fully sialylated enzyme produced by the modified 293ST-2D6 cell line which coexpresses high levels of recombinant α2,6-sialyltransferase (Chitlaru *et al.*, 1998). The effect of enzyme subunit assembly on circulatory residence of the recombinant AChE was evaluated by examining the pharmacokinetic behavior of fully sialylated enzyme following its complete conversion into tetramers in the presence of the synthetic ColQ Proline Rich Association Domain (PRAD) peptide (Kronman *et al.*, 2000; Simon *et al.*, 1998).

Pharmacokinetic analyses of the various recombinant bovine AChE forms in rhesus macaques demonstrated that each of the differently processed forms was characterized by a unique circulatory retention pattern (Fig. 1A, Table 1). Recombinant bovine AChE totally devoid of sialic acid residues displayed a monophasic elimination curve and was cleared rapidly from the circulation within a very short period of time (Mean residence time (MRT) = 3.9±0.6 min). In contrast, all recombinant bovine enzyme forms containing sialic acid residues displayed biphasic elimination curves with different circulatory residence values in accordance with the level of sialic acid occupancy and enzyme subunit assembly. Thus, rBoAChE preparations consisting of partially sialylated, fully sialylated and fully sialylated/tetramerized forms of the enzyme exhibited increasingly higher circulatory retention rates, as demonstrated by the corresponding MRT values of 66±2, 205±7 and 1510±45 minutes, respectively. These results establish that both sialic acid levels and enzyme subunit assembly strongly influence circulatory retention of BoAChE in non-human primates and that enzyme sialylation and oligomerization operate in a synergistic manner, resulting in the generation of an enzyme form which resides in the circulation of rhesus macaques for very long periods of time.

The MRT values of the various rBoAChE forms in monkeys are very similar to those obtained in mice (Kronman *et al.*, 2000; See also Fig. 5). Thus, the ratios of the MRTs in

rhesus to the MRTs in mice (MRT_{Rh}:MRT_{M}) for the asialylated, partially-sialylated, fully-sialylated and fully-sialylated/tetramerized forms of rBoAChE are 1.0±0.05, 1.2±0.09,

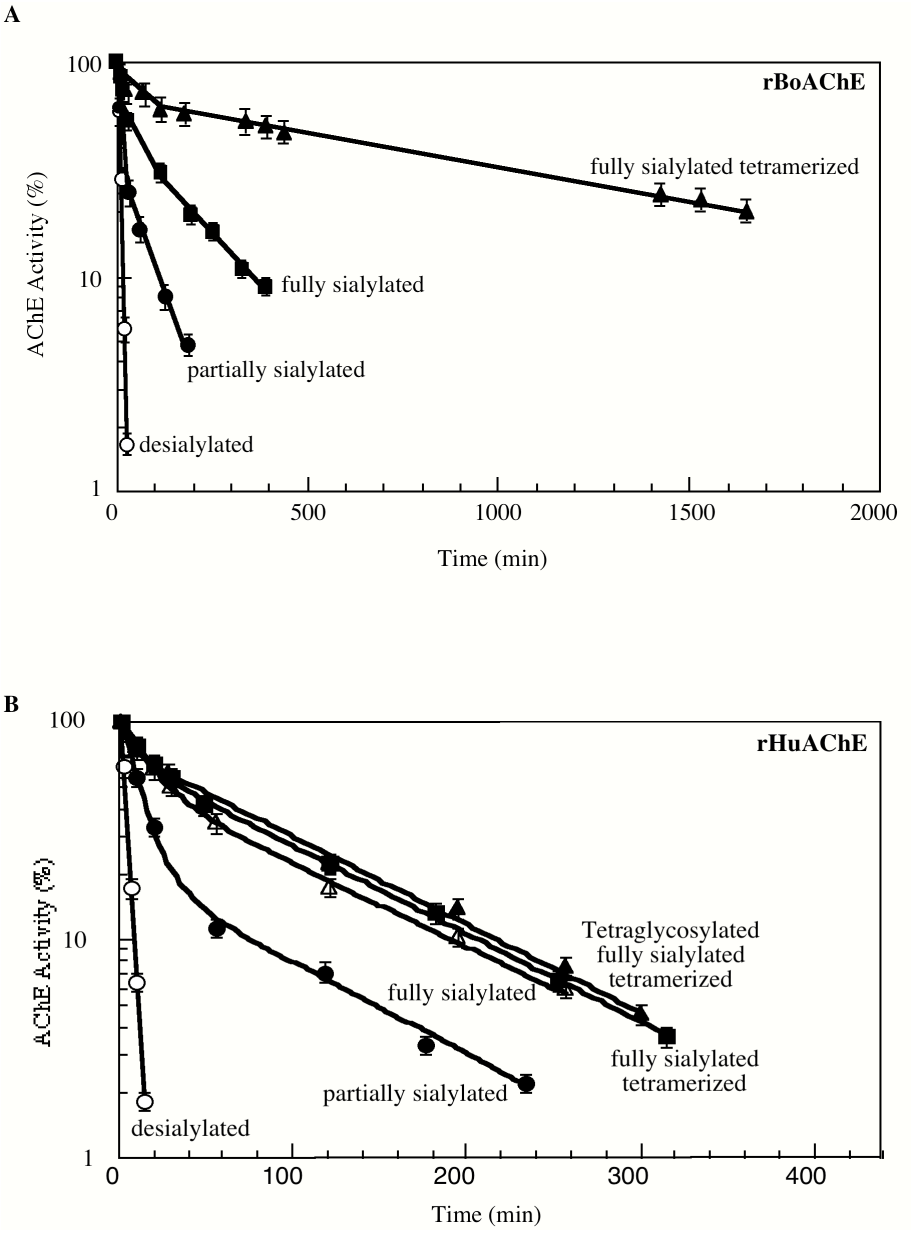

Figure 1: Comparison of the circulatory elimination profiles of various molecular forms of rBoAChE and rHuAChE in rhesus macaques. Purified preparations of various molecular forms of rBoAChE (***A***) or rHuAChE (***B***), differing in their post-translation processing (glycan sialylation level, subunit assembly state, N-glycan loading) were administered to 3 rhesus macaques and residual AChE activity in the circulation was assayed at the indicated time points. Circulatory removal curves were determined for all the AChE forms and the derived pharmacokinetic parameters are presented in Table 1. Note the difference in timescales in panels A and B.

1.0±0.06 and 1.1±0.08, respectively. The finding that the MRT_{Rh}:MRT_{M} values for all the differently processed forms of rBoAChE are approximately 1, demonstrates that the pharmacokinetics of rBoAChE is determined in the rhesus animal system by the same set of principles revealed in the past in mice (Kronman *et al*., 2000), reflecting the hierarchical rules of fully-sialylated/tetramerized > fully-sialylated > partially-sialylated > asialylated.

Table 1: Pharmacokinetic parameters of rBoAChE and rHuAChE in rhesus macaques

AChE source	AChE type	A (%)	B (%)	$T_{1/2}\alpha$ (min)	$T1_{/2}\beta$ (min)	MRT (min)
rBoAChE	sialidase treated	100	-	3.5±0.5	-	3.9±0.6
	partially sialylated	85±6	20±5	5±0.5	57±4	66±2
	fully sialylated	56±6	46±5	17±4	163±25	205±7
	fully sialylated, tetramerized	34±2	68±2	14±2	1080±30	1510±45
rHuAChE	sialidase treated	100	-	2±0.5	-	2.7±0.4
	partially sialylated	85±5	17±4	6±1	54±6	59±1
	fully sialylated	37±4	65±6	6±2	73±4	99±3
	fully sialylated, tetramerized	31±4	72±5	5±1	74±4	96±5
	Tetraglycosylated, fully sialylated, tetramerized	40±3	64±4	6±1.5	73±5	97±6

The circulatory elimination patterns of recombinant human AChEs in rhesus macaques appear to deviate from the classical hierarchical rules established in mice

The generation of a therapeutically effective bioscavenger of organophosphate compounds based on exogenously administered cholinesterase, would ideally require the use of an enzyme form of homologous or closely related origin. We therefore addressed the question, whether the set of rules governing bovine AChE pharmacokinetics in monkeys apply to primate enzyme species as well. To this end, we monitored the circulatory performance of human AChE in rhesus macaques. Pharmacokinetic analyses of differently processed forms of human rAChE in monkeys revealed a unique pattern of elimination profiles (Fig. 1B, Table 1). Human rAChE entirely devoid of sialic acid residues was eliminated rapidly from the circulation (MRT =2.7±0.4 min) and partial sialylation of the rHuAChE resulted in

improved circulatory residence (MRT = 59±1 min), yet, full sialylation of the human enzyme resulted in an additional 1.7-fold increase in circulatory retention only (MRT = 99±3 min), while tetramerization of the fully sialylated human enzyme did not further contribute to the circulatory retention of the human enzyme (MRT = 96±5 min). Thus, while to full sialylation of the bovine enzyme and its following conversion into tetramers resulted in a 2.8-fold and 7-fold increase in circulatory residence time, respectively, full sialylation of the human enzyme form resulted in only a modest increase in MRT, and its subsequent tetramerization did not affect its circulatory retention at all. Notably, when examined in mice (Chitlaru *et al.*, 2001, see also Fig. 5B), the circulatory residence of the fully sialylated human enzyme could be significantly extended by tetramerization ($MRT_{fully\text{-}sialylated}$ and $MRT_{fully\text{-}sialylated/tetrameric}$ = 195±9 and 740±30 min, respectively) These results indicate that the inability to significantly extend the circulatory life-time of rHuAChE by tetramerization in rhesus macaques does not reflect an intrinsic property of the human enzyme *per se*, but rather some property of the rhesus macaque animal system with regard to the enzyme form of human source.

Human rAChE differs from the bovine enzyme in its number of appended N-glycans. The human enzyme contains three N-glycans at amino acid positions, which are homologous to those of three N-glycans of the bovine enzyme, while the latter carries an additional fourth N-glycan at amino acid 61 (Mendelson *et al.*, 1998; Velan *et al.*, 1993). Previous findings showed that a mutated form of fully sialylated, tetramerized rHuAChE, which contains, like the bovine enzyme, a fourth N-glycan at amino acid 61, resides in the circulation of mice for longer periods of time than its triglycosylated counterpart (Chitlaru *et al.*, 2002, see also Fig. 5B). To examine whether increasing the number of N-glycans contributes to the retention of rHuAChE in the rhesus macaque background as well, the pharmacokinetic behavior of the tetraglycosylated D61N enzyme in its fully sialylated/tetramerized configuration was monitored in monkeys. Pharmacokinetic profiling of this enzyme form demonstrated that its residence was virtually identical to that of its triglycosylated counterpart (MRT values = 97±6 and 96±5 min, respectively, Table 1 and Fig. 5B), and thus, unlike in the mouse animal system, where both enzyme tetramerization and addition of N-glycans, increased the circulatory retention of human AChE, in the rhesus animal system, neither tetramerization nor addition of N-glycans, contributed in a measurable manner to the circulatory residence of the fully sialylated enzyme.

These findings suggest that rHuAChE pharmacokinetics in the rhesus animal system deviate from the classical hierarchical rules found for the same enzyme in mice due to the operation

of a process which specifically promotes elimination of the human enzyme from the circulation of monkeys, while mitigating the positive effect of post-translation-related processes (i.e. enzyme assembly and glycan loading) on circulatory retention. This inability to augment circulatory retention of AChE in monkeys cannot be attributed to quantitative or qualitative differences in glycan processing of the two enzymes, since: (a) the tetraglycosylated mutant form of rHuAChE possesses the same number of appended N-glycans at the same amino acid positions as the bovine enzyme (Mendelson *et al.*, 1998), and (b) extensive structural analyses carried out in the past (Kronman *et al.*, 2000; Chitlaru *et al.*, 2001; see also Fig. 3B) have clearly demonstrated that both the bovine and human versions of rAChE generated in the HEK-293 cell line contain almost identical N-glycan forms in similar abundances. Thus, the differential pharmacokinetic hierarchical patterns exhibited by human and bovine AChEs in the rhesus animal system cannot be attributed to points of variance in their post-translation modifications, but most likely stem from differences in their primary amino acid sequences.

Cloning, expression and N-glycan analysis of various posttranslationally modified recombinant RhAChE forms

The presence of butyrylcholinesterase (BChE) and not acetylcholinesterase in the circulation of primates (e.g. rhesus and human) at the adult stage (Li *et al.*, 2000), may suggest that AChE is actively removed from the bloodstream. Such a mechanism could provide an explanation for the unique elimination of human AChE from the circulation of monkeys, since unlike bovine AChE, this species of the enzyme may be sufficiently similar to the "self" AChE of rhesus macaques and therefore be subject to active removal. To examine whether the pharmacokinetic patterns of human AChE enzyme forms may indeed be attributed to the action of "self" AChE circulatory elimination mechanisms, we set out to examine the pharmacokinetics of rhesus AChE in its homologous animal system. Determination of the genomic sequences of rhesus macaque AChE corresponding to exons 2 to 6 (Fig. 14A) revealed that at the DNA level, the rhesus and human AChEs differ at 32 out of 1971 nucleotides. Only three of these divergences result in changes in amino acids within the coding region of the mature enzyme: $M42_{human}->T42_{rhesus}$, $H284_{human}->N284_{rhesus}$ and $A467_{human}->T467_{rhesus}$ (Fig. 2B). The rRhAChE coding sequences were introduced into HEK-293 cells, or the modified 293ST-2D6 cell line expressing high levels of recombinant α-2,6 sialyltransferase (Chitlaru *et al.*, 1998), to generate authentic rhesus macaque recombinant AChEs, which are partially or fully sialylated, respectively.

A.

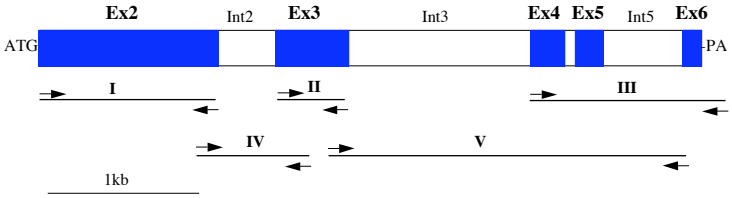

B.

```
Mature T - subunit
bovine --P--P----M--------L--MA-R---------------V--------
rhesus EGREDAELLVTVRGGRLRGIRLKTPGGPVSAFLGIPFAEPPTGPRRFLPP  50
human  ------------------------------------------M--------

bovine ---R--P--LN--A-----------------------------------
rhesus EPKQPWSGVVDATTFQSVCYQYVDTLYPGFEGTEMWNPNRELSEDCLYLN 100
human  --------------------------------------------------

bovine --------S------------------------------T---G-------
rhesus VWTPYPRPTSPTPVLVWIYGGGFYSGASSLDVYDGRFLVQAERTVLVSMN 150
human  --------------------------------------------------

bovine --------------------------------------------------
rhesus YRVGAFGFLALPGSREAPGNVGLLDQRLALQWVQENVAAFGGDPTSVTLF 200
human  --------------------------------------------------

bovine ----------------------------------------V--------L
rhesus GESAGAASVGMHLLSPPSRGLFHRAVLQSGAPNGPWATVGMGEARRRATQ 250
human  --------------------------------------------------

bovine --R--------A------------A----D--D---R-------------
rhesus LAHLVGCPPGGTGGNDTELVACLRTRPAQVLVNNEWHVLPQESVFRFSFV 300
human  ---------------------------------H----------------

bovine --------------------------------------------------
rhesus PVVDGDFLSDTPEALINAGDFHGLQVLVGVVKDEGSYFLVYGAPGFSKDN 350
human  --------------------------------------------------

bovine -------Q-----------A------------------------------
rhesus ESLISRAEFLAGVRVGVPQVSDLAAEAVVLHYTDWLHPEDPARLREALSD 400
human  --------------------------------------------------

bovine ----------------------------I---------------------
rhesus VVGDHNVVCPVAQLAGRLAAQGARVYAYVFEHRASTLSWPLWMGVPHGYE 450
human  --------------------------------------------------

bovine ------L--E--L---I--RT-------------------D---------
rhesus IEFIFGIPLDPSRNYTTEEKIFAQRLMRYWANFARTGDPNEPRDPKAPQW 500
human  ----------------A---------------------------------

bovine -------------N----------------------------------
rhesus PPYTAGAQQYVSLDLRPLEVRRGLRAQACAFWNRFLPKLLSATDTLDEAE 550
human  --------------------------------------------------

bovine ----------------------------------
rhesus RQWKAEFHRWSSYMVHWKNQFDHYSKQDRCSDL                  583
human  ----------------------------------

Signal peptide
bovine --------------------------------
rhesus MRPPQCLLHTPSLASPLLLLLLWLLGGGVGA
human  --------------------------------

Exon#5
bovine --------------------RP--------------   ------
rhesus ASEAPSTCPGFTHGEAAPRP  GLPLPLLLLHQLLLLFLSHLRRL
human  --------------------  ----------------------
```

Figure 2: Determination of rhesus AChE gene sequence (*A*) Map of the *Macaca mulatta* AChE gene and DNA genomic fragments generated by PCR amplification for sequence determination. **(*B*)** Amino acid sequence of RhAChE. The deduced sequence of the mature T-subunit, signal peptide and the C-terminus of the H subunit (Exon 5) of RhAChE, and the corresponding regions of HuAChE and BoAChE are shown. The conserved N-glycosylation consensus sequences are underlined. The rhesus/bovine and rhesus/human diverging amino acids are highlighted in bold and shadowed fonts, respectively.

As expected, the levels of production of the partially and fully sialylated rRhAChEs were similar to those of the human enzyme expressed in the same cell systems (approx. 50 units/ml/24h, (Chitlaru *et al*., 1998). The rRhAChE products exhibited a migration pattern on SDS-PAGE (Fig. 3A, inset), indistinguishable from that of their human counterparts (Chitlaru *et al*., 1998). As shown previously for the human enzyme, the rhesus AChE derived from the modified 293ST-2D6 cell line displayed a slower mobility, reflecting the efficient sialylation of the enzyme product in these α-2,6 sialyltransferase expresser cells. This was further verified by the pharmacokinetic analysis of the enzyme product in mice, as described below.

Examination of the sucrose-gradient profile of partially or fully sialylated rRhAChE demonstrated that these enzyme preparations consist of a mixture of differently assembled forms, most of which are dimers. Incubation of these rRhAChE preparations with the synthetic human ColQ PRAD peptide (Kronman *et al*., 2000) resulted in the quantitative conversion of the enzymes into assembled tetramers (Fig. 3A), in manner similar to that reported previously for human AChE (Chitlaru *et al*., 2001).

To determine that the basic structures of the N-glycans appended to rRhAChE generated in HEK-293 cells are similar to those of rBoAChE and rHuAChE derived from the same cells, the glycan structures of rRhAChE (partially and fully sialylated) were analyzed by MALDI-TOF (Fig 3B). Inspection of the MALDI-TOF-MS profiles of desialylated glycans of rRhAChE produced by HEK-293 cells and sialyltransferase-modified 293ST-2D6 cells revealed that both glycan pools consist of a similar array of varied structures, displaying an overall pattern which is similar to that of the N-glycans associated with partially sialylated and fully sialylated rHuAChE and rBoAChE (Fig. 3B). Thus, the major glycan species (41-46% of total glycans) correspond to complex-type biantennary forms carrying a fucose moiety, while triantennary glycans (22-30% of the total glycans) were represented to a higher extent by the non-fucosylated form. The single significant difference between the glycan structures of rRhAChE and those of rHuAChE and rBoAChE is in the level of tetraglycosylated forms, which is higher in the rhesus enzymes. Taken together, characterization of the recombinant RhAChE demonstrates that this enzyme displays a strikingly high degree of similarity to the human enzyme both in its primary sequence and in its post-translation processing.

A

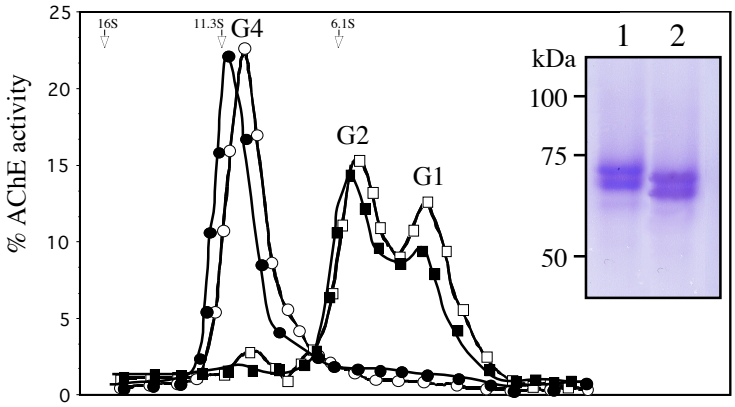

B

biantennary		triantennary		tetraantennary	
	rAChE:	rAChE-ST:	rAChE:	rAChE-ST:	rAChE:	rAChE-ST:
Rh:	5.8±1	3.9±0.5	20±2	17±1.8	11±1.5	19±2
Hu:	4.9±0.8	5.2±0.6	13.6±1	19±1	<0.8	<0.8
Bo:	6.9±1	5.9±0.7	25±2	23±2	<0.8	<0.8
biantennary fucosylated		**triantennary fucosylated**		**tetraantennary fucosylated**	
	rAChE:	rAChE-ST:	rAChE:	rAChE-ST:	rAChE:	rAChE-ST:
Rh:	41±4	46±5	10±1.8	5.5±0.8	5.8±1	9±1
Hu:	65±6	61±5	11.2±2	14.5±2	2.2±0.3	2.8±0.8
Bo:	57±5	54±5	5.9±2	8±2	1.5±0.4	3.5±0.6

Figure 3: Characterization of recombinant rhesus AChE (***A***) Sucrose gradient sedimentation profiles of partially sialylated (filled symbols) and fully sialylated (empty symbols) rRhAChE respectively, before (squares) and after (circles) *in vitro* tetramerization. *G1, G2,* and *G4* annotate the monomeric, dimeric, and tetrameric RhAChE forms, respectively. *Arrows* denote the elution position of the sedimentation markers alkaline phosphatase (6.1 S), catalase (11.3 S), and β-galactosidase (16 S) included in all samples. **Inset:** SDS-PAGE analysis of rRhAChE produced in the sialyltransferase-expresser 293ST-2D6 cells (lane 1) or in non-modified HEK-293 cells (lane 2). **(*B*)** The basic structures of the glycans of rAChEs (produced by HEK-293 cells) and rAChE-STs (produced by 293ST-2D6 cells). Glycans are classified according to their branching and fucosylation. Desialylated glycan structures were deduced from the mass spectral data obtained by MALDI-TOF as described in the Method section. The relative abundance (% of total glycans) of each glycan species is shown and compared to the abundances of the corresponding glycan structures in rHuAChE and rBoAChE determined previously (Kronman *et al.*, 2000; Chitlaru *et al.*, 2001). *Open square*, GlcNAc; *open circle,* Mannose; *solid circle,* β-Galactose; *solid square,* GalNAc; *elongated diamond*, Fucose. Rh, rhesus; Hu, human; Bo, Bovine.

Pharmacokinetic profiles of recombinant RhAChE in Rhesus macaques and mice

Examination of the pharmacokinetic behavior of the various forms of rRhAChE in mice (Fig. 4A, Table 2), demonstrated that rRhAChE is retained in the circulation in a manner similar to that displayed by recombinant human AChE (Kronman *et al*., 2000). This was manifested both by the increase in circulatory residence time observed for enzyme forms displaying increasing amounts of appended sialic acid residues (MRT for asialylated, partially sialylated, and fully sialylated rRhAChE = 3.2±0.6, 92±4 and 171±8 min, respectively), and by the significant combined effect of both full sialylation and enzyme tetramerization (MRT of fully sialylated tetrameric rRhAChE = 805±25 min). Thus, rRhAChE pharmacokinetics in mice is governed, like rHuAChE, by post-translation-related processes that operate in a hierarchical manner leading to the extension of the circulatory residence by efficient sialylation and tetramerization. The strikingly similar pharmacokinetic behaviors of human and rhesus AChEs in the mice animal system and the fact that they are equally influenced by the same set of post-translation processes, is in accordance with the high degree of resemblance of the two primate AChE enzyme forms.

Table 2: Pharmacokinetic parameters of rRhAChE in rhesus macaques and mice

Animal **system**	**AChE type**	**A (%)**	**B (%)**	**T1/2α (min)**	**T1/2β (min)**	**MRT (min)**
Rhesus	**sialidase treated**	100	-	3.6±0.6	-	3.4±0.4
	partially sialylated	75±5	32±5	7±1	72±10	86±6
	fully sialylated	46±4	57±5	16±2	113±8	143±7
	fully sialylated, tetramerized	57±3	46±3	26±3	255±24	290±25
Mouse	**sialidase treated**	100	-	2.9±0.6	-	3.2±0.6
	partially sialylated	56±8	34±9	8±3	71±16	92±4
	fully sialylated	51±7	49±7	11±3	118±12	171±8
	fully sialylated, tetramerized	46±3	52±3	45±10	666±38	805±25

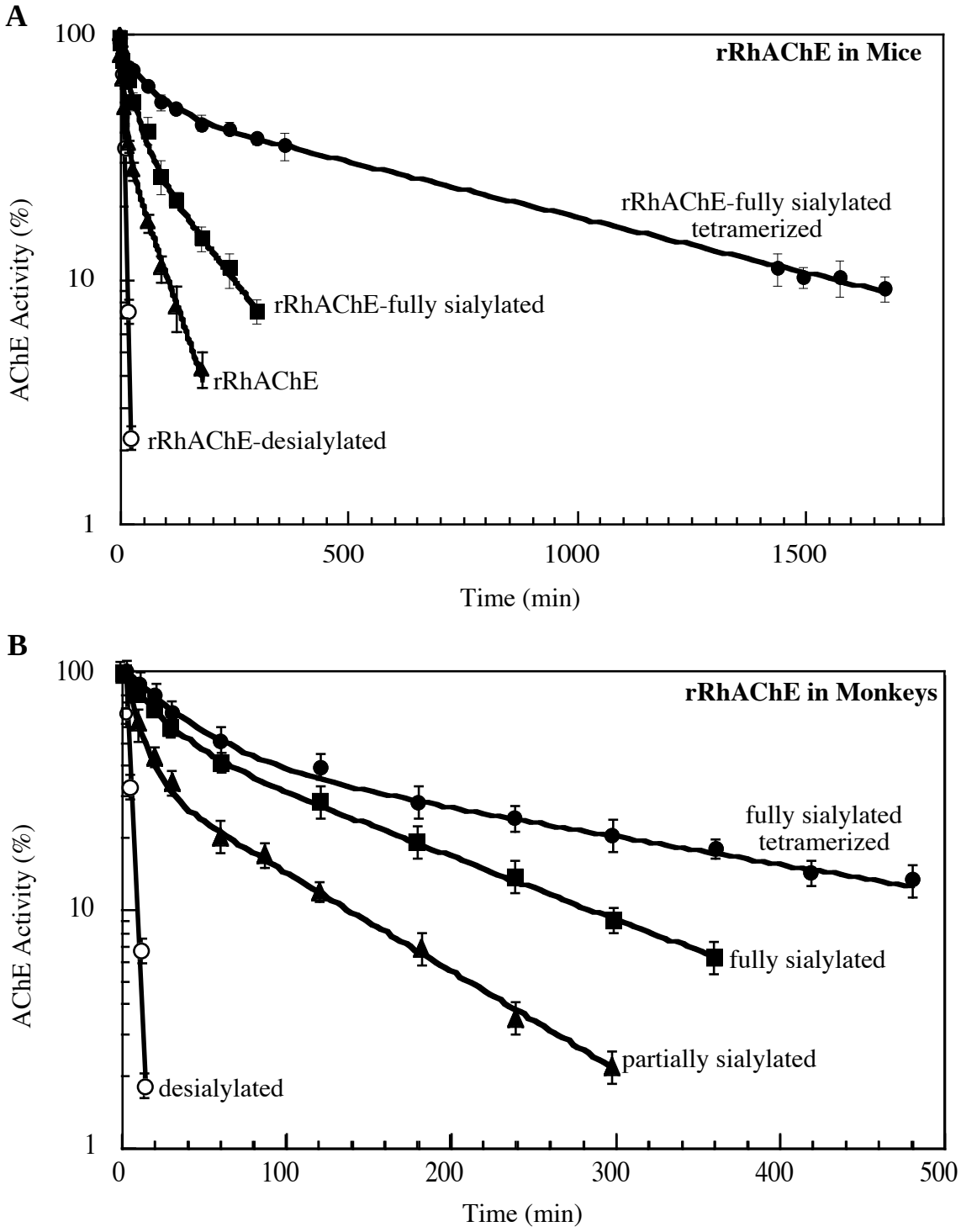

Figure 4: Circulatory elimination profiles of various molecular forms of rRhAChE in mice and in rhesus macaques Purified preparations of various molecular forms of rRhAChE, differing in their post-translation processing (glycan sialylation level, subunit assembly state), were administered to mice **(*A*)** or rhesus macaques **(*B*)** and residual AChE activity in the circulation was assayed at the indicated time points. Circulatory removal curves were determined for all the AChE forms and the derived pharmacokinetic parameters are presented in Table 2. Note the difference in timescales in panels A and B.

Pharmacokinetic analyses of the various recombinant rhesus AChE forms in monkeys demonstrated (Fig. 4B) that rhesus AChE pharmacokinetics abides by the classical rules of hierarchy to a lesser extent in this animal system. This is manifested by the finding that conversion of rRhAChE to its fully tetramerized state resulted in a 2-fold increase (MRT rRhAChE $_{\text{fully-sialylated}}$ = 143±7 min; MRT rRhAChE $_{\text{fully-sialylated/tetramerized}}$ = 290±25 min) in circulatory retention only, as opposed to a 4.7-fold increase in mice (MRT rRhAChE $_{\text{fully-sialylated}}$ = 171±8 min; MRT rRhAChE $_{\text{fully-sialylated/tetramerized}}$ = 805±25 min). Thus, while the MRT_{Rh}:MRT_{M} values of asialylated, partially-sialylated, and fully-sialylated rRhAChE are 1.0±0.06, 0.93±0.04, and 0.84±0.04, respectively, the MRT_{Rh}:MRT_{M} value of the fully-sialylated/tetramerized form of rRhAChE sharply declines to 0.36±0.02. Thus, unlike bovine AChE which displayed a similar pharmacokinetic behavior in both mice and monkeys as exemplified by MRT_{Rh}:MRT_{M} values of approximately 1 for all the differently processed forms of rBoAChE, the rhesus enzyme resembles its human counterpart in its differential pharmacokinetic behavior in the mouse and monkey animal systems; circulatory retention of both primate enzymes was clearly less susceptible to post-translation modifications in monkeys.

Taken together these findings demonstrate that the circulatory residence of bovine and primate AChEs in rhesus macaques are governed in a different manner. Increasing sialic acid levels of the different enzyme species results in extension of their circulatory lifetime in rhesus macaques (Fig. 5A), emphasizing the pivotal role of glycan sialylation in determining the circulatory residence of AChEs in rhesus macaques. Yet, one can notice that the effect of full sialylation on AChE pharmacokinetics in rhesus macaques is slightly less prominent in the case of the primate enzymes. The differential pharmacokinetic performance of bovine and primate AChEs in rhesus macaques is fully manifested when examining the effect of enzyme tetramerization on circulatory residence (Fig. 5B). While assembly of the bovine enzyme into tetramers resulted in a striking increase in its retention, tetramerization affected the circulatory duration of the primate AChEs to a much lower extent, or not at all. The deviation from the classical hierarchical rules established for the different enzyme species in the mice animal system, is further manifested by the inability to extend circulatory residence of the human enzyme by increasing the glycan loading of the enzyme (Fig. 5C). Thus, unlike the bovine enzyme, AChEs of primate source appear to be actively eliminated from the circulation of monkeys in a manner that counteracts the positive effect of post-translation processing on circulatory longevity. The somewhat surprising observation that the human

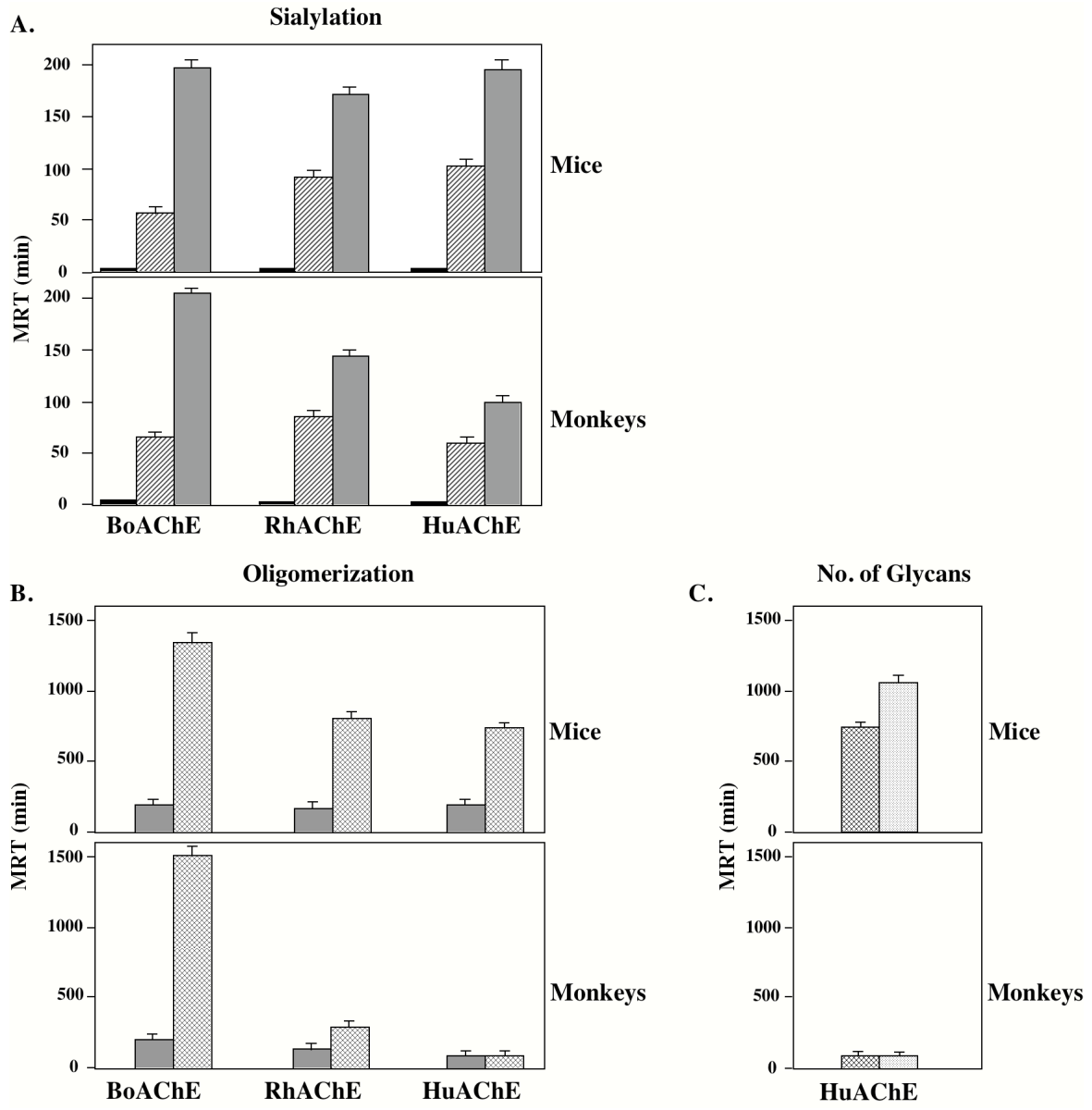

Figure 5: Effect of sialylation, oligomerization and glycan loading on the circulatory residence of bovine, human and rhesus AChEs in mice or rhesus macaques Bars represent the MRT values in mice and monkeys of the different molecular forms of BoAChE, HuAChE and RhAChE as calculated from the circulatory elimination data obtained in this and previous studies (Kronman *et al.*, 2000; Chitlaru *et al.*, 2001, 2002). (***A***) Effect of sialylation of AChEs: sialidase treated (■), partially sialylated (▨) and fully sialylated (■). (***B***) Effect of oligomerization of sialylated AChEs: dimeric (■) and tetrameric (▩). (***C***) Effect of number of glycans in fully sialylated tetrameric HuAChEs: Wild type (wt) triglycosylated (▩) and D61N tetraglycosylated (□).

enzyme is even more prone than the rhesus enzyme to elimination from the circulation of rhesus macaques suggests that the differential pharmacokinetics of bovine and primate AChEs in monkeys cannot be fully explained in terms of "self"-specific enzyme removal. Specific structural features which are common to the primate enzymes under examination, and not to the bovine enzyme, seem to facilitate the active removal of AChEs in rhesus macaques, while the observed differences in the clearance patterns of the human and rhesus enzymes in rhesus macaques may be attributed to subtle differences in structures of the two primate AChEs species.

Facilitated elimination of cholinesterases from the circulation of rhesus macaques is restricted to primate AChE but not to primate BChE

The presence of significant levels of circulating BChE in rhesus macaques (Carmona *et al.*, 1996) seems to suggest that active removal of primate cholinesterase in this animal system is restricted to AChE. However, primate BChE may also be actively and effectively eliminated from the circulation at rates similar to those of AChE, while its apparent prevalence in the circulation may be a reflection of its high turnover rate. To examine this issue, BChE from rhesus monkey serum was purified on procainamide columns and subjected to pharmacokinetic profiling in rhesus macaques. To enable the monitoring of the administered enzyme over the high background of endogenous BChE (~10U/ml), purified rhesus serum BChE was radiolabeled by incubating the enzyme with a tritiated organophosphorus compound, [^{3}H]-DFP. The inactivated enzyme was then administered to rhesus macaques, and its circulatory residence was followed by determining radioactivity in blood samples removed at various periods of time (Fig. 6). This quantization, which enables detection of relatively small amounts of administered enzyme was repeated in three monkeys, and allowed us to determine that rhesus BChE resides in the circulation of rhesus macaques for long periods of time, displaying an MRT value of 9,950±1300min. However, to rule out the possibility that the coupling of the organophosphorus DFP compound to the enzyme affected significantly its circulatory retention, the experiment was performed with native non-labeled rhesus serum BChE, using large enough amounts of enzyme to allow significant quantization of the administered enzyme over background, by monitoring BChE enzymatic activity. As in the case of the radiolabeled BChE, the native non-labeled form of rhesus BChE resided in the circulation for extended periods of time and displayed a similar MRT value of 10,600±1200min (Fig. 6, inset). These values, which testify to the fact that RhBChE resides in the circulation of monkeys for very long periods of time, are in good agreement with those

reported recently (Rosenberg *et al.*, 2002), and are similar to those determined in the past for human BChE in humans (Cascio *et al.*, 1988; Jenkins *et al.*, 1967). The occurrence of BChE in the circulation of rhesus macaques reflects therefore the long-term circulatory retention of this enzyme form, rather than the presence at steady state of high levels of short-lived species of ChE. These findings show that removal of rhesus AChE cannot be attributed to a general mechanism responsible for the elimination of all forms of primate cholinesterase, but rather depends on the operation of an elaborate clearance system, which recognizes and removes the soluble self acetylcholinesterase, RhAChE, and the very closely related HuAChE, in a unique manner.

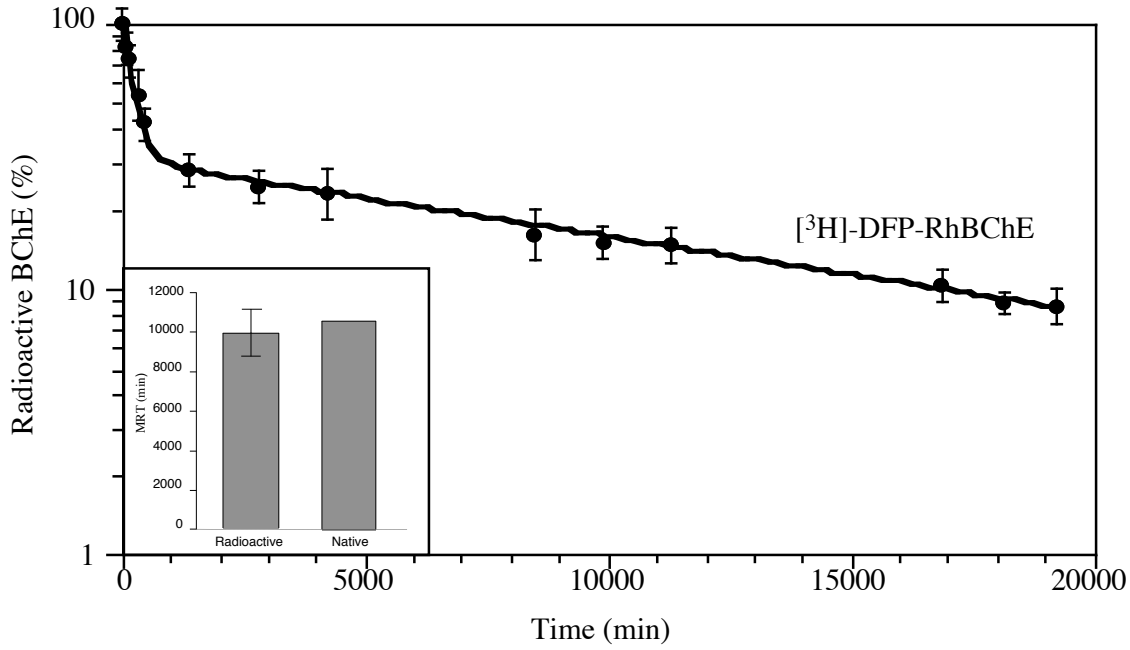

Figure 6: Circulatory elimination profiles of labeled and non-labeled rhesus butyryl (BChE) in rhesus macaques. Native rhesus BChE, labeled with [^{3}H]-DFP was administered to 3 rhesus macaques and residual circulatory radiolabeled BChE was assayed at the indicated time points post-administration. **Inset:** Comparison of the MRT values of the radioactively labeled rhesus BChE and enzymatically active non-labeled BChE, see "Methods" section.

A possible role for amino acid domains in the differential pharmacokinetic behavior of bovine and primate AChEs in rhesus macaques

As reported above, the glycan pool of rRhAChE consists of an array of varied structures whose basic structures displayed an overall pattern, similar to that of the N-glycans associated with rBoAChE and rHuAChE (Fig. 3B), the only notable difference being the

relatively high level of tetraantennary glycan forms which is observed in the rhesus enzyme. Differences in the basic structures of appended N-glycans cannot therefore provide an explanation for the differential pharmacokinetic performances of bovine versus primate AChEs. Likewise, the dissimilar pharmacokinetic patterns of bovine and primate AChEs in monkeys cannot be attributed to differences in terminal sialylation, since the various AChEs are all efficiently sialylated in a similar manner when expressed in the genetically modified 293ST 2D6 cells that express high levels of heterologous 2,6-sialyltransferase (Fig. 3A, inset, see also (Chitlaru *et al.*, 1998). Examination of the amino acid divergences between the human and rhesus AChEs (Fig. 2) demonstrates that these are not involved in the generation or abolishment of N-glycosylation consensus sequences, while SDS-PAGE analysis (Fig. 3A inset, and Chitlaru *et al.*, 1998) suggests that the human and rhesus enzymes carry similar amounts of glycans. Thus, both primate AChEs carry 3 N-glycans per enzyme subunit, while the bovine enzyme contains 4 N-glycans per enzyme subunit. However, this quantitative difference in N-glycan loading of bovine AChE and primate AChEs is also apparently not responsible for the less efficient retention of the latter in the circulation of monkeys, since addition of a fourth N-glycan to the human enzyme at aa 61, the position which is analogous to that of the fourth N-glycan of the bovine enzyme, did not alter human AChE circulatory residence in monkeys (Fig. 5C). Furthermore, incubation of both primate and bovine forms of AChE with the synthetic ColQ PRAD peptide resulted in the quantitative conversion of the all the various enzyme forms into tetramers in a similarly highly efficient manner, attesting to the fact that their disparate pharmacokinetics in monkeys are not related to differences in subunit organization.

Taken together, all these findings suggest that the dissimilarity between bovine and primate AChE circulatory residence does not stem from differences in glycosylation or assembly state, but rather from points of divergence in their primary structure which differentially affect circulatory residence. The divergent amino acid domains may in themselves constitute ligands for receptor-directed clearance or can lead to appendage of yet undefined structures involved in clearance. Such species-specific amino acid domains which facilitate circulatory elimination of primate AChEs from the circulation of monkeys, operate through a mechanism of considerable potency as judged by their ability to counteract the positive effect of post-translation modifications on circulatory residence of primate AChEs, and function as clearance epitopes in an enzyme assembly-independent manner, as demonstrated by their ability to abolish tetramerization-induced circulatory life-time extension (Fig. 5B).

Alterations in plasma clearance of proteins by amino-acid replacements that affect interactions of the protein with its clearance receptor in a direct or indirect manner have been documented previously in other systems. In the case of insulin-like growth factor (IGF-I), the single and double amino acid mutants F49A and E3A/F49A were cleared more rapidly from the circulation due to their diminished ability to form high-molecular mass soluble complexes with insulin-like growth factor binding proteins, without changing the affinity of the mutant forms towards the insulin growth factor type I receptor (Dubaquie *et al.*, 2001). On the other hand, apolipoprotein E plasma clearance is severely compromised by a single Arg-158->Cys mutation, which prevents efficient binding of ApoE to the low-density lipoprotein receptor (van Vlijmen *et al.*, 1996). Amino acid substitutions were also demonstrated to affect tissue plasminogen activator (t-PA) clearance from the circulation, yet in this case the altered pharmacokinetic properties were due to changes in the N-glycan contents of the protein, rather than to the presence of altered amino acids *per se*. Thus, the 9-fold reduction in circulatory clearance of the Thr-110->Asn t-PA mutant is probably due to the addition of a complex-type N-glycan structure (Keyt *et al.*, 1994), while the 6.5-fold reduction in plasma clearance of the Asn117->Gln t-PA mutant was attributed to the prevention of high-mannose glycosylation at this site (Aoki *et al.*, 2001). As noted above, in the case of AChE the differential circulatory behavior of primate and bovine enzymes cannot to be attributed to glycosylation-related factors.

Comparison of the sequences of the bovine and rhesus enzymes (Fig. 2B) demonstrates that the diverging amino acids are dispersed throughout the primary enzyme structures, yet, examination of the 3D structure of AChE reveals that all of these diverging amino acids are clustered within three domains, A, B and C (Fig. 7). These divergence patches are located at the surface of the enzyme, both in its monomeric (Fig. 7A) and tetrameric (Fig. 7C) states of assembly, only part of Domain B being obscured by tetramerization (Fig. 7C). The bovine version of AChE as well as the tetraglycosylated form of the human enzyme mentioned above carry an additional N-glycan at aa 61, which maps to a central position within Domain A (Fig. 7B). Interestingly, human AChE carrying this additional N-glycan, displayed enhanced circulatory retention in mice (Chitlaru *et al.*, 2002). We note that the three human/rhesus diverging amino acids, 42, 284 and 467, which are apparently responsible for the somewhat differential pharmacokinetic patterns of these two enzymes in the rhesus animal system, indeed map within Domains B (42 and 284) and C (467).

The effect of masking of primate-specific amino-acid domains by PEGylation on the circulatory lifetime of AChE in rhesus macaques.

Previous studies carried out in mice (Cohen *et al*., 2001) demonstrated that the conjugation of PEG chains to lysine residues of AChE resulted in the generation of a molecule which resides in the circulation for exceedingly long periods of time. Most importantly, PEG conjugation prevented plasma clearance of undersialylated rHuAChE as well, suggesting that the appendage of PEG chains obstructs accessibility of domains at the surface of the enzyme to the hepatic asialoglycoprotein receptors. It was therefore interesting to examine whether PEGylation can prevent the putative species-specific amino-acid domain removal process, as well. To address this issue, partially sialylated rHuAChE and rRhAChE produced in HEK-293 cells and consisting mostly of dimeric forms were subjected to PEG appendage. To allow efficient PEG-conjugation of the two primate AChEs without compromising AChE bioactivity, the enzymes were reacted with succinimidyl propionate activated PEG at molar ratios and under conditions determined in the past (Cohen *et al*., 2001). Under these conditions, the PEGylated product carries an average of 4 PEG chains per enzyme subunit and retains full enzymatic activity.

The PEGylated rHuAChE and rRhAChE were administered to rhesus macaques and the pharmacokinetic profiles of the chemically modified enzymes were monitored (Fig. 8). The PEGylated enzymes were retained in the circulation for exceedingly long periods of time, exhibiting MRT values of 10,360±280 min and 9,900±390 min for PEGylated rHuAChE and PEGylated rRhAChE, respectively. Thus, the chemical conjugation of PEG to the primate enzymes resulted in an extraordinarily high increase in the residence of the human and rhesus enzymes, over 100-fold, in the circulation of monkeys, demonstrating that PEGylation of AChE indeed leads to the efficient masking of the various determinants that promote enzyme clearance in monkeys. The finding that the PEGylated forms of the primate enzymes exhibit MRT values which are exceedingly higher than that of rBoAChE even in its fully processed form (1510±45 min, See Table 5), demonstrates that the appendage of PEG chains masks not only the elements which cause the minor inequality in the pharmacokinetics of human and rhesus AChEs, but also overcomes the contribution of the primate-specific amino acid sequences to the inferior pharmacokinetic performance in monkeys of both rHuAChE and rRhAChE as compared to the bovine enzyme. In fact, the MRT values of the PEGylated primate AChEs are similar to that exhibited by native long-lived rhesus BChE (Fig. 6),

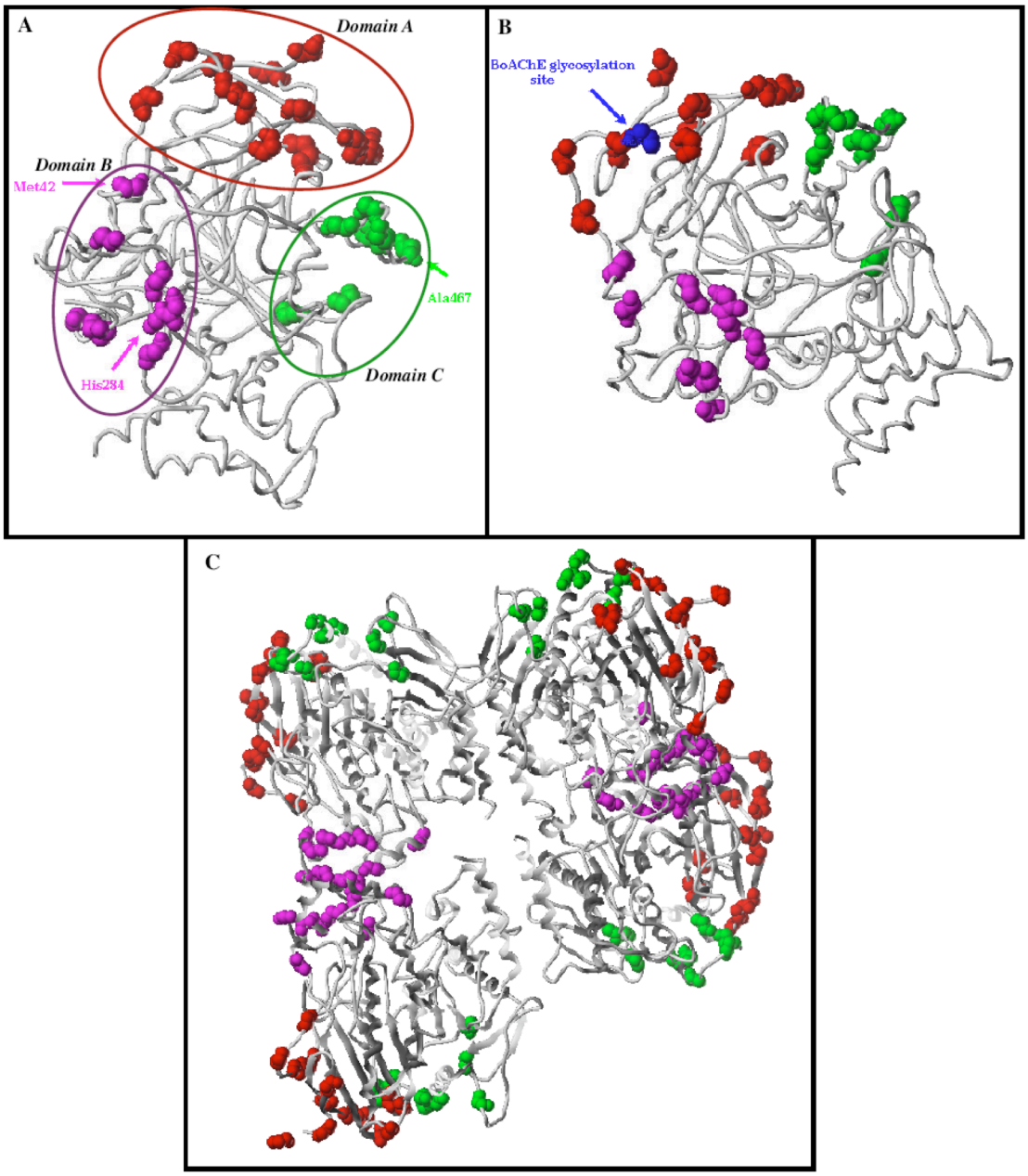

Figure 7: Mapping of divergent amino acids between BoAChE and RhAChE/HuAChE onto the three-dimensional model of HuAChE The protein backbone is depicted as a line ribbon and the divergent residues are shown as space-fill spheres. Note that all divergent residues map to the enzyme surface. (***A***) Mapping of the BoAChE/RhAChE diverging amino acid residues within three enzyme surface-located domains. The BoAChE/RhAChE diverging amino acid residues are colored according to their location: red, Domain A; magenta, Domain B; and green, Domain C. Arrows point to the three divergent residues (Met42, His284 and Ala467) between RhAChE and HuAChE. (***B***) Mapping of the fourth glycosylation site (Asn 61) of BoAChE to the center of Domain A. (***C***) Mapping of the BoAChE/RhAChE divergent domains within the tetrameric structure of human AChE.

indicating that PEG appendage results in the generation of enzyme forms which are no longer accessible to circulatory removal systems which recognize and interact with the self primate acetylcholinesterase-specific domains.

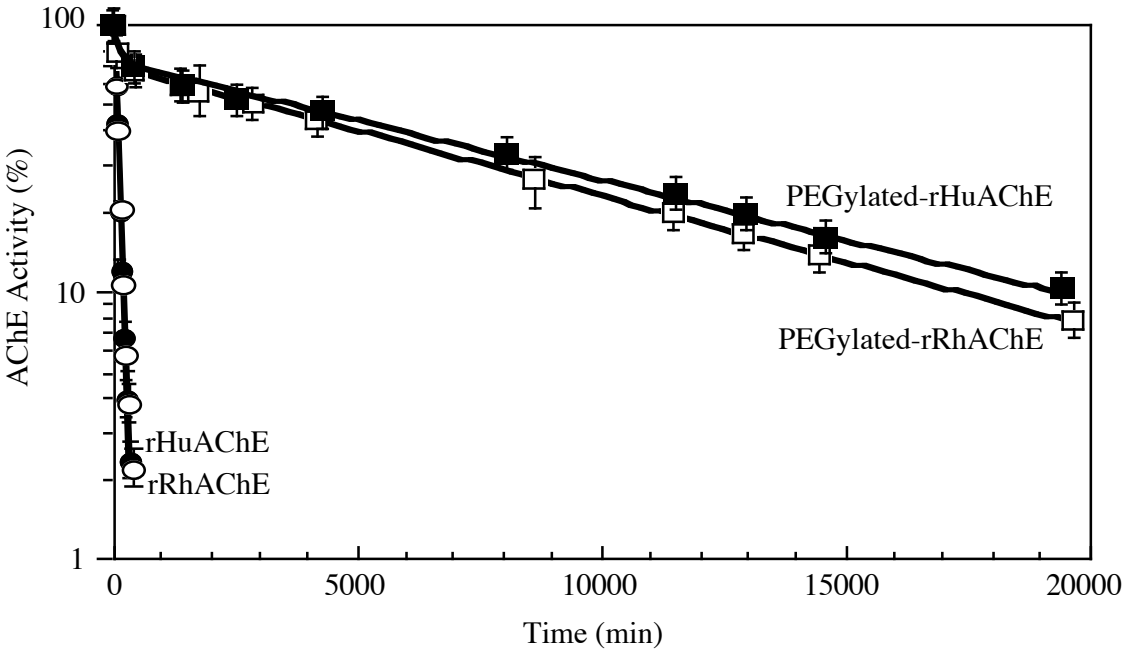

Figure 8: Pharmacokinetic profiles of PEGylated rRhAChE and PEGylated rHuAChE in rhesus macaques Purified recombinant rhesus (empty symbols) or human (filled symbols) AChE generated in HEK-293 cells (partially sialylated, dimeric forms), were administered to 3 rhesus macaques before (circles) or after (squares) chemical conjugation to polyethylene glycol. The residual AChE activity in the circulation was assayed at the indicated time points as described in the "Experimental" section

In conclusion, the present study defines amino acid-related domains as an important element, which together with post-translation related factors such as oligosaccharide sialylation, enzyme assembly and glycan loading, determines the circulatory lifetime of acetylcholinesterase in the circulation of non-human primates. In fact, in the rhesus macaque animal system, amino-acid-related elimination of AChE is effective to a degree that it prevents full manifestation of the positive effect of efficient sialylation on the circulatory retention of the enzyme. Even so, chemical conjugation of PEG to AChE species containing amino acid epitopes which promote circulatory elimination, could effectively protect these enzymes from amino acid-related removal. The amino acid configurations that promote enzyme clearance in rhesus macaques seem to be restricted to those presented by "self" or "self-like" AChE species. Unlike in rhesus macaques, differences in amino-acid sequences had only a minor effect on the differential clearance of bovine, human and rhesus AChE in

the mouse animal system yet this apparent insensitivity to amino acid alterations may stem from the fact that the three AChE species examined, BoAChE, HuAChE and RhAChE, are equally "foreign" and therefore do not present amino-acid epitopes which promote enzyme removal in mice. Indeed, primates are characterized by a paucity of soluble AChE in the circulation at the adult stage (Li *et al.*, 2000). The predominance of butyryl ChE in the circulation of adults, and the finding that "self" acetyl ChE is eliminated from the circulation, may suggest that organisms have evolved elaborate mechanisms to support circulatory residence of butyryl cholinesterase in particular. Although the biological significance of active elimination of soluble acetylcholinestereases from the bloodstream remains to be elucidated, it may be speculated that this process has to do with one or more of the non-catalytic functions attributed to this enzyme, which include cell differentiation, haematopoietic and thrombopoietic activities and involvement in cell-adhesion (Balasubramanian and Bhanumathy, 1993; Grisaru *et al.*, 1999; Soreq and Seidman, 2001).

III. THE EFFECT OF POLYETHYLENE GLYCOL CONJUGATION ON THE CIRCULATORY LIFETIME OF ACETYLCHOLINESTERASE MOLECULAR FORMS DIFFERING IN THEIR POST-TRANSLATIONAL PROCESSING

INTRODUCTION

Studies carried out in our laboratory demonstrated that PEG modification of AChE can result in the generation of bioactive enzyme exhibiting an improved pharmacokinetic profile (Cohen *et al.*, 2001). Examination of a set of conditions for the attachment of PEG to AChE, allowed us to determine that under certain conditions, 4 PEG molecules may be appended to monomeric rHuAChE, with minimal effect on the catalytic activity of the enzyme or on the reactivity towards active center inhibitors (e.g. edrophonium and diisopropylfluorophosphate (DFP)), peripheral site ligands (e.g. propidium), and even towards the bulky snake-venom toxin fasciculin II. The PEGylated AChE demonstrated prolonged circulatory retention rates which were characterized by an MRT exceeding 2000 minutes. Examination of MRTs of an array of PEGylated AChEs which differed one from another by their degree of modification, as well as by the length of the appended PEG chains, suggested that the overall increase in MRT is directly dependent on the molecular size of the modified enzyme (Cohen *et al.*, 2001).

In our previous studies under Contract DAMD17-00-C-0021, we demonstrated that recombinant AChE can be converted into a long-term circulating protein by a two-step modification procedure that results in high-level glycan sialylation and enzyme subunit tetramerization. These findings suggest that receptor-mediated removal and limited protein size, which are respectively remedied by sialylation and tetramerization, indeed play a crucial role in determining the circulatory behavior of rAChE. However, the possible interrelationship between PEG-conjugation and the post-translation modifications of proteins with regard to the overall pharamacokinetic profile of the protein product has not been explored. It therefore remains to be clarified whether PEGylation of rAChE exhibiting sub-optimal post-translation modifications will give rise to an enzyme species exhibiting maximal

circulatory residence, or whether efficient AChE post-translation processing is required for the full scale manifestation of the effect of PEGylation on circulatory residence. For instance, the quantitative and qualitative features of enzyme glycosylation may contribute to the overall circulatory residence of PEGylated proteins resulting in the increased retention of glycosylated, fully-sialylated PEGylated AChE, as compared to nonglycosylated or undersialylated forms of PEGylated enzyme. Elucidation of the interrelationship between the state of post-translation processing and AChE PEGylation, might lead to the design of long-lived PEGylated-AChE, which benefits from the combined effect of post-translation modifications with chemical modification. Conversely, these studies may prove that the overriding effect of PEGylation allows in itself maximal retention of AChE in the circulation, circumventing the need for optimized post-translation processing of the enzyme.

In the present study, we conducted a series of experiments designed to probe the interrelationship between either AChE lysine contents or AChE differential post-translational processing and PEG-conjugation with regard to the overall pharamacokinetic profile of the protein product. The data resulting from this study are provided herein, and the implications of our findings on the large-scale production of rHuAChE for therapeutic use are discussed.

METHODS

PEG-conjugation reaction and analysis of the products

Attachment of PEG chains to primary amines in the AChE enzymes was performed using succinimidyl propionate activated methoxy PEG (SPA-PEG; Shearwater polymers, Inc.). Purified recombinant enzymes (10μM) was incubated with PEG-20000 at a ratio of 100:1 $[PEG]_0/[AChE\ primary\ amines]_0$ in 50mM borate buffer pH 8.5 for 2 hours at room temperature. The modified products were dialyzed extensively against phosphate buffer saline (PBS) using cellulose acetate membranes (cutoff 50KDa; Nest Group Inc.). Samples of the proteins were resolved on 5% SDS-polyacrylamide gels. To reduce the interaction of PEG with SDS (Odom *et al*., 1997), Tris–HCl concentration in the stacking gel was decrease by 25%, to 93.8mM and concentration of SDS in the electrode buffer was lowered to 0.05%. PEGylated proteins were visualized by Coomassie staining or by BaI_2 staining which allows visualization of PEG. Preservation of AChE enzymatic activity was monitored by activity measurements as described below.

Enzyme activity

AChE activity was measured according to Ellman *et al*. (1961). Assays were performed in the presence of 0.5 mM acetylthiocholine, 50 mM sodium phosphate buffer pH 8.0 0.1 mg/ml BSA and 0.3 mM 5,5'-dithiobis-(2-nitrobenzoic acid). The assay was carried out at 27^0C and monitored by a Thermomax microplate reader (Molecular Devices).

Pharmacokinetics in mice

Clearance experiments in mice (3 to 6 ICR male mice per enzyme sample) and analysis of pharmacokinetic profiles were carried out as described previously (Kronman *et al*., 1995). The study was approved by the local ethical committee on animal experiments. Residual AChE activity in blood samples was measured and all values were corrected for background activity determined in blood samples withdrawn 1 hour before performing the experiment. The clearance patterns of the various enzyme preparations were usually biphasic and fitted to a bi-exponential elimination pharmacokinetic model ($C_t=Ae^{-k\alpha t}+Be^{-k\beta t}$) as described previously (Kronman *et al*., 1995). This model enables determination of the parameters A and B which represent the fractions of the material removed from the circulation in the first-fast and second-slow elimination phases respectively, and $T_{1/2}\alpha$ and $T_{1/2}\beta$ which represent the circulatory half-life values of the enzyme in the fast and slow phases. The

pharmacokinetic parameters MRT (mean residence time, which reflects the average length of time the administered molecules are retained in the organism) and CL (clearance, which represents the proportionality factor relating the rate of substance elimination to its plasma concentration (CL=dose/area under the concentration-time curve), (Rowland and Tozer, 1989) were independently obtained by analyzing the clearance data according to a noncompartmental pharmacokinetic model using the WinNonlin computer program (Laub and Gallo, 1996).

Sucrose gradient

Analytical sucrose density gradient centrifugation was performed on 5-25% sucrose gradients containing 0.1M NaCl/50 mM sodium phosphate buffer pH 8.0. Centrifugation was carried out in an SW41 Ti rotor (Beckman) for 26h at 160000 Fractions of 0.2 ml were collected and assayed for AChE activity. Alkaline phosphatase was used as a sedimentation marker.

Non-denaturing deglycosylation of AChE

Purified recombinant AChE (500μg of either the wild-type or the C-terminal truncated enzyme) was subjected to two consecutive treatments with 250mU of N-glycanase plus (Glyko Inc.) at room temperature for 24 hours. AChE was cleared from the N-glycanase enzyme and the removed glycan chains by purification on procaine-amid column as described before (Kronman *et al.*, 1992, 1995). The complete removal of the glycans from AChE was monitored by SDS-PAGE analysis. Using these mild conditions for glycan removal results in the full preservation of the enzymatic activity of AChE.

MALDI-TOF Analysis of Basic Glycan Structures

- Release, recovery, purification and labeling of N-glycans:

N-glycans of purified enzyme preparations (~100 μg protein) were released by N-glycosidase-F (Glyko, USA) treatment as described before (Kronman *et al.*, 1992). Deglycosylated protein was removed by ethanol-precipitation and glycans were recovered and purified from the supernatant as described by Kuster *et al.* (1997). To increase sensitivity (Anumula and Dhume, 1998; Okafo *et al.*, 1996, 1997) purified glycans were fluorescently labeled. Fluorescent labeling of purified glycans with 2-aminobenzamide (2-AB) was performed according to Bigge *et al.,* 1995, using a commercial labeling kit (Glyko, USA).

- Sialic acid removal:

Agarose-bound sialidase (0.04U, Sigma) was prewashed 5 times with water and incubated at room temperature for 16h with 2AB labeled N-glycans released from 1.5 -2.0 nmol AChE. Sialidase was removed by Eppendorf centrifugation. Desialylated N-glycans were vacuum dried, resuspended in 30 μl of water and stored at -20^{0}C until use.

- Mass spectrometry:

Mass spectra were acquired on a Micromass TofSpec 2E reflectron time-of-flight (TOF) mass spectrometer. 2AB-labeled desialylated or 2AB-labeled esterified glycan samples were mixed with an equal volume of freshly prepared DHB (10mg/ml in 70% acetonitrile) and loaded onto the mass spectrometer target. Routinely, 1 μl and 1 μl of glycan samples diluted 1:10 in water were subjected to analysis. Dried spots were recrystallized by adding 0.5 μl ethanol and allowed to redry. Neutral glycans were observed as $[M+Na]^+$ ions. 1 μl of peptide mixture (renin substrate, ACTH fragment 18-39, and angiotensin, 10pMole/μl, all from Sigma) which served as a three-point external calibrant for mass assignment of the ions was mixed with freshly prepared α-cyano-4-hydroxycinnamic acid (10 mg/ml in 49.5% acetonitrile; 49.5% ethanol; 0.001% TFA), loaded on the mass spectrometer target and allowed to dry. All oligosaccharides were analyzed at 20 kV with a single-stage reflectron in the positive-ion mode. Between 100 and 200 scans were averaged for each of the spectra shown.

RESULTS AND DISCUSSION

Effect of enzyme subunit assembly on the circulatory retention of PEGylated rHuAChE

To examine whether the circulatory life-time of enzyme forms which are assembled into tetramers can be extended more efficiently by PEGylation than non-assembled enzyme forms, we compared the pharmacokinetic performance of PEGylated ΔC-rHuAChE to that of native fetal bovine serum (FBS) AChE. The latter consists solely of tetramers, while the truncated rHuAChE enzyme is of monomeric nature in its entirety, as determined by sucrose gradient analysis (Fig. 9).

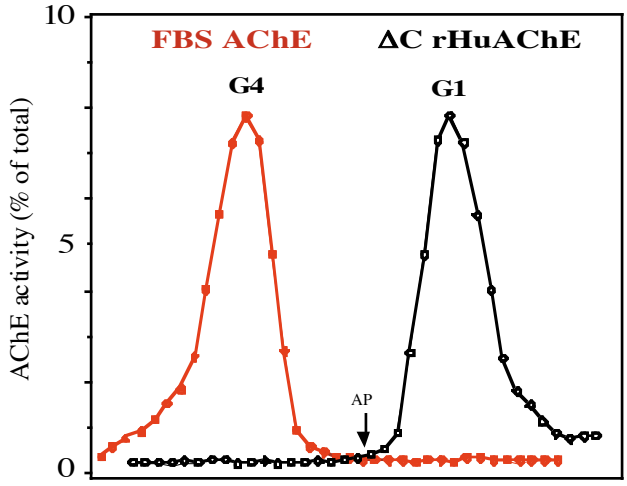

Figure 9: Sucrose-gradient sedimentation profiles of FBS-AChE and ΔC-rHuAChE. G4 indicates the sedimentation position of AChE tetramers and G1 indicates the sedimentation position of monomers. The arrow denotes the sedimentation position of the alkaline phosphatase marker (6.1 S) added to the samples.

The conjugation of PEG to FBS-AChE resulted in the generation of an enzyme form which is characterized by improved $T_{1/2}$ and MRT values (Table 3) and resides in the circulation of mice for extended periods of time (Fig. 10), allowing us to conclude that PEGylation of serum-derived AChE can improve its circulatory residence. Yet these values were essentially the same as those determined for the PEGylated monomeric ΔC-rHuAChE. Thus, although enzyme tetramerization has been shown in the past to contribute to the circulatory longevity of AChE (Kronman *et al.*, 2000; Chitlaru *et al.*, 2001), it does not provide an additional pharmacokinetic value to PEG-conjugation. We conclude therefore, that following PEG-conjugation, monomeric and tetrameric AChEs are retained in the circulation for extended periods of time in an equal manner.

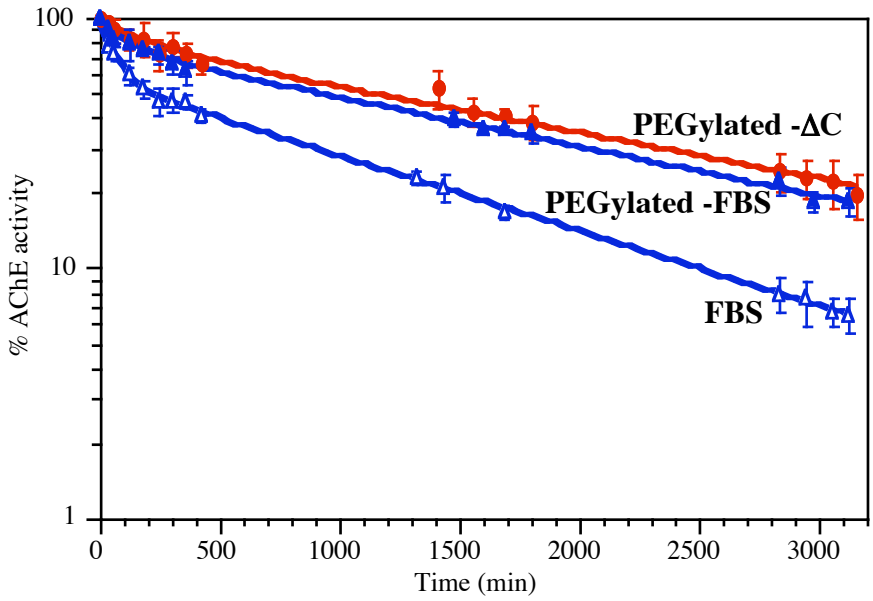

Figure 10: Pharmacokinetic profiles of non-modified and PEG-modified FBS-AChE and PEG-modified ΔC-rHuAChE. The various exogenous rHuAChEs were introduced into mice at levels that were at least 30-fold higher than background levels. Residual AChE activity was determined in blood samples removed at various time periods.

Table 3: Pharmacokinetic parameters of non-modified and PEG-modified FBS-AChE and PEG-modified ΔC-rHuAChE.

AChE type	A (%)	B (%)	$T_{1/2}\alpha$ (min)	$T_{1/2}\beta$ (min)	MRT (min)
AChE-FBS	43±2	57±2	41±5	990±67	1390
PEGylated-FBS	21±5	75±6	65±26	1535±150	2065
PEGylated -ΔC	23±4	76±3	35±15	1550±120	2100

Effect of glycan quantity and composition on the circulatory retention of PEGylated rHuAChE

Unlike the human version of AChE, which contains three appended N-glycans (Velan *et al.*, 1993), the bovine enzyme carries a fourth oligosaccharide unit at amino acid 61 (Mendelson *et al.*, 1998). The finding that the circulatory lifetime of PEGylated FBS-AChE is similar to that of the C-terminal truncated version of the human AChE, ΔC-rHuAChE, demonstrates that the presence of an additional glycan unit in the bovine enzyme does not contribute to the ability of the PEG-conjugation process to extended circulatory residence. To further examine whether HuAChE forms carrying less than 3 N-glycans are negatively affected in their ability to reside in the circulation for extended periods of time following PEGylation, we monitored the pharmacokinetic behavior of the N350Q/N464Q rHuAChE mutant. The N-glycosylation consensus sequences at positions 350 and 464 of this enzyme form have been altered by Asn-to-Gln mutations, resulting in the generation of rHuAChE containing a single N-glycan unit at position 265 (Velan *et al.*, 1993). N350Q/N464Q rHuAChE is characterized by low circulatory retention ($T_{1/2}\beta$ and MRT values = 37 and 50 mins, respectively, Table 4). PEG-conjugation of this hypoglycosylated AChE mutant resulted in a significant extension of its circulatory retention (Fig. 11 and Table 4). Most importantly, the pharmacokinetic values displayed by the hypoglycosylated enzyme did not differ substantially from those of the triglycosylated ΔC-rHuAChE, ($T_{1/2}\beta$ = 1540 and 1550 mins and MRT values = 2035 and 2100 mins, for the monoglycosylated and triglycosylated enzyme forms, respectively). Taken together, these results demonstrate that even low levels of enzyme glycosylation suffice for efficient circulatory lifetime extension of AChE, provided the enzyme is efficiently PEGylated.

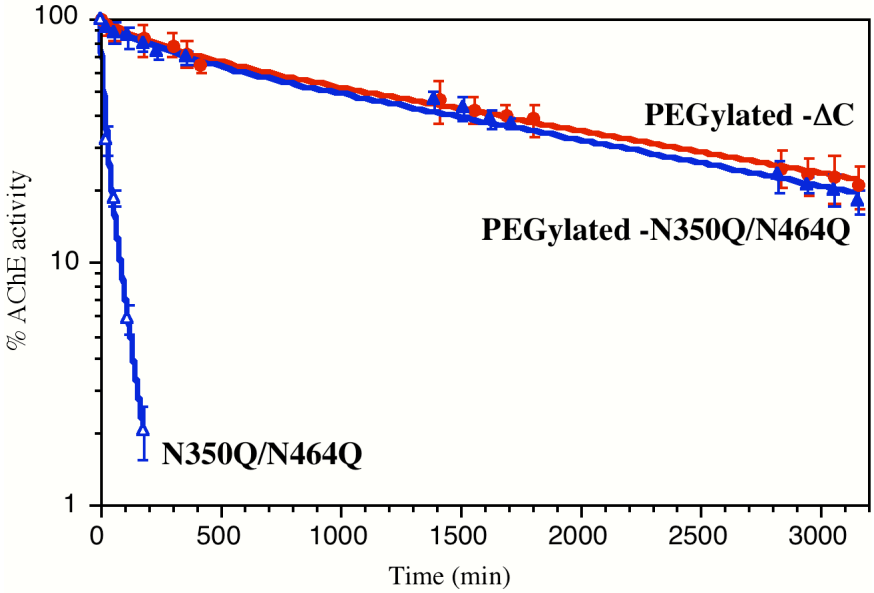

Figure 11: Pharmacokinetic profiles of non-modified and PEG-modified monoglycosylated N350Q/N464Q rHuAChE and PEG-modified ΔC-rHuAChE. The experiments were performed as detailed in the legend to Fig. 10.

Table 4: Pharmacokinetic parameters of non-modified and PEG-modified monoglycosylated N350Q/N464Q rHuAChE and PEG-modified ΔC-rHuAChE.

AChE type	A (%)	B (%)	$T_{1/2}\alpha$ (min)	$T_{1/2}\beta$ (min)	MRT (min)
AChE- N350Q/N464Q	43±6	57±5	3.5±1	37±3	50
PEGylated- N350Q/N464Q	21±6	79±5	25±13	1540±110	2035
PEGylated -ΔC	23±4	76±3	35±15	1550±120	2100

Examination of the basic glycan forms appended to the hypoglycosylated N350Q/N464Q rHuAChE by MALDI-TOF analysis, displayed that this enzyme form differs from wild-type HuAChE not only in its glycan quantity, but also in the actual glycan structures, which it contains (Fig. 12). While the wild-type enzyme carries an array of oligosaccharides consisting only of complex-type glycan forms, the monoglycosylated rHuAChE mutant contains glycans of both complex and high-mannose type. The high-mannose glycans form a series, which differ one from another in the number of mannose residues per glycan unit,

ranging from 5 mannose/glycan (MW = 1377.8 Da) to 9 mannose/glycan (MW = 2025.8 Da), and those containing 5 to 7 mannose units appear in both non-acetylated and acetylated versions (Fig. 12, upper panel). In addition, the monoglycosylated rHuAChE displays (Fig. 12, upper panel) unique complex-type N-glycans, which were not detected in the wild-type enzyme or in other rHuAChE or rBoAChE forms examined previously (Kronman *et al*., 2000; Chitlaru *et al.,* 2001, 2002). These include glycan structures that carry 2 GalNac (MW = 2011.0 Da) or 2 fucose (MW = 2117.8 Da) moieties. It therefore appears that the severe reduction in the number of appended N-glycans causes the hypoglycosylated rHuAChE to undergo a different pattern of oligosaccharide processing within the cells. The finding that PEGylation of the hypoglycosylated rHuAChE leads to the generation of an enzyme form which is retained for periods of time in a manner similar to that of ΔC-rHuAChE, confirms that PEG appendage can not only efficiently extend the circulatory residence of enzyme forms which carry significantly lower amounts of appended glycans, but that PEGylation can also extend the circulatory life-time of enzyme forms displaying altered glycan structures.

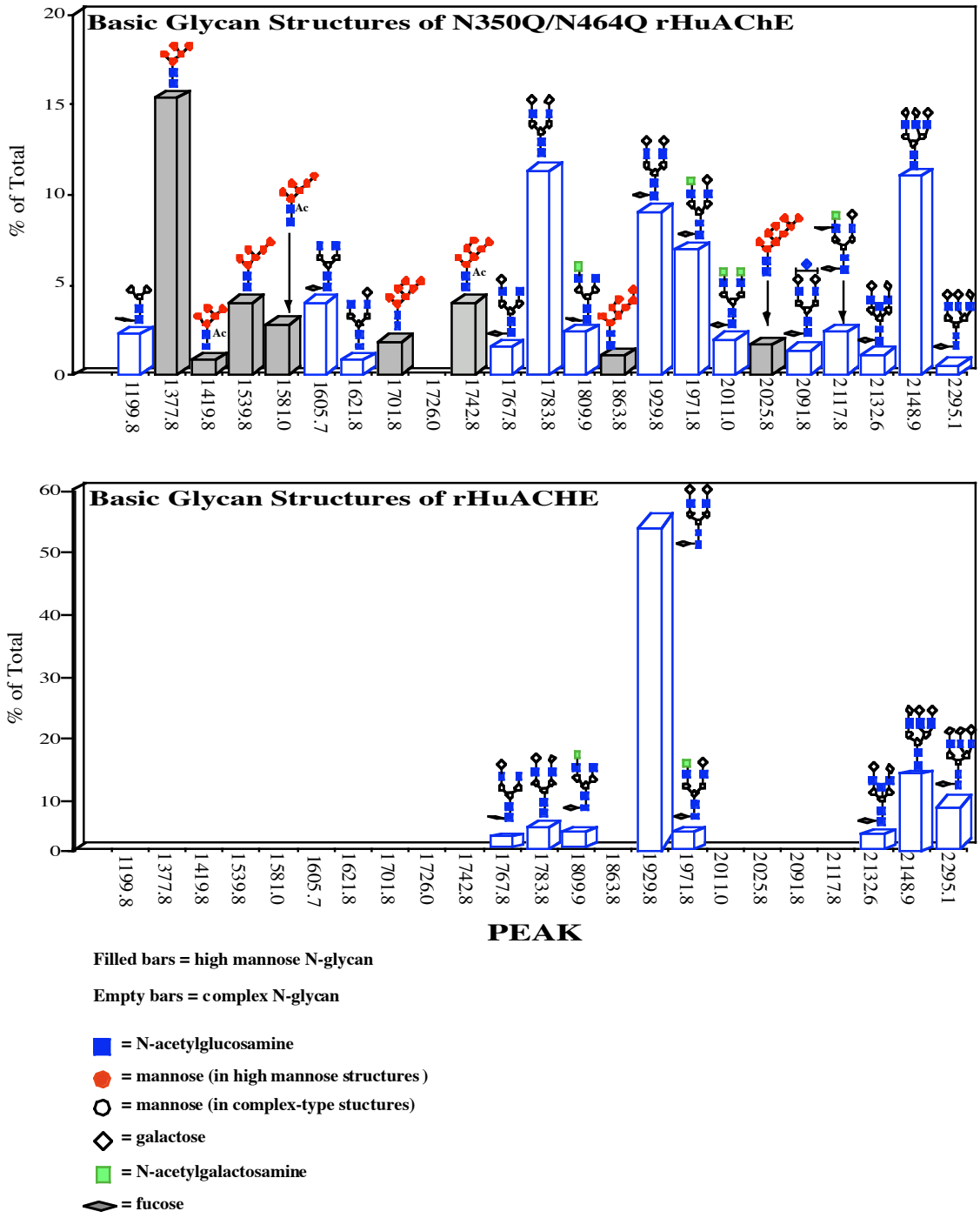

Figure 12: The basic structures and relative abundances of desialylated N-glycans released from monoglycosylated N350Q/N464Q rHuAChE and from wild-type rHuAChE. Purified N-glycans released from the two enzyme forms were subjected to sialidase treatment and 2-AB labeling before MALDI-TOF analysis. Molecular masses and schematic structures are shown for the various glycan forms. Molecular weights represent monoisotopic masses of the respective $[M+Na]^+$ ions of the glycan species.

Effect of glycan sialylation on the circulatory retention of PEGylated rHuAChE

Since our previous studies have shown that circulatory longevity of AChE is influenced mainly by the level of sialic acid capping of the glycans (Kronman *et al.*, 2000; Chitlaru *et al.*, 2001) rather than by their basic structures, we extended these studies to examine whether differences in sialic acid occupancy affect the ability to prolong circulatory retention by PEGylation of AChE. This was achieved by using three different preparations of the C-terminal truncated ΔC-rHuAChE: (1) Partially sialylated enzyme produced in non-modified HEK-293 cells; (2) Fully sialylated ΔC-rHuAChE produced in the genetically modified 2D6ST cell line, which coexpress high levels of α-2,6 sialyltransferase (Chitlaru *et al.*, 1998, 2001), and (3) Desialylated ΔC-rHuAChE, generated by subjecting the rHuAChE to sialidase treatment. All three enzyme forms were PEGylated and subjected to pharmacokinetic studies in mice. As shown in Fig. 13, desialylated, partially sialylated and fully sialylated ΔC-rHuAChEs which exhibit mean residence time (MRT) values of 4, 42 and 163 minutes, respectively, are all characterized by MRTs of approximately 2000 minutes following PEGylation. Thus, the ability to confer extended circulatory longevity to ΔC-rHuAChE by PEG conjugation is not affected by differences in levels of sialic acid capping.

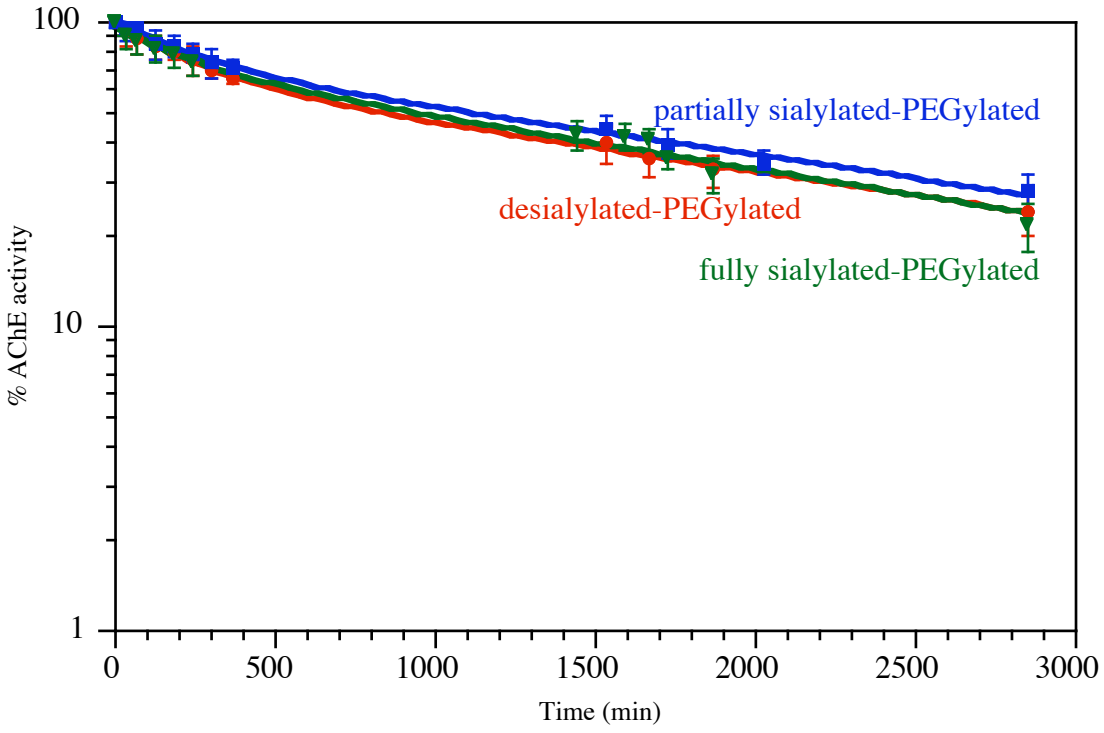

Figure 13: Pharmacokinetic profiles of PEG-modified ΔC-rHuAChE containing different levels of sialic acid. The PEGylated rHuAChEs were introduced into mice at levels that were at least 30-fold higher than background. Residual AChE activity was determined in blood samples removed at various time periods.

Pharmacokinetic performance of PEGylated rHuAChE devoid of glycans

Since even low levels of enzyme glycosylation suffice for efficient circulatory lifetime extension of AChE by PEGylation, as manifested by the finding that PEG-conjugation of the AChE mutant carrying a single N-glycan unit at amino acid 265 resulted in a significant extension of its circulatory retention, we asked whether a minimal level of glycosylation is required at all for extension of circulatory residence by PEG conjugation. To answer this question we set out to monitor the pharmacokinetic performance of PEGylated deglycosylated-AChE. Since the efficient removal of N-glycans normally requires the full denaturation of the substrate protein prior to glycan removal, this method of generation of AChE totally devoid of glycans is not suitable for the monitoring of the residual enzymatic activity of the enzyme in the bloodstream of the administered mice. We therefore performed the enzymatic removal of AChE glycans under a different set of conditions, to allow glycan removal from enzyme preparations in their native conformation. This was achieved by incubating the hypoglycosylated N350Q/N464Q AChE in the presence of highly concentrated N-glycanase at room temperature for 48 hours, without prior heat denaturation.

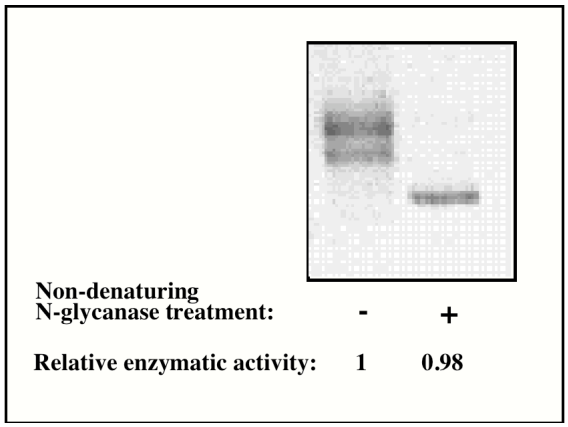

Figure 14: SDS-PAGE analysis of ΔC-HuAChE before and after non-denaturing N-glycan treatment. N-glycans were enzymatically removed from ΔC-rHuAChE as described in the text. Relative enzymatic activities before and after N-glycan removal are indicated.

This procedure resulted in the generation of AChE in which enzymatic activity is fully preserved, while SDS-PAGE analysis demonstrated that the N-glycanase-treated enzyme appears as a single faster-migrating band, attesting to the fact that glycans were indeed efficiently removed from the non-denatured enzyme (Fig. 14). This deglycosylated AChE was subjected to PEG-conjugation, and the chemically modified enzyme was administered to mice to evaluate its pharmacokinetic performance (Fig. 15). As in the case of glycan-bearing

enzyme species, the circulatory retention of the deglycosylated AChE was significantly extended by PEG appendage, displaying a mean residence time (MRT) value of 1910±75 mins. This value, is very similar to that observed for the wild-type triglycosylated AChE (MRT = 2100 mins.) Thus, the ability to extend the circulatory residence time of HuAChE by PEG, is not dependent on the presence of N-glycans, and can be effectively carried out using AChE, which is totally devoid of oligosaccharide appendages.

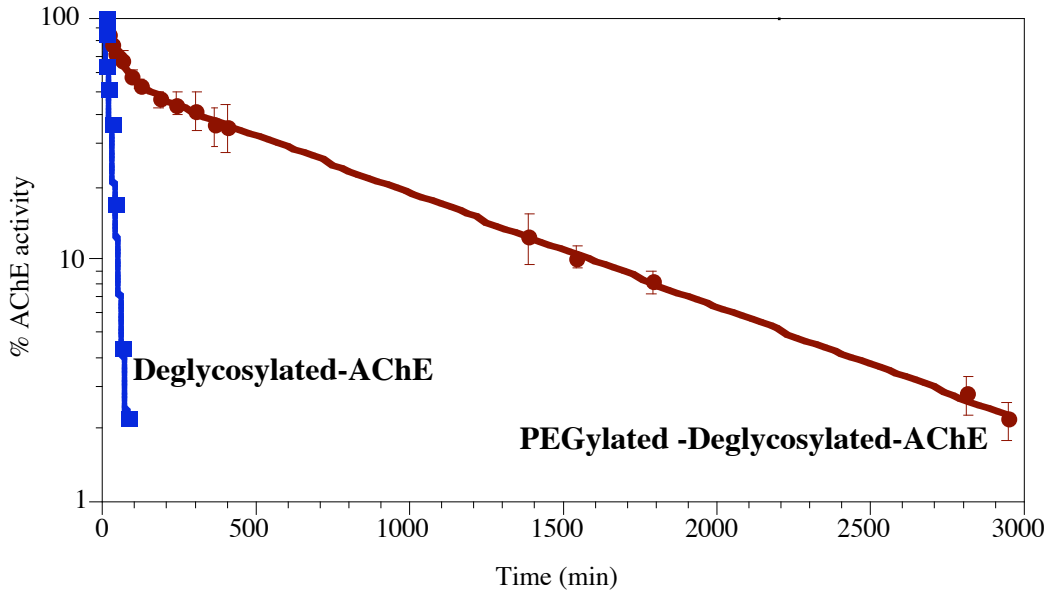

Figure 15: Pharmacokinetic profiles of non-modified and PEG-modified ΔC-rHuAChE devoid of N-glycans. N-glycans were enzymatically removed from ΔC-rHuAChE as described in the text. The non-modified and PEGylated deglycosylated rHuAChEs were introduced into mice at levels that were at least 30-fold higher than background. Residual AChE activity was determined in blood samples removed at various time periods.

Taken together, this series of experiments leads to the conclusion that various post-translational modification-related characteristics of AChE such as its state of assembly, alterations in N-glycosylation levels or even their total absence, as well as variations in the basic structure and terminal capping of the appended glycans, do not affect the ability of the enzyme to undergo PEGylation in a manner which will allow it to reside in the circulation for extended periods of time. These findings are in line with the idea that protein PEGylation enhances circulatory longevity by forming a shielding cloud around the modified protein which thereby prevents access to receptors involved in protein clearance, and by increasing the overall molecular size of the modified protein and thus which preventing or decreasing its

glomerular filtration (Monfardini and Veronese, 1998). These studies point towards the potential ability to utilize recombinant human AChE produced in bacterial production systems, and therefore lack all eukaryotic-related post translation modifications, as a cost-effective source for large-scale amounts of enzyme which can be thereby be efficiently PEGylated to generate circulatory long-lived enzyme species for therapeutic use.

IV. GENERATION OF HYPOLYSINE MUTANTS OF rHuAChE AS SUBSTRATES FOR PEGYLATION

INTRODUCTION

The conversion of AChE into PEG-modified long-lived molecules that can serve as effective therapeutic bioscavengers requires that the chemically modified product: (i) reside in the circulation for sufficiently-long periods of time, (ii) retain its biological activity and, (iii) exhibit maximal homogeneity. The amount of appended PEG moieties may crucially affect each of the three requirements mentioned above: while increasing the PEG load of AChE may positively contribute to long-term circulatory residence, the enhanced pharmacokinetic performance of the enzyme may be associated with a concomitant loss in biological activity and/or may display increased heterogeneity.

Previous studies carried out in our laboratory demonstrated that under various sets of conditions, different amounts of PEG moieties can be appended to rHuAChE. This study led to the generation of an array of PEGylated AChEs that differed one from another by their degree of modification. Subjecting the differently PEGylated AChEs to pharmacokinetic studies allowed us to determine that the circulatory residence time values of the various enzyme forms is linearly correlated with the number of appended PEGs. PEGylated AChE containing an average of 4 to 5 PEG moieties per enzyme, displayed maximal pharmacokinetic performance, while retaining full catalytic activity (Cohen *et al.*, 2001). However, examination of the enzyme product revealed that it comprised a mixture of 3 major products, differing one from another in their PEG contents. Further attempts to increase the number of appended PEG units or to achieve uniform PEGylation under stringent conditions which favor highly effective PEG appendage, resulted in the generation of enzyme forms displaying severely reduced catalytic activity.

The generation of PEGylated AChE arrays displaying different characteristics in terms of pharmacokinetics, enzymatic activity and homogeneity may be achieved not only by altering reaction conditions, but also by reducing or increasing the number of lysine target residues in AChE. High levels of PEGylation may be achieved even under mild reaction conditions, if lysine target residues are added to the enzyme. On the other hand, the elimination of some lysine residues to prevent their appendage to PEG may be required to generate uniformly modified enzyme forms which retains full catalytic activity following PEGylation under stringent conditions which would otherwise reduce catalytic activity. For instance,

PEGylation of the lysine at position 348 of human AChE, which is located at the entrance to the gorge leading to the catalytic site of the enzyme, may prove to sterically hinder the diffusion of substrate to the active center, and therefore should be eliminated. However, elimination of selected lysine residues should be restricted to those that are not required for catalytic activity, nor play a role in the reactivity of the enzyme towards organophosphates. One should also keep in mind that one or more of the lysine residues may be crucial for maintaining the native enzyme architecture, as has been proven in the past for selected residues (Shafferman *et al*., 1992a). For example, localization of the lysine residues within the 3D model of rHuAChE demonstrates that some of these lysines are located within well-defined conformational structures such as α-helices, raising the question whether their replacement might negatively influence the conformational integrity of the enzyme. These various considerations suggest that a wide spectrum of PEGylated lysine-modulated AChE forms need to be examined empirically to determine the optimal AChE configuration in terms of biological activity and pharmacokinetic performance. Such studies should include examination of the relationship between the number of available lysines and the pharmacokinetic performance of the PEGylated enzyme product. Another point of consideration should take into account that the various lysines display an unequal distribution at the enzyme surface. Lysine elimination should therefore be designed not only in terms of the number of sites remaining for PEG appendage, but also should take into account the spatial location of the various lysine moieties, to avoid the generation of enzyme-surface exposed regions that are not protected by nearby PEGylated lysine residues.

In this section, we summarize the work carried out in our laboratory to determine the effect of lysine reduction on the enzymatic performance, thermostability and pharmacokinetic properties of PEGylated and non-PEGylated rHuAChEs.

METHODS

Cell culture techniques, enzyme production and purification of rAChEs

HEK-293 cell lines stably expressing high levels of ΔC-rHuAChE, C580A-rHuAChE and various hypolysine mutants rHuAChE, and rBoAChE were generated as described previously (Kronman *et al*., 2000; Chitlaru *et al*., 2001). The method for purification of the secreted rHuAChE enzymes was described previously (Kronman *et al*., 1995).

Generation of rHuAChE mutants

The generation of the C580A rHuAChE and the C-terminal tail deleted version of rHuAChE, ΔC-rHuAChE, were described previously (Velan *et al.*, 1991; Kryger *et al*., 2000). To generate the various hypolysine recombinant human AChEs, the human ΔC-AChE gene cloned in the prHuAChE-nc vector (Velan *et al*., 1991; Kronman *et al*., 1992) was subjected to site-directed mutagenesis to replace one, or in some cases two lysine codons with alanine codons using the QuikChange site-directed mutagenesis kit (Stratagene, USA). Additional rHuAChE mutants in whom two or three lysine residues were replaced were generated by exchanging relevant fragments between the various single and double lysine mutants. All mutant rHuAChEs were verified by DNA sequencing (ABI prism rhodamine kit using the ABI310 Genetic Analyzer, Applied Biosystems).

Enzyme activity, specific activity and thermostability

AChE activities of purified AChE preparations were measured according to Ellman *et al*. (1961). Assays were performed in the presence of 0.5 mM acetylthiocholine, 50 mM sodium phosphate buffer pH 8.0, 0.1 mg/ml BSA and 0.3 mM 5,5'-dithiobis-(2-nitrobenzoic acid). The assay was carried out at 27^0C and monitored by a Thermomax microplate reader (Molecular Devices). The various hypolysine AChE protein products were quantitified by ELISA, and the specific activity of each mutant product was calculated by dividing the enzymatic activity to protein quantity. The various hypolysine mutants were examined for thermal stability by incubating the mutated AChEs at 51^0C for various periods of time followed by measurement of residual enzymatic activity. The thermal decay curve of each of the mutant AChE forms was profiled and half-life time values were determined.

Conjugation of polyethylene glycol to AChE

Attachment of PEG chains to primary amines in the various rHuAChEs was performed using succinimidyl propionate activated methoxy PEG (SPA-PEG; Shearwater polymers, Inc.), as

described previously (Cohen *et al.*, 2001). Briefly, purified rHuAChE or rRhAChE (5mM) were incubated with PEG-20000 at a ratio of 50:1 $[PEG]_0/[AChE\ primary\ amines]_0$ in 50mM phosphate buffer pH 8.0 for 2 hours at room temperature. The chemically modified products were dialyzed extensively against phosphate buffer saline (PBS) and analyzed on 6% SDS-PAGE gels.

Clearance experiments and analysis of pharmacokinetic profiles in mice

Male outbred ICR mice (Charles River Laboratories, UK) were maintained at 20-22^{0}C and relative humidity of 50±10% on a 12-hr light-dark cycle, fed with commercial rodent chow (Koffolk, Inc., Tel-Aviv, Israel) and provided with tap water *ad libitum*. Treatment of animals was in accordance with regulations outlined in the USDA Animal Welfare Act and the conditions specified in *The Guide for Care and Use of Laboratory Animals* (National Institute of Health, 1996). All pharmacokinetic studies were approved by the local ethical committee on animal experiments.

Clearance experiments (3 to 6 mice per enzyme sample) were carried out essentially as described previously (Kronman *et al.*, 1995). Mice were injected i.v. with the various rHuAChE preparations (100 units/mouse in 0.2 ml PBS). Residual AChE activity in blood samples was measured and all values were corrected for background hydrolytic activity in the blood (using samples withdrawn 1 hour before performing the experiment). AChE activity values in samples removed 1 minute after injection were assigned a value of 100% and used for calculation of residual activity. Background cholinesterase levels in blood of pre-administered mice were less than 2 units/ml.

The clearance patterns of the various enzyme preparations were usually biphasic and fitted to a bi-exponential elimination pharmacokinetic model ($C_t=Ae^{-k\alpha t}+Be^{-k\beta t}$) as described previously (Kronman *et al.*, 2000, Chitlaru *et al.*, 2001). This model enables determination of the parameters A and B which represent the fractions of the material removed from the circulation in the first-fast and second-slow elimination phases respectively, and $T_{1/2}\alpha$ and $T_{1/2}\beta$ which represent the circulatory half-life values of the enzyme in the fast and slow phases. The pharmacokinetic parameter MRT (mean residence time, which reflects the average length of time the administered molecules are retained in the organism) was independently obtained by analyzing the clearance data according to a noncompartmental pharmacokinetic model using the WinNonlin computer program (Laub and Gallo, 1996).

RESULTS

Effect of removal of the C-terminal tail lysine residues on the circulatory retention of PEGylated rHuAChE

To determine whether the pharmacokinetic performance of PEGylated rHuAChE is affected by the number of sites available for PEG-appendage, we compared as a first step, the pharmacokinetic profiles of PEGylated mutated rHuAChE species in which either cysteine 580 was substituted by alanine (C580A, Velan *et al.*, 1991), or the C-terminal portion of the enzyme corresponding to amino-acids 544 to 583 was deleted (ΔC-rHuAChE, Kryger *et al.*, 2000). Both of these enzyme forms are impaired in their ability to form dimers due to the absence of cysteine 580, involved in interchain disulphide bonding. The two monomeric AChE forms differ however one from another in the number of lysine residues available for PEG conjugation. While the C580A AChE carries 10 lysines, the ΔC-rHuAChE C-terminus-truncated enzyme contains only 7 (Fig. 16).

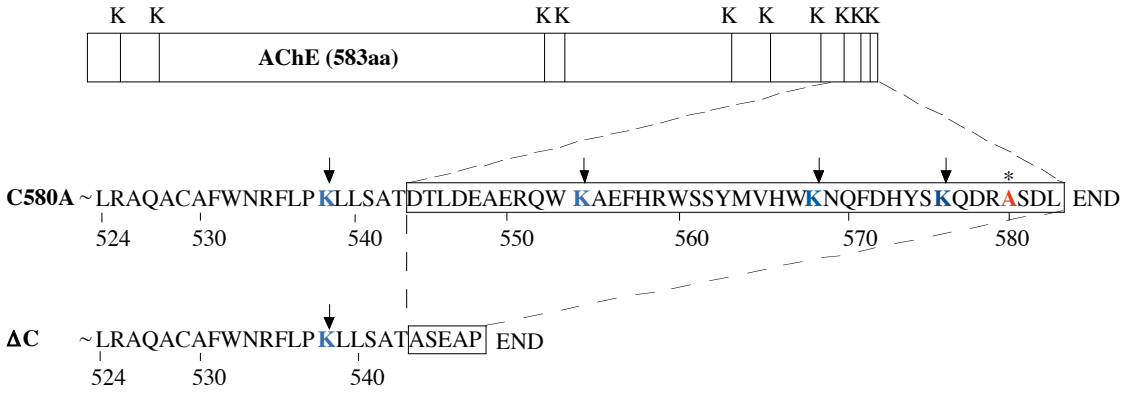

Figure 16: Schematic representation of the distribution of lysine residues along the HuAChE sequence and the C-terminal sequence of the C580A and ΔC-rHuAChE forms. Lysine residues are marked by arrows. The C580A mutation is marked by asterisk.

The two enzyme forms were conjugated to PEG (approx. MW =20,000) using succinimidyl-propionate-activated PEG, which specifically targets the PEG moieties to lysine residues. The chemically modified preparations were administered to mice, residual AChE activity was monitored in blood samples removed at various periods of time, and the elimination curves of the two enzyme forms were plotted (Fig. 17).

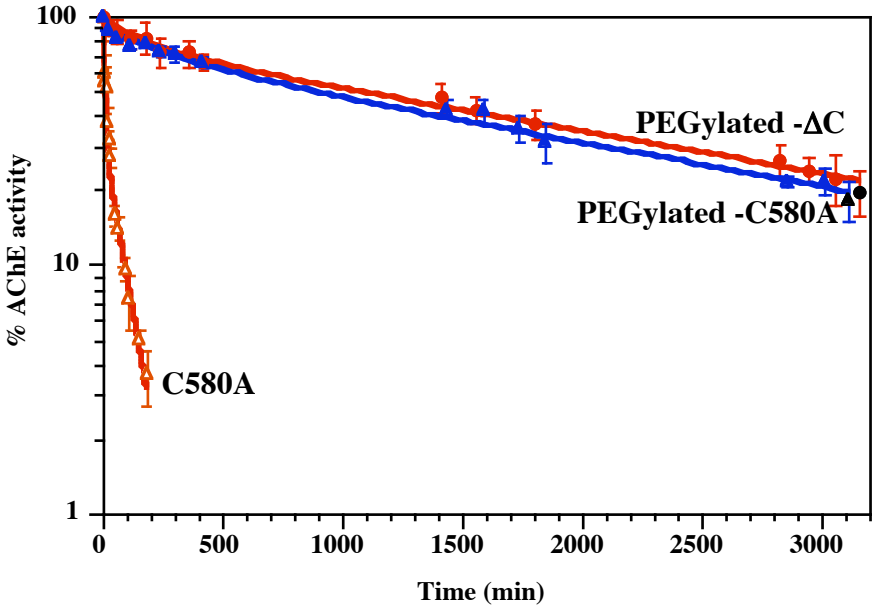

Figure 17: Pharmacokinetic profiles of non-modified and PEG-modified C580A rHuAChE and PEG-modified ΔC-rHuAChE. The experiments were performed as detailed in the Methods section.

Table 5: Pharmacokinetic parameters of non-modified and PEG-modified C580A rHuAChE and PEG-modified ΔC-rHuAChE.

AChE type	A (%)	B (%)	$T_{1/2}\alpha$ (min)	$T_{1/2}\beta$ (min)	MRT (min)
AChE-C580A	65±3	35±2	4±1	50±8	73
PEGylated-C580A	19±5	75±7	55±16	1590±150	2085
PEGylated -ΔC	23±4	76±3	35±15	1550±120	2100

The two PEGylated rHuAChEs, C580A and ΔC- rHuAChE, displayed nearly identical pharmacokinetic profiles, characterized by very similar half-life and mean residence time values (Table 5). These findings demonstrate that the variance in number of accessible lysines in the two enzyme preparations (10 versus 7 for the C580A and ΔC- rHuAChEs, respectively) does not affect the ability of the enzyme to undergo efficient PEGylation.

Generation and characterization of hypolysine mutant rHuAChEs

The apparent insensitivity to lysine number noted above, may simply reflect the fact that in both of the enzyme species under examination, the lysine contents exceeds the maximal amount required for optimal circulatory retention, and that enzyme species characterized by lower lysine contents may display differential circulatory longevity following PEGylation. As a first step towards the evaluation of the effect of lower lysine contents on AChE pharmacokinetics, we generated by site-directed mutagenesis a series of different hypolysine AChE expression vectors. Each of the seven constructs (K23A, K53A, K332A, K348A, K470A, K496A, K538A), code for C-terminal truncated AChE in which a single lysine residue is replaced by alanine. These constructs were introduced into HEK-293 cells, and stable pools of each of these seven AChE mutants were generated. Protein quantities of the various hypolysine AChEs were determined by ELISA and their specific activities were calculated. In all cases, the specific activity of the hypolysine mutants did not deviate in a significant manner from that of the wild type enzyme (6.5 U/μg, see Figure 18); at most, a ~3-fold decrease or increase in specific activities as compared to the wild type enzyme were observed. Taken together, these results indicate that the removal of any of the individual lysine residues does not alter the kinetic performance of the enzyme. Based solely on this criterion, any of the lysine residues may be eliminated to generate modified AChE for PEGylation, yet pertinent differences in the functional roles of the different lysine residues that were not detected by determining their specific activities, may yet be revealed by subjecting the various hypolysine forms to other examinations. To this end, the various hypolysine mutants were examined for thermal stability, to determine whether some of the lysines play a greater role in maintenance of the functional integrity of the enzyme, and thereby should not be replaced. This was achieved by incubating the monolysine mutated AChEs at 51^0C for various periods of time followed by measurement of residual enzymatic activity. The thermal decay curve of each of the mutant AChE forms was profiled and half-life time values were determined. Nearly all of the hypolysine forms displayed thermal decay values, which did not differ significantly from that of the wild-type enzyme ($T_{1/2}51^0C$ = 8.9 min.). Only one of the hypolysine AChE forms (K470A) exhibited a greater than 5-fold reduction in thermostability as compared to the wild-type enzyme (Figure 18).

AChE type	Specific activity (U/μg)	$T_{1/2}$ at 51^{0}C (min.)
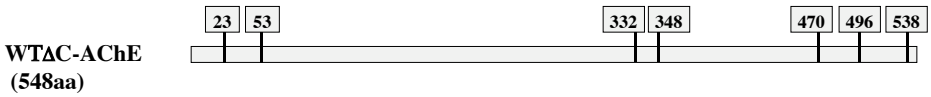 WTΔC-AChE (548aa)	6.5	8.9
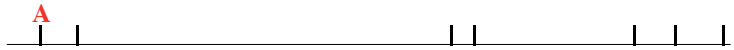 ΔC-K23A	12.0	10.2
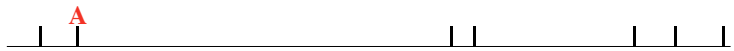 ΔC-K53A	4.1	8.4
 ΔC-K332A	4.5	3.1
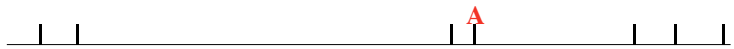 ΔC-K348A	2.2	4.6
 ΔC-K470A	6.3	1.5
 ΔC-K496A	20.0	8.9
 ΔC-K538A	5.7	4.6
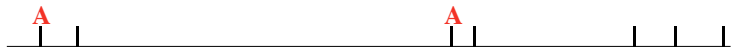 ΔC-K23A/K332A	10.8	3.3
 ΔC-K23A/K348A	4.0	4.9
 ΔC-K332A/K348A	2.5	3.0
 ΔC-K470A/K496A	12.7	1.3
 ΔC-K23A/K332A /K348A	2.5	2.6

Figure 18: **Specific activity and thermostability values of WT and hypolysine ΔC-AChEs.** Framed numbers (upper line) designate positions of lysine residues in wild-type ΔC-AChE.

The finding that replacement of single lysine residues did not significantly alter the catalytic performance or thermostability of the enzyme, suggests that any of the various lysines may be replaced to generate hypolysine enzyme for controlled PEGylation. Preparation of homogenous PEGylated AChE, however, requires the generation of enzyme forms carrying multiple lysine replacements. As an intermediate step towards the generation of an array of such multilysine mutant AChEs, we generated several AChE forms, in which two lysine residues were replaced by alanine. These were introduced into HEK-293 cells and enzyme secreted from stable cells was characterized (Figure 18). As in the case of the single lysine

replacements, the specific activities of the various double lysine mutants did not deviate significantly from that of the wild-type enzyme; at most, a 2.5-fold an increase or decrease in specific activities as compared to of the wild-type enzyme was observed. Examination of the various double lysine mutants for thermal stability allowed us to determine the thermal decay values of the various hypolysine mutants. Only enzyme forms which contained the K470A mutation exhibited a greater than 5-fold reduction in thermostability as compared to the wild-type enzyme.

Biochemical and pharmacokinetic characterization of tetralysine mutant rHuAChE before and after PEG conjugation

Based on these findings we decided to generate different multilysine AChE mutants in which three lysine residues are replaced by alanine. As a first step, the mutant K23A/K332A/K348A AChE gene was constructed. This multilysine AChE mutant (containing 4 lysine residues at positions 53, 470, 496 and 538) was introduced into HEK-293 cells, produced at-large-scale and purified. Measurement of the AChE activity of this multilysine enzyme mutant allowed us to determine that its specific activity did not deviate in a significant manner for that of the wild type enzyme. Likewise, examination of the K23A/K332A/K348A multilysine mutant for thermal stability allowed us to determine that its thermal decay compared to that of the wild-type enzyme.

To further evaluate the properties of this multilysine mutant AChE form, we monitored its pharmacokinetic behavior before PEG-conjugation. To this end, 100 units of highly purified K23A/K332A/K348A AChE were administered to three mice and residual AChE activity in blood samples removed at various time points, was determined. Determination of the clearance profile of the triple-lysine mutated enzyme (Fig. 19), demonstrated that this enzyme form is removed from the circulation at a rate which is similar to that demonstrated by the wild-type enzyme (mean residence time value of K23A/K332A/K348A AChE = 53±7 minutes; mean residence time value of the wild type enzyme = 46±4 minutes). Thus, substitution of these three lysine residues did not compromise the pharmacokinetic performance of the AChE enzyme, and therefore this hypolysine HuAChE enzyme form may serve as the template for the generation of an optimized AChE-based bioscavenger.

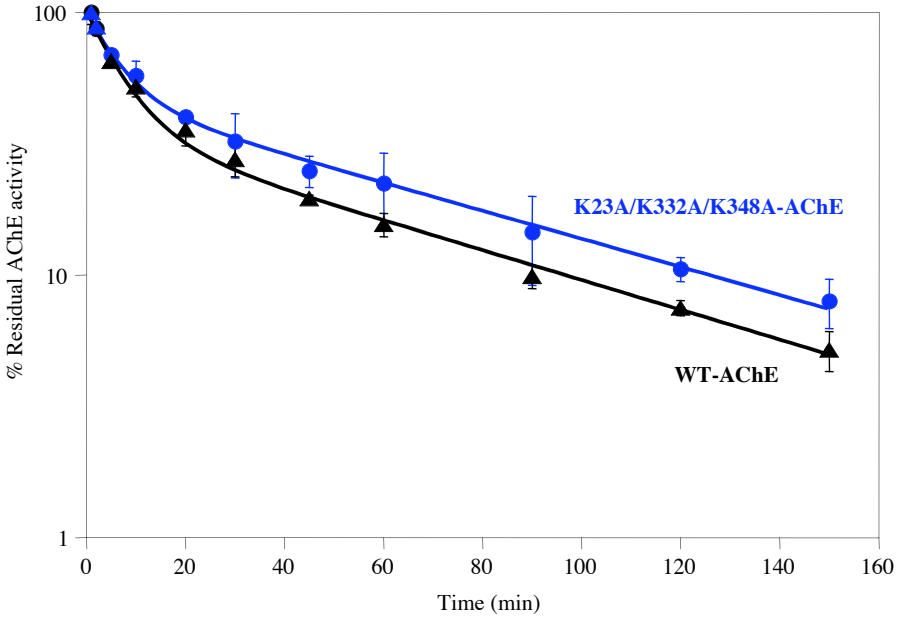

Figure 19: **Pharmacokinetic profile of the K23A/K332A/K348A ΔC-AChE enzyme form.** The wild-type ΔC-AChE and the K23A/K332A/K348A mutant proteins were introduced into mice at levels that were at least 30-fold higher than background levels. Residual AChE activity was determined in blood samples removed at various time periods.

The K23A/K332A/K348A hypolysine enzyme form was then subjected to PEG-conjugation, and tested for enzymatic activity conservation, homogeneity and thermostability. Analysis of the enzyme product following PEGylation on SDS-PAGE (Fig. 20) revealed the presence of a single protein band, which corresponds to AChE carrying 5 PEG chains. This observation implies that the PEG target sites of the tetralysine AChE (4 remaining lysines, and the C-terminus of the protein) are fully occupied. Most importantly, under the set of conditions chosen for carrying out the PEGylation process, loss of enzymatic activity was very low (<10%).

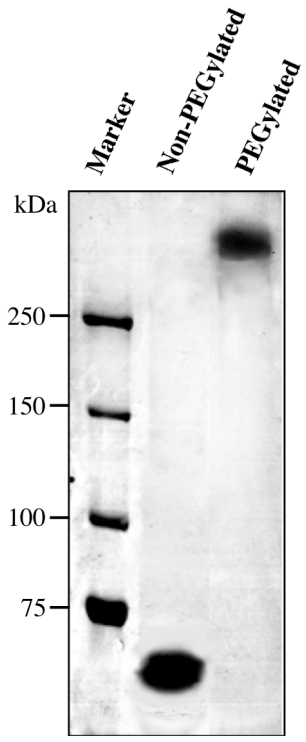

Figure 20: SDS-PAGE analysis of PEGylated and non-PEGylated tetralysine human AChE. PEGylated and non-PEGylated K23A/K332A/K348A hypolysine AChE (40 μg/lane) were resolved on 6% SDS-polyacrylamide gels and stained with Coomassie blue.

Examination of the stability of PEGylated tetralysine AChE was conducted by incubating this enzyme at 51^0C for various periods of time followed by measurement of residual enzymatic activity. The thermal decay curve of each of the mutant AChE forms was profiled and half-life time values were determined (Fig. 21). This analysis allowed us to determine that PEGylation of the tetralysine AChE results in increased thermostability, the $T_{1/2}$ values for the PEGylated and non-PEGylated enzyme forms being 6.7 and 2.6 minutes, respectively.
Taken together, this line of studies allowed us to determine that the tetralysine AChE enzyme form can be fully PEGylated, and yield a homogeneous enzyme product while fully conserving its enzymatic activity.

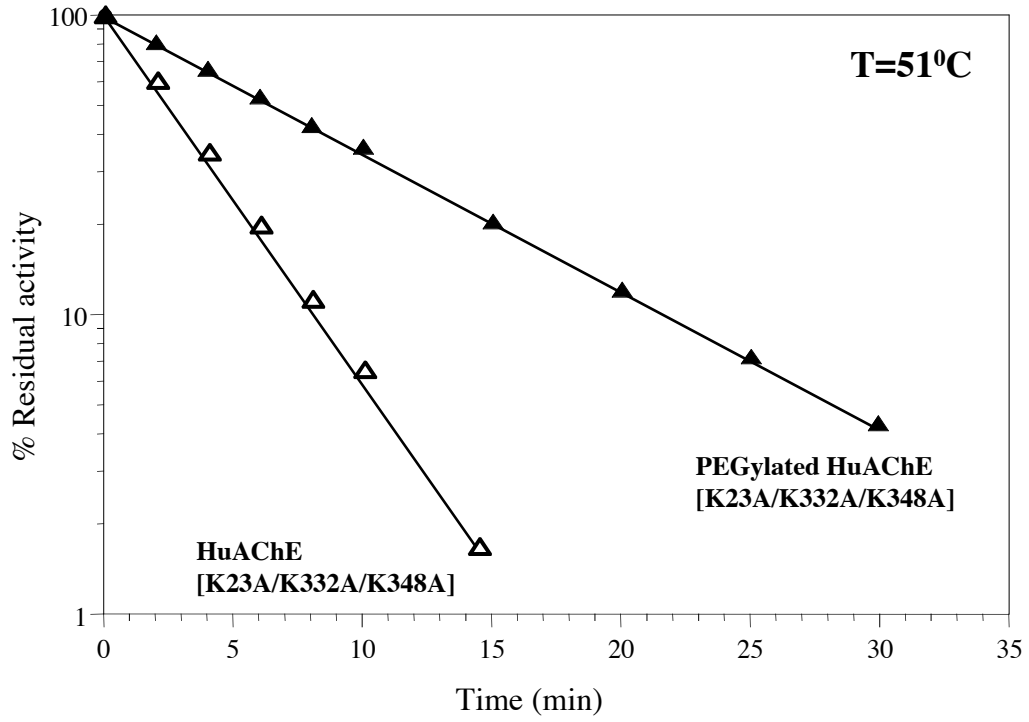

Figure 21: **Thermostability profiles of PEGylated and non-PEGylated wild type and tetralysine human AChEs.** Wild-type and K23A/K332A/K348A hypolysine AChEs before or after PEGylation were incubated at 51^0C and residual AChE activity was determined in samples withdrawn at the indicated time points.

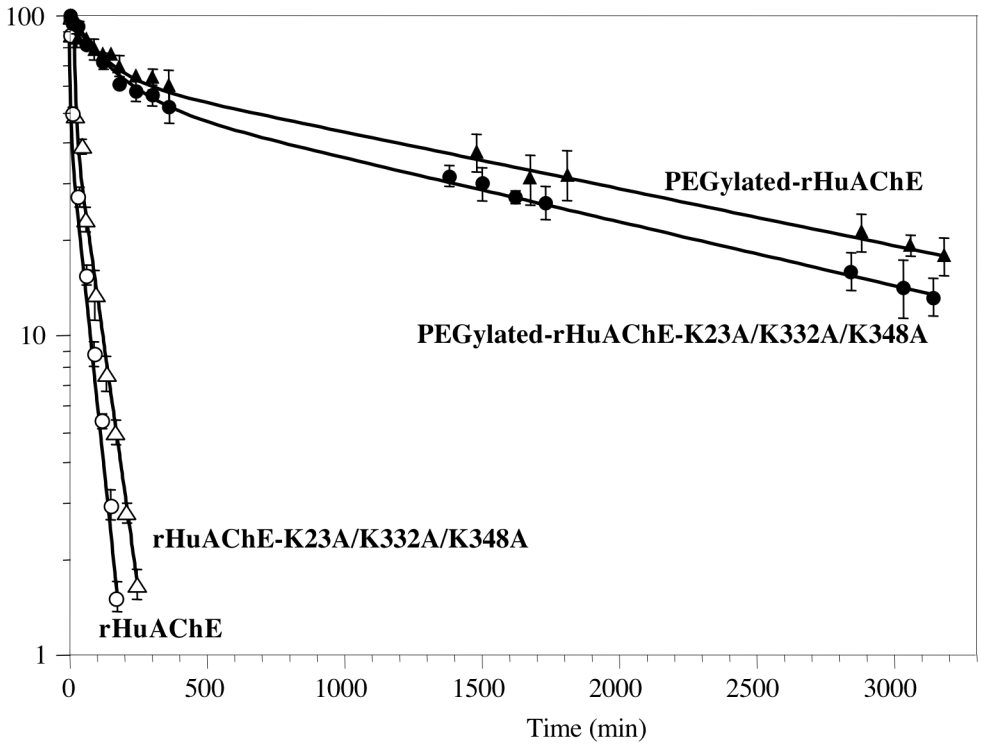

Figure 22: **Pharmacokinetic profile of the PEGylated K23A/K332A/K348A-HuAChE enzyme form.** The wild-type rHuAChE and the K23A/K332A/K348A mutant proteins and their PEGylated forms were introduced into mice at levels that were at least 30-fold higher than background levels. Residual AChE activity was determined in blood samples removed at various time periods.

PEGylated K23A/K332A/K348A AChE was examined for its pharmacokinetic performance, to determine whether it resides in the circulation for extended periods of time. To this end, 100 units of the PEGylated-hypolysine AChE mutant, PEGylated-rHuAChE and the corresponding non-PEGylated HuAChEs were administered to mice (three mice for each enzyme form), blood samples were removed at various time points, and residual AChE activity was determined. Determination of the clearance profile of the PEGylated triple-lysine mutated enzyme (Fig. 22), demonstrated that this enzyme form is removed from the circulation at a rate which is similar to that demonstrated by the PEGylated wild-type enzyme, which is loaded with an average of 4-5 PEGs per AChE subunit (Cohen *et al*., 2001) - the mean residence time value of PEGylated K23A/K332A/K348A AChE is 1795 minutes, while the mean residence time value of the PEGylated wild type enzyme is about 2000 minutes. Thus, substitution of these three lysine residues did not compromise the ability to significantly improve the pharmacokinetic performance of rHuAChE enzyme by PEGylation. Altogether, the biochemical and the pharmacological studies of the K23A/K332A/K348A hypolysine HuAChE, suggest that the PEGylated form of this enzyme may serve as the template for the generation of an optimized AChE-based bioscavenger. Further studies are required to determine whether hypolysine AChE forms displaying lesser amounts of PEGylation target sites than the K23A/K332A/K348A HuAChE, may also allow long-term circulatory residence following their PEGylation.

V. DETERMINATION OF THE ANTIGENIC AND IMMUNOGENIC PROPERTIES OF PEGYLATED rHuAChES

INTRODUCTION

The use of mutagenized forms of human AChE and the possible requirement in certain situations for repeated administration of the prophylactic agent are a cause for concern regarding the possible development of unfavorable immunogenic responses to the bioscavenger. As detailed above, we have demonstrated that conjugation of PEG chains to rHuAChE impedes physical interactions between the PEGylated AChE and membrane-bound protein receptors such as the hepatic asialoglycoprotein receptor, or receptors involved in amino-acid-mediated removal of AChEs (Section II). The attachment of a linear, flexible uncharged hydrophilic polymer such as PEG, may prevent recognition of the enzyme by the host immune system as well, so that the PEGylated version of AChE will elicit a lesser immune response than the non-modified version of AChE. The effective shielding of PEGylated AChE from immunorecognition may also depend on the amount and specific locations of the appended PEG molecules on the enzyme surface. The array of PEGylated-AChE enzymes in which one or more lysine target sites were removed (Section IV), can serve to examine the contribution of different amounts of PEG or their specific locations at the enzyme surface to the immunogenic and antigenic properties of the PEGylated AChE product. Determination of the antigenic potential of different surface regions of the enzyme will allow judicious selection of specific configurations of lysine residues for PEGylation, on the basis of their ability to support the generation of modified enzyme displaying both homogeneity and low immunogenicity.

In this section, we summarize the work carried out in our laboratory to determine whether PEGylated and non-PEGylated rHuAChEs differ in their antigenic and immunogenic properties.

METHODS

Enzymes

Procedures of transfection of the human embryonal kidney derived cell line (HEK-293) with the expression vector of the C-terminus truncated HuAChE enzymes (Cohen *et al.*, 2001) and the generation of stable cell clones expressing high levels of recombinant ChE products, were described previously (Kronman *et al*., 1992, 1995).

Attachment of PEG chains to primary amines in rHuAChE was performed using succinimidyl propionate-activated methoxy-PEG (SPA-PEG; Nektar Inc.) as described previously (Cohen *et al*., 2001). Briefly, purified rHuAChE (5 μM) was incubated with PEG-20000 at a ratio of 30:1 (mol/mol) $[PEG]_0/[AChE\ primary\ amines]_0$ in 50 mM borate buffer, pH 8.5, for 2 h at room temperature. The chemically modified products were dialyzed extensively against PBS and analyzed on 6% SDS/PAGE gels.

Antigenicity and Immunogenicity of the non-modified and PEGylated rHuAChEs

For antigenicity studies, HuAChE or PEGylated-HuAChE (160 ng) were incubated in the presence of different amounts of mouse polyclonal anti-ChE antiserum (Shafferman *et al*., 1992a; titer = 1:320,000) and then precipitated with Protein G-sepharose beads (Sigma). Residual ChEs activity in the soluble nonbound fraction was determined.

For immunogenicity studies, mice (10 mice/group) were administered at monthly intervals with 10 μg/mouse of either rHuAChE or PEGylated rHuAChE. Antibody titers in blood samples removed at various periods of time were determined by direct ELISA (Shafferman *et al*., 1992a).

RESULTS

Comparison of the antigenic and immunogenic properties of wild-type rhuAChE before and after PEG conjugation

As an initial step towards determination of the immunological properties of PEGylated rHuAChE, antigenicity studies were carried out with nonmodified ΔC-rHuAChE and PEGylated rHuAChE. To this end, 160 ng of either ΔC-rHuAChE or PEGylated rHuAChE were incubated with different amounts of polyclonal mouse anti-HuAChE (Shafferman *et al.*, 1992a), and then precipitated with Protein G sepharose beads. Immunoprecipitation was evaluated by determining residual AChE activity in the supernatant. The results (Fig. 23) clearly demonstrate that, unlike the nonmodified enzyme, the PEGylated version of the enzyme is ineffectively precipitated by the anti-AChE antibodies, suggesting that the appendage of PEG moieties efficiently "shield" the enzyme from immuno-recognition.

To further evaluate the effect of PEGylation on the immunological properties of AChE, we compared the immunogenic potential of PEGylated rHuAChE to that of nonmodified rHuAChE, following their administration to mice. To this end, non-modified or PEG-modified AChE (no adjuvant included) were repeatedly administered to mice (n=10) at monthly intervals, and anti-AChE antibody formation was monitored (Fig. 24). Mice administered with non-modified AChE displayed substantial levels of anti-AChE antibody even after the second administration (antibody titers = 1500 at 7 weeks), and antibody levels increased significantly following the administration of a third dose (antibody titers = 7800 at 11 weeks). In contrast, anti-ChE levels were consistently low throughout the experiment (antibody titers were less than 400 at 11 weeks). The failure of PEG-AChE to elicit significant antibody formation even in a heterologous animal model (human AChE in mice), strongly suggests that the PEG appendage results in the conversion of the AChE molecule into an "immunologically inert" form.

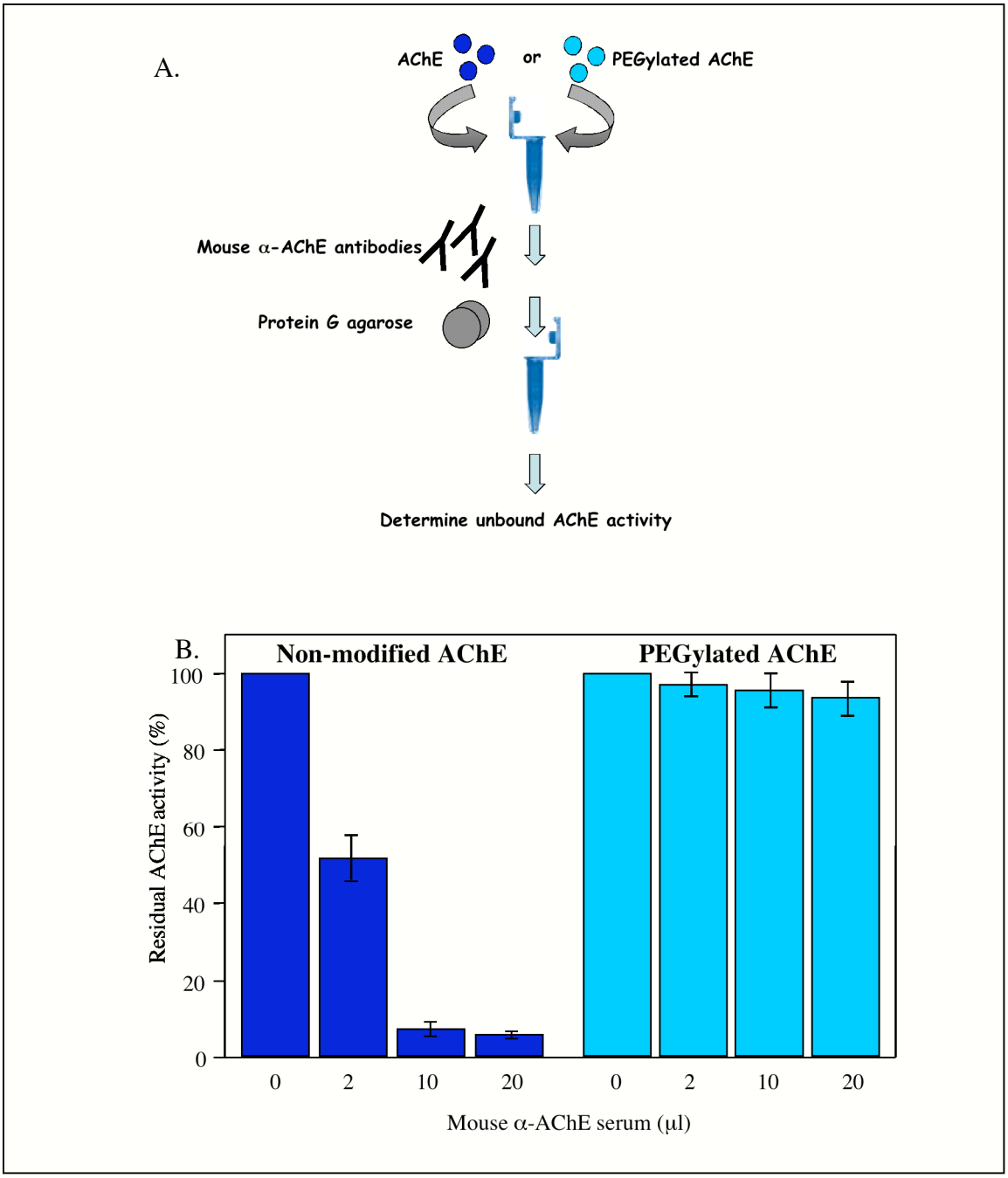

Figure 23: **Determination of antigenicity of AChE and PEGylated AChE.** A. Presentation of the immunoprecipitation scheme: AChE or PEGylated AChE proteins were incubated in the presence of different amounts of mouse polyclonal anti-AChE antiserum and then precipitated with Protein G-agarose beads. Residual AChE activity in the soluble nonbound fraction was determined. B. Residual AChE activity following immunoprecipitation with the indicated amounts of antiserum.

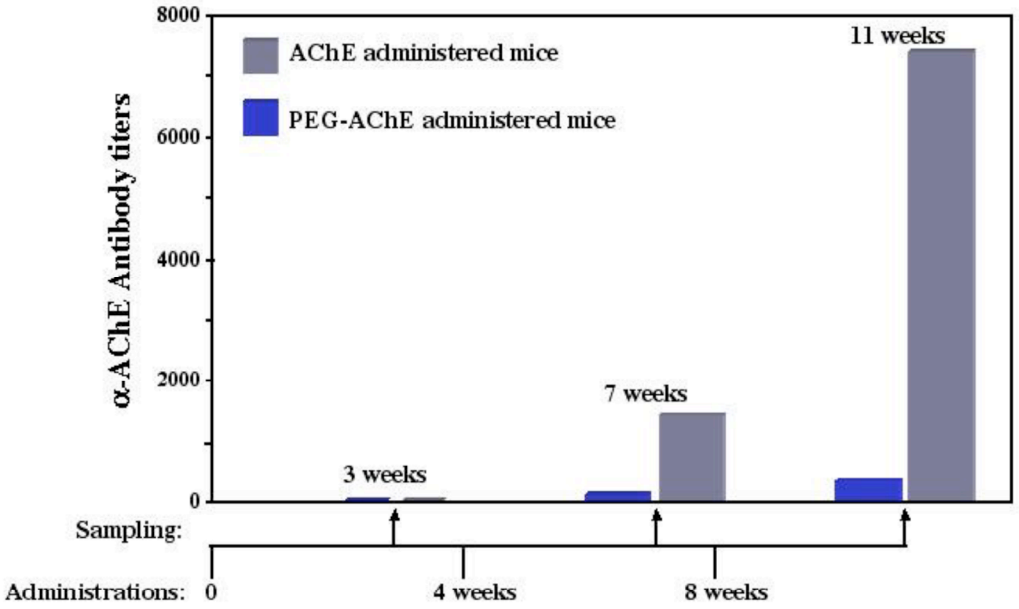

Figure 24: **Anti HuAChE antibody titers in mice administered with rHuAChE or PEGylated rHuAChE.** Mice (10 mice/group) were administered at monthly intervals with 10 μg/mouse of either rHuAChE or PEGylated rHuAChE without adjuvant. Antibody titers were determined in blood samples removed at various periods of time, as indicated in the figure. Antibody titers were determined by direct ELISA, in 96-well microtiter plates coated with highly purified rHuAChE.

Comparison of the antigenic and immunogenic properties of tetralysine rHuAChE before and after PEG conjugation

One of the hypolysine AChE mutants, K23A/K332A/K348A, which contains only four lysine residues, was shown to be retained in the circulation of mice following PEG appendage for extended periods of time (Section IV). To examine whether the lower levels of PEGylation and altered spatial location of the PEG residues on the surface of this mutated version of AChE affect its immunorecognition, the antigenicity and immunogenicity of PEGylated K23A/K332A/K348A AChE were compared to those of PEGylated wild type AChE.

To this end, 160 ng of wild type AChE, hypolysine K23A/K332A/K348A-AChE or the corresponding PEGylated forms of these enzymes were incubated with 20μl polyclonal mouse anti-HuAChE Abs and then precipitated with Protein G sepharose beads. The nonPEGylated wild type and hypolysine K23A/K332A/K348A-AChE enzymes were effectively recognized by the anti-HuAChE Abs, yet as expected, both the PEGylated wild

type and hypolysine AChEs could not be immunoprecipitated by these antibodies, as manifested by the fact that nearly all of the enzymatic activity remained in the non-bound supernatant fraction (Figure 25).

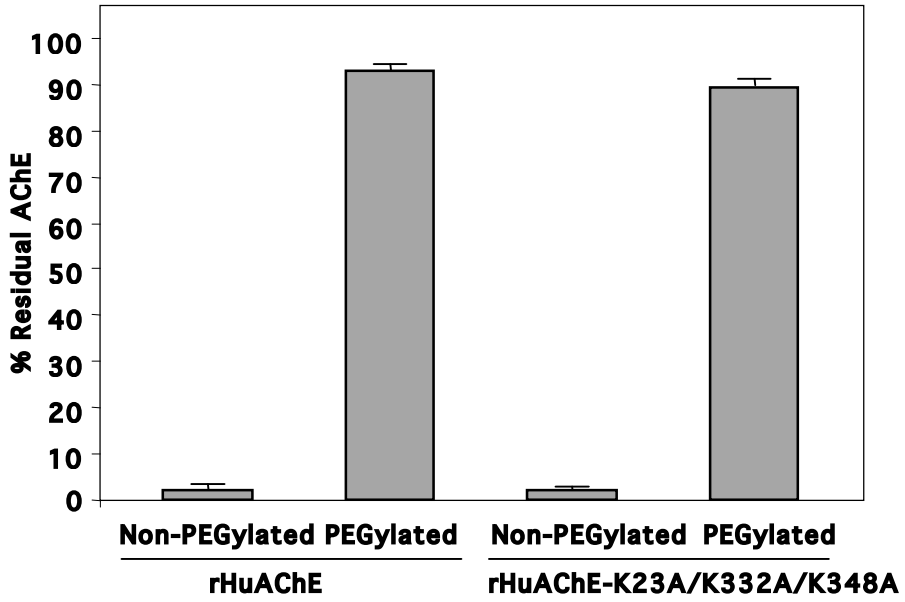

Figure 25: **Determination of antigenicity of wild type and hypolysine AChEs and their PEGylated forms.** Wild type AChE or K23A/K332A/K348A AChE in their non-PEGylated and PEGylated forms were incubated in the presence of 20 μl of mouse polyclonal anti-AChE antiserum and then precipitated with Protein G-agarose beads. Residual AChE activity in the soluble nonbound fraction was determined and expressed as percent of input activity prior to immunoprecipitation.

In accordance with these findings, we compared the immunogenic potential of PEGylated K23A/K332A/K348A rHuAChE to that of nonmodified K23A/K332A/K348A rHuAChE. To this end, non-modified or PEG-modified K23A/K332A/K348A AChEs were administered to mice (n=10) at monthly intervals (no adjuvant included), and anti-AChE antibody formation was monitored (Fig. 26). This set of experiments allowed us to determine that the nonmodified and PEGylated versions of the hypolysine rHuAChE differ significantly in their ability to elicit an immune response in an heterologous animal system (Fig. 26). Thus, mice administered with non-modified K23A/K332A/K348A rHuAChE displayed substantial levels of anti-AChE antibody even after the second administration (antibody titers = ~10,000 at 7 weeks), and antibody levels increased significantly following the administration of a third and fourth dose (antibody titers = ~40,000 and ~60,000 at 11 and 15 weeks, respectively). In contrast, anti-ChE levels were consistently low in mice, which were administered with PEGylated K23A/K332A/K348A rHuAChE (antibody titers were less than

5000 at 15 weeks). We can therefore conclude that controlled PEG appendage effectively reduces the immunogenicity, even of the hypolysine AChE molecule.

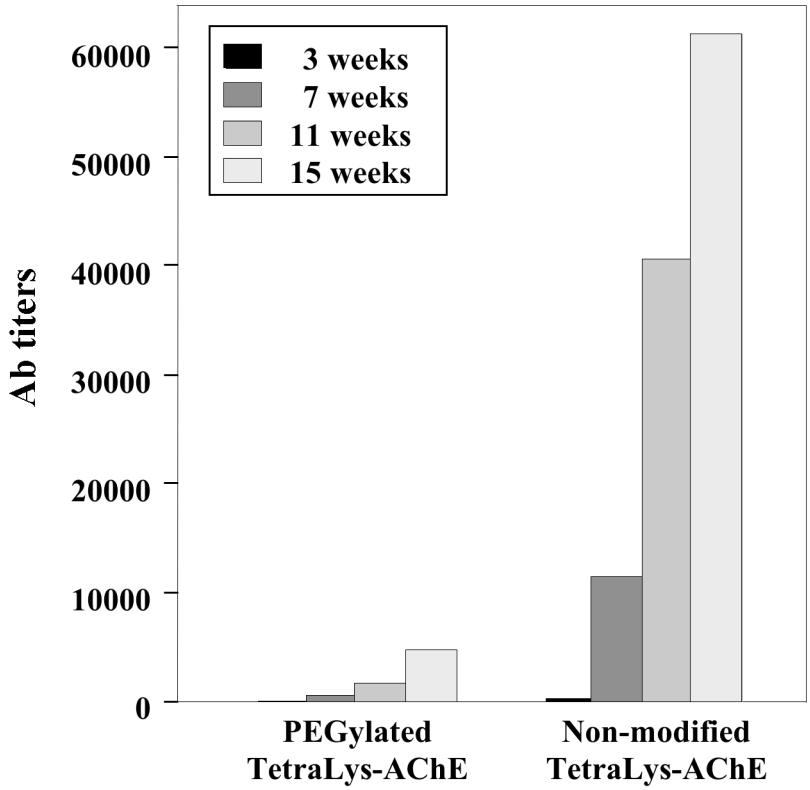

Figure 26: Anti HuAChE antibody titers in mice administered with tetralysine rHuAChE or PEGylated tetralysine rHuAChE. Mice (10 mice/group) were administered at monthly intervals with 10 μg/mouse of either tetralysine (K23A/K332A/K348A) rHuAChE or PEGylated tetralysine rHuAChE without adjuvant. Antibody titers were determined in blood samples removed at various periods of time, as indicated in the figure. Antibody titers were determined by direct ELISA, in 96-well microtiter plates coated with highly purified rHuAChE.

Taken together, the pharmacokinetic and antigenic/immunogenic analyses of PEGylated K23A/K332A/K348A rHuAChE demonstrate that the judicious elimination of selected HuAChE lysine residues, necessary for the generation of a homogenous product upon PEGylation, may provide the means to generate an AChE-based OP-compound bioscavenger which is characterized by both long-term circulatory residence and reduced immunogenicity. Further studies with the full array of hypolysine rHuAChEs (see Section IV) will enable us to define in a more precise manner, the relationship between the number and locations of the PEG target sites, and the immunogenic and pharmacokinetic properties of the PEGylated enzymes.

VI. GENERATION OF rHuAChE IN MICROORGANISM-BASED EXPRESSION SYSTEMS

INTRODUCTION

As documented at length in the previous section, optimized PEG-conjugation results in the long-term retention of AChEs in the circulation even when these are not optimally processed. Thus, proteins lacking glycan moieties or containing glycans which are not capped by sialic acid, exhibit extended circulatory retention following PEG-conjugation, probably due to the masking effect of the appended PEG which obstructs removal via receptor-dependent elimination systems. Likewise, assembly of AChE into tetramers is not a prerequisite for circulatory longevity, most likely since the molecular size of the PEGylated enzyme decreases or prevents clearance through glomerular filtration. This body of data point towards the potential ability to utilize recombinant human AChE produced in non-mammalian production systems, as a cost-effective source for large-scale amounts of enzyme that can then be efficiently PEGylated to generate circulatory long-lived enzyme species for therapeutic use.

Generation of human acetylcholinesterase in an *E. coli*-based production system was documented in the past (Fischer *et al.*, 1993). However, the recombinant enzyme produced in this system segregated as misfolded protein forms in insoluble inclusion bodies, and only 3% of the recombinant AChE could be successfully refolded into enzymatically active forms. Different approaches were explored in the past for the prevention of inclusion body segregation of recombinant proteins in *E. coli*. These included expression of the protein of interest fused to a solubilizing protein, targeting of the recombinant protein to the periplasm, coexpression of chaperones together with the protein of interest, and facilitation of disulfide bond formation in the cytoplasm. However, each of these strategies had serious drawbacks. The use of fused proteins for the generation of soluble recombinant bioactive products was complicated by the need for enzymatic cleavage which resulted in non-specific cleavage within the product protein, while the presence of highly bioactive proteases requires additional purification steps, increase production costs and can prohibit drug approval. Targeting of recombinant proteins to the oxidizing environment of the periplasm to allow their correct folding, proved to be a particularly complex and incompletely understood process (Pugsley, 1993), while the presence of a targeting signal peptide did not always ensure efficient protein translocation through the inner membrane. Coexpression of

chaperones for the solubilization of recombinant proteins was complicated by the fact that (i) the correct substrate-chaperone combination has to be found by trial and error, (ii) overexpression of chaperones led in some cases to undesirable phenotypes that were detrimental to viability and protein expression (Blum *et al*., 1992) and (iii) the increase in yield of properly folded proteins as a result of chaperone coexpression proved to be inconsistent (Wall and Pluckthun, 1995; Yasukawa *et al*., 1995; Makrides, 1996).

Bacillus species synthesize and secrete many extracellular enzymes directly into the medium in high yields and therefore serve as an attractive alternative to *E. coli*, for expression and secretion of biotechnologically important proteins (Simonen and Palva, 1993). The successful production/secretion of high levels of uniformly processed recombinant product in *Bacillus* requires the introduction of specific modifications both in the expression vector and in the host strain which will result in a favorable combination of biochemical and genetic traits. For instance, proteases of various species of *Bacillus* may severely affect production and secretion of foreign proteins by these bacteria. To remedy this situation, mutant strains that produce less proteases were generated (Sloma *et al*., 1990; Wu *et al*., 1991; Ye *et al*., 1999; Lee *et al*., 2000). Progressive mutagenesis of *Bacillus subtilis* resulted in the generation of strains that are deficient in two (subtilisin and neutral protease, the major *B. subtilis* proteases), five, six and seven proteases. The latter strain, WB700, allowed 8-fold higher production/secretion of staphylokinase, than wild type *B. subtilis* (~340mg/ml under optimized conditions, Ye *et al*., 1999). An alternative approach to overcome the problem of extensive proteolytic degradation, is to use *B. brevis* rather than *B. subtilis*. This bacillus strain naturally secretes very low amounts of proteases, or none at all. For example, extracellular protease activity of *B. brevis* 47 is 1.6% of that of *B. subtilis*, and that of *B. brevis* HPD31 is below detection level (Tagaki *et al*., 1989). Several foreign proteins such as *B. stearothermophilus* α-amylase, swine pepsinogen, human epidermal growth factor and human interleukin-6, have been successfully produced by using these two *B. brevis* strains as hosts (Tsukagoshi *et al*., 1985; Takao *et al*., 1989; Udaka *et al*., 1989; Yamagata *et al*., 1989; Sagiya *et al*., 1994; Ebisu *et al*., 1996; Nagao *et al*., 1997; Shiga *et al*., 2000).

In recent years high level production and extracellular secretion of recombinant enzymes were achieved in *Bacillus*-based systems using different combinations of parameters that affect production. In most cases the host strain were either the six or seven protease-deficient strains of *B. subtilis* (WB600, WB700, W751) or low protease strains of *B. brevis* (HPD31, *B. brevis* 47). In some cases, the signal peptide of the protein of interest was modified to comply with the general structure of *Bacillus* signal peptides, but in most cases the original

signal peptide was replaced with a *B. subtilis* or *B. brevis* signal. Likewise, the promoter driving transcription was usually of *Bacillus* origin (e.g. Pamy of *B. amyloliquefaciens,* P43 of *B. subtilis*, cell wall protein promoter of *B. brevis*). Extensive studies designed to find an optimal combination of host cells (*B. subtilis* vs. *B. brevis*, examination of specific strains), signal-peptide, signal-protein joining procedure, and transcription promoter, led to high-level production and secretion of recombinant proteins within the 200-1000 mg/liter range. In the case of recombinant human epidermal growth factor produced in a *B. brevis*-based system, large-scale production levels reached up to 1.5 gram per liter (Ebisu *et al*., 1996).

An additional cost-effective system for large-scale production of heterologous proteins is based on the methylotrophic yeast *Pichia pastoris*. The increasing popularity of this particular expression system can be attributed to several factors, most importantly: (1) The foreign proteins produced at high levels in *Pichia pastoris* may be directed to the extracellular medium (2) the capability of performing many eukaryotic posttranslational modifications, including disulfide bond formation and proteolytic processing, and (3) the ability to rapidly grow on inexpensive media to high cell densities. An optimized combination of *Pichia* strain, transcription promoter, gene nucleotide composition, signal peptide and signal peptide-to-mature protein tailoring, can lead to high-level production and secretion of recombinant proteins. For example, human insulin (Wang *et al.*, 2001) and human albumin (Sreekrishna *et al*., 1998) were secreted into the medium, reaching levels of 1.5 g/l and 3.0 g/l, respectively. Expression of mammalian AChE in *Pichia*-based systems was documented in few cases, yet the data concerning production levels are not consistent and differ by two to three orders of magnitude, even when the AChE enzyme expressed was of the same species (rat AChE).

The promoter most commonly used to drive high levels of expression of heterologous proteins in the *P. pastoris* system is the *P. pastoris* AOX1 promoter, which is controlled at transcription level by the presence of methanol. Due to the strict regulation of the AOX1 promoter, this promoter is well fitted for driving inducible expression of recombinant proteins, however, in certain circumstances in which constitutive expression may be preferable, several promoters such as the *P. pastoris* GAP, FLD1, PEX8, and YPT1 can be used. Both Northern analysis and reporter activation experiments indicate that the *P. pastoris* glyceraldehyde 3-phosphate dehydrogenase (GAP) gene promoter provides strong constitutive expression with glucose as a carbon source, at a level comparable to that achieved by the AOX1 promoter (Waterham *et al.*, 1997). A certain advantage of using the

GAP promoter is that methanol is not required for induction, nor is it necessary to shift cultures from one carbon source to another, making strain growth more straightforward.

The effective secretion of the heterologous protein product depends largely on the fusion of the mature enzyme to an appropriate signal peptide that can be efficiently processed in the production system of choice. As the secretion efficiency of a protein sometimes improves dramatically when a different signal sequence is utilized, a match between *cis*-acting information in the signal sequence and the foreign protein partner appears to be crucial for effective targeting to the extracellular medium. The secretion signal sequence of the *Saccharomyces cerevisiae* MATα factor is most commonly used as signal peptide for expression of heterologous proteins in *P. pastoris*. Recently, other signal peptides were shown to be effective in secreting and/or being properly processed in cases where the standard *S. cerevisiae* MATα prepro signal gave unsatisfactory results. These include the secretion signal of *P. pastoris* acid phosphate (PHO1) and a phytohemagglutinin signal sequence (PHA-E) from *Phaseolus vulgaris* (Cereghino and Cregg, 2000). Unfortunately, there is no way to predict which signal will work best. Trial and error experiments using several signals are often required to find the optimum secretion signal for a specific protein.

When expression vectors are introduced into *P. pastoris*, individual transformants typically express widely varying amounts of protein. In some cases, maximum levels of expression frequently depend on integration of several copies of the expression cassette (Romanos *et al.*, 1995). The selection of a *P. pastoris* high-level AChE expressor clone, may therefore require high throughput screening procedures. Though screening for rare transformants that express the highest amounts of protein can, in some circumstances, be labor-intensive and time-consuming, the sensitive colorimetric method for measurement of secreted AChE activity, should allow rapid and straightforward screening for high-level AChE expressing clones.

In this section, we summarize the work carried out in our laboratory, aimed at the generation of recombinant human AChE in both *Bacillus brevis* and *Pichia pastoris* microorganism-based production systems.

METHODS

Planning and construction of a synthetic human AChE gene

Analyses of nucleotide frequencies, codon usage, restriction site contents and potential RNA secondary structures, were carried out using several programs in the GCG Wisconsin software package (Accelrys Inc.) including StemLoop and mFold softwares.

For the assembly of the synthetic gene, 46 oligonucleotides (65-83 bases) were synthesized by Sigma Inc., Israel. Oligonucleotides were resolved on urea-PAGE gels, extracted with butanol and purified on G-50 columns. Phosphorylation of the 5' ends of inner oligonucleotides was carried out using T4 kinase (BioLab, Inc.). Pairs of oligonucleotides were denatured at 95ºC, annealed at 42ºC and ligated overnight at 4ºC with T4 ligase. Ligated oligonucleotides were mixed, denatured and allowed to re-ligate, to form larger segments corresponding to the N-terminal, mid-gene, and C-terminal regions of the synthetic gene, which were then amplified by PCR. The PCR products were resolved and excised from a 1% agarose gel, cut with restriction enzymes (SacI and BstEII, BstEII and EcoRV, EcoRV and BamHI for the first, second and third segments respectively) and ligated to pGEM3Z vector. The segments were assembled in tandem to generate the full-length coding region of the synthetic human AChE gene in the pGEM vector.

The synthetic AChE coding region and the upstream *B. brevis* ribosome binding site and signal-peptide were completely sequenced by ABI310 genetic analyzer using T7, SP6 and inner primers. Erroneous codons were replaced by proper codons by site-directed mutagenesis using the Quickchange system (Stratagene, Inc.)

In-vitro expression system

The pGEM-sAChE plasmid (1μg) was subjected to ^{35}S-methionine labeled *in-vitro* transcription-translation (TNT Quick Coupled Transcription/Translation Systems, Promega Inc.). The reaction products were immunoprecipitated with polyclonal mouse anti-HuAChE (Shafferman *et al.*, 1992a) antibodies, or with non-related control anti-GFP antibodies and protein G agarose beads (Sigma Inc.). Immunoprecipitated proteins were resolved by SDS-PAGE and visualized by fluorography (Amplify, Amersham Biosciences).

Expression of the Synthetic Human AChE Gene in *Bacillus brevis*

The synthetic AChE coding region, including a *Bacillus*-oriented ribosome binding site and the *B. brevis* cell wall protein signal peptide (Tsuboi, *et al.*, 1986; Yamagata *et al.*, 1987), was cloned into the *E. coli-Bacillus* shuttle vector pXX_{MCS-5} (Gat *et al.*, 2003) downstream to the α-amylase promoter of *Bacillus amyloliquefaciens* (P*amy*), or the *Bacillus anthracis* surface antigen protein promoter, (Psap_L) or the *Bacillus brevis* cell wall protein promoter (P*cwp*). The $psAChE_{amy}$ and $psAChE_{sapL}$, constructs were generated by excising the synthetic HuAChE gene, together with the *B. brevis* cell-wall protein ribosomal binding site (RBS) and signal peptide (SP) from the pGEM3-sAChE vector, to replace the GFP coding region and RBS in the $pGuv_{amy}$ and $pGuv_{sapL}$ vectors (Gat *et al.*, 2003). The $psAChE_{cwp}$ construct was generated utilizing P*cwp* specific primers for PCR amplification of the P*cwp* region (Adachi *et al.*, 1991), using *B. brevis* chromosomal DNA as template. The resulting PCR product was verified by sequencing, and was used to replace the Pamy promoter of $psAChE_{amy}$.

Competent *B. brevis choshinensis* cells were prepared as described previously (Okamoto *et al.*, 1997), and plasmid DNA was introduced by electroporation. Transformed cells were then selected for neomycin resistance. Selected neomycin resistant clones were examined for the presence of the expression plasmid by PCR analysis, utilizing internal primers for the synthetic AChE gene.

Expression of the Synthetic Human AChE Gene in *Pichia pastoris*

The synthetic and non-modified human AChE coding regions were cloned into the *P. pastoris* expression vector, pPICZα. Cloning was achieved by PCR amplification of the open reading frames of the synthetic and non-modified AChE genes, utilizing primers which include appropriate restriction sites for the in-frame insertion, downstream to the α-factor signal sequence and Kex2/STE13 cleavage sequence. AChE coding sequences, as well as sequences spanning the *Saccharomyces cerevisiae* MATα factor/AChE junction, were verified by DNA sequencing.

Competent yeast cells of the two *Pichia pastoris* strains: KM71H and GS115 were prepared according to the manufacturer's instructions, and conditions for optimal electroporation yields (1500V; 50μF; 10msec; 5 μg linearized linear DNA) were determined. The transformed yeast cells were selected on YPD plates containing 100μg/ml zeocin.

Pichia transformant cells were propagated at 30^0C in BMGY medium (1% yeast extract, 2% peptone, 100 mM potassium phosphate, pH 6.0, 1.34% yeast nitrogen base, 4 $x10^{-5}$ % biotin,

1% glycerol). For production of AChE, cells were transferred after 72 hrs to BMMY medium (1% yeast extract, 2% peptone, 100 mM potassium phosphate, pH 6.0, 1.34% yeast nitrogen base, 4 $x10^{-5}$ % biotin, 0.5% methanol) for 96 hours and additional methanol (0.5%) was added daily. Secreted AChE activity was determined in samples removed from the medium at various time points.

Western blot analysis

Analysis of rHuAChE or GFP products was performed by resolving intracellular protein extracts on 10% SDS-PAGE followed by Western blot analysis using anti-HuAChE polyclonal antibodies (Shafferman *et al.*, 1992a) or anti-GFP polyclonal antibodies (Clontech Inc.).

Northern blot analysis

Total RNA isolated from transformed *B. brevis* cells was denaturing with glyoxal/DMSO, and resolved on agarose gels. Following capillary transfer to nylon membranes, the respective mRNAs were detected by hybridization to ^{33}P-ATP labeled 100-bp probes complementary to the 3'-end of the corresponding transcripts, followed by fluorography.

Pulse-chase

Transformed cell clones were subjected to metabolic labeling for 30 minutes with [^{35}S] methionine/cysteine and then chased by adding non-labeled methionine/cysteine at excess. At various chase periods, culture media was collected and washed cells were lysed by sonication. Recombinant GFP and AChE proteins were immunoprecipitated from cleared cell lysates with rabbit anti-GFP antibodies (Clontech Inc.) and mouse anti-AChE antibodies (Shafferman *et al.*, 1992a), respectively, and then adsorbed with Protein G. Immunoprecipitates were analyzed by reducing SDS-PAGE followed by fluorography, and fluorograms were quantified by densitometry.

RESULTS

Construction of a Human AChE Synthetic Gene

Comparison between the human AChE gene and the genomes of *E. coli, B. subtilis, P. pastoris and S. cerevisiae* (Nakamura *et al.*, 2000) demonstrates that while the genomes of these microorganisms display an average GC content of 45%, the coding sequence for ΔC-HuAChE gene is characterized by a significantly higher GC content of 65.2%. In fact, the GC content of the first 100 base pairs of the coding sequence for ΔC-HuAChE gene reaches even higher values of 72%. Codon usage in ΔC-HuAChE also differed significantly from that of microorganisms such as *Bacillus* or *Pichia* (see Table 6 A,B; Fig. 27A).

To allow optimal expression of human AChE in microorganisms, we set out to design a synthetic HuAChE gene (sAChE) of lower GC content, which codes for authentic human AChE, utilizing nucleotide codons which will be compatible with efficient expression in microorganisms-based systems.

Meticulous planning led to the proposal of a candidate nucleotide sequence coding for human AChE in which: (1) The overall GC content is 51.7%, as opposed to 65.2% in the original ΔC-HuAChE gene (Fig. 27B); (2) The probability of generation of RNAs with stable secondary structures, which might have an unfavorable effect on the translation process is considerably lower; (3) Additional unique restriction sites for future manipulation of individual lysine residues have been introduced, and (4) Codon usage conforms to that of microorganisms such as *Bacillus* or *P. pastoris* to a much greater extent (Table 6 A, B, C, Fig. 27A). For example, the usage frequency values of codons CCC(Pro), GTG(Val), GCC(Ala), CTG(Leu), which in the native HuAChE sequence are 44-79 per 1000 nucleotides , are now reduced to 5.5-22 per 1000 nucleotides, in a manner similar to that displayed by various microorganisms. Similarly, codons displaying in the native HuAChE coding sequence very low usage frequency values of 0-5 per 1000 nucleotides, such as AGA(Arg) and TTA(Leu), and GTT(Val), were elevated in the synthetic coding region to 18-31 per 1000 nucleotides, conforming with their usage in microorganisms (Fig. 27A).

To construct the modified human AChE gene (synthetic rHuAChE), we synthesized 46 DNA oligonucleotide fragments (65 to 83 nucleotides each), spanning the full length of both strands of the synthetic rHuAChE. Oligonucleotide fragments corresponding to the ribosome binding site and signal peptide of the *B. brevis* cell wall protein (CWP, Tsuboi, *et al.*, 1986; Yamagata *et al.*, 1987) were synthesized as well. The oligonucleotides were grouped according to their location within the gene (N-terminal and *B. brevis* sequences, mid-gene, C-

terminal), and oligonucleotide members of each group were joined one to another in a stepwise manner, as depicted in Fig. 28. Briefly, phosphorylated oligonucleotides corresponding to contiguous sequences were allowed to anneal and were then ligated. Nearest neighbor ligation products (comprised of 4 oligonucleotides) were then paired and subjected to a second round of annealing/ligation. These were then joined in a similar manner to form a segment corresponding to a one third length of the synthetic AChE gene. The three double stranded products corresponding to the one-third *ache* gene segments, were then amplified by PCR, and the PCR products were cloned into the pGEM3 vector. These segments, which also include a *B. brevis* ribosome-binding site and signal peptide, were assembled in tandem to generate the full-length coding region of the synthetic human AChE gene (Fig. 29A). Sequence verification of the synthetic AChE coding region allowed us to determine that three of the codons did not code for correct human AChE amino acids. These erroneous codons were exchanged with the proper codons by site-directed mutagenesis using the Quickchange system (Stratagene, Inc.).

Table 6: Comparison of the codon usage of native rHuAChE to that of several microorganisms and the synthetic HuAChE

A.

Codons in native HuAChE

Nucleotide triplet

Amino-acid

Codons in *B. subtilis*

TTT	Phe	16.4	30.2	TCT	Ser	5.5	12.9	TAT	Tyr	5.5	22.6	TGT	Cys	1.8	3.6
TTC		32.9	14.2	TCC		14.6	8.1	TAC		29.2	12.0	TGC		9.1	4.3
TTA	Leu	0	19.1	TCA		3.7	14.8	TAA	Stop			TGA	Stop		
TTG		5.5	15.3	TCG		5.5	6.4	TAG				TGG	Trp	23.7	10.3
CTT		3.7	23.0	CCT	Pro	12.8	10.6	CAT	His	3.7	15.2	CGT	Arg	9.1	7.6
CTC		16.4	10.8	CCC		43.8	3.3	CAC		16.4	7.5	CGC		14.6	8.6
CTA		1.8	4.9	CCA		16.4	7.1	CAA	Gln	5.5	19.7	CGA		12.8	4.1
CTG		74.8	23.1	CCG		14.6	16.1	CAG		31.0	18.7	CGG		25.6	6.5
ATT	Ile	1.8	36.8	ACT	Thr	49.3	8.7	AAT	Asn	9.1	22.1	AGA		9.1	6.6
ATC		14.6	27.0	ACC		14.6	8.6	AAC		20.1	17.3	AGG		18.3	14.2
ATA		0	9.3	ACA		12.8	22.3	AAA	Lys	5.5	49.1	AGT	Ser	0	10.6
ATG	Met	12.8	26.9	ACG		14.6	14.6	AAG		7.3	20.8	AGC		9.1	3.9
GTT	Val	5.5	19.2	GCT	Ala	14.6	19.0	GAT	Asp	12.8	33.0	GGT	Gly	14.6	12.8
GTC		20.1	17.3	GCC		63.9	15.9	GAC		31.0	18.8	GGC		38.3	23.4
GTA		9.1	13.4	GCA		9.1	21.7	GAA	Glu	5.5	48.9	GGA		12.8	21.7
GTG		60.2	17.7	GCG		9.1	20.2	GAG		52.9	23.1	GGG		32.9	11.1

B.

Codons in native HuAChE

Nucleotide triplet

Amino-acid

Codons in *P. pastoris*

TTT	Phe	16.4	38.3	TCT	Ser	5.5	9.1	TAT	Tyr	5.5	23.7	TGT	Cys	1.8	7.3
TTC		32.9	11.0	TCC		14.6	5.5	TAC		29.2	11.0	TGC		9.1	3.7
TTA	Leu	0	23.7	TCA		3.7	12.8	TAA	Stop			TGA	Stop		
TTG		5.5	16.4	TCG		5.5	7.3	TAG				TGG	Trp	23.7	23.7
CTT	Leu	3.7	29.2	CCT	Pro	12.8	27.4	CAT	His	3.7	12.8	CGT	Arg	9.1	12.8
CTC		16.4	7.3	CCC		43.8	5.5	CAC		16.4	7.3	CGC		14.6	16.4
CTA		1.8	7.3	CCA		16.4	27.4	CAA	Gln	5.5	23.7	CGA		12.8	9.1
CTG		74.8	18.3	CCG		14.6	27.4	CAG		31.0	12.8	CGG		25.6	9.1
ATT	Ile	1.8	7.3	ACT	Thr	49.3	9.1	AAT	Asn	9.1	18.3	AGA		9.1	11.0
ATC		14.6	5.5	ACC		14.6	7.3	AAC		20.1	11.0	AGG		18.3	11.0
ATA		0	3.7	ACA		12.8	18.3	AAA	Lys	5.5	9.1	AGT	Ser	0	18.3
ATG	Met	12.8	12.8	ACG		14.6	9.1	AAG		7.3	3.7	AGC		9.1	5.5
GTT	Val	5.5	31.0	GCT	Ala	14.6	21.9	GAT	Asp	12.8	29.2	GGT	Gly	14.6	21.9
GTC		20.1	21.9	GCC		63.9	21.9	GAC		31.0	14.6	GGC		38.3	38.3
GTA		9.1	20.1	GCA		9.1	31	GAA	Glu	5.5	42	GGA		12.8	25.6
GTG		60.2	21.9	GCG		9.1	21.9	GAG		52.9	16.4	GGG		32.9	12.8

C.

Codons in native HuAChE

Nucleotide triplet

Amino-acid

Codons in synthetic HuAChE

TTT	Phe	16.4	23.9	TCT	Ser	5.5	23.5	TAT	Tyr	5.5	14.7	TGT	Cys	1.8	8.3
TTC		32.9	19.1	TCC		14.6	16.3	TAC		29.2	18.3	TGC		9.1	4.5
TTA	Leu	0	14.9	TCA		3.7	15.6	TAA	Stop			TGA	Stop		
TTG		5.5	31.4	TCG		5.5	7.2	TAG				TGG	Trp	23.7	9.9
CTT	Leu	3.7	16.0	CCT	Pro	12.8	15.3	CAT	His	3.7	10.5	CGT	Arg	9.1	6.9
CTC		16.4	7.6	CCC		43.8	6.7	CAC		16.4	8.9	CGC		14.6	2.3
CTA		1.8	11.2	CCA		16.4	17.1	CAA	Gln	5.5	23.9	CGA		12.8	4.6
CTG		74.8	15.3	CCG		14.6	4.1	CAG		31.0	14.5	CGG		25.6	2.2
ATT	Ile	1.8	31.7	ACT	Thr	49.3	23.3	AAT	Asn	9.1	23.5	AGA		9.1	12.1
ATC		14.6	19.3	ACC		14.6	13.7	AAC		20.1	25.7	AGG		18.3	7.4
ATA		0	11.5	ACA		12.8	14.3	AAA	Lys	5.5	30.2	AGT	Ser	0	19.9
ATG	Met	12.8	19.2	ACG		14.6	6.3	AAG		7.3	34.4	AGC		9.1	6.6
GTT	Val	5.5	26.7	GCT	Ala	14.6	29.6	GAT	Asp	12.8	37.2	GGT	Gly	14.6	26.6
GTC		20.1	14.5	GCC		63.9	16.7	GAC		31.0	26.2	GGC		38.3	8.6
GTA		9.1	10.1	GCA		9.1	15.9	GAA	Glu	5.5	40.2	GGA		12.8	20.0
GTG		60.2	12.8	GCG		9.1	3.7	GAG		52.9	29.6	GGG		32.9	6.4

A.

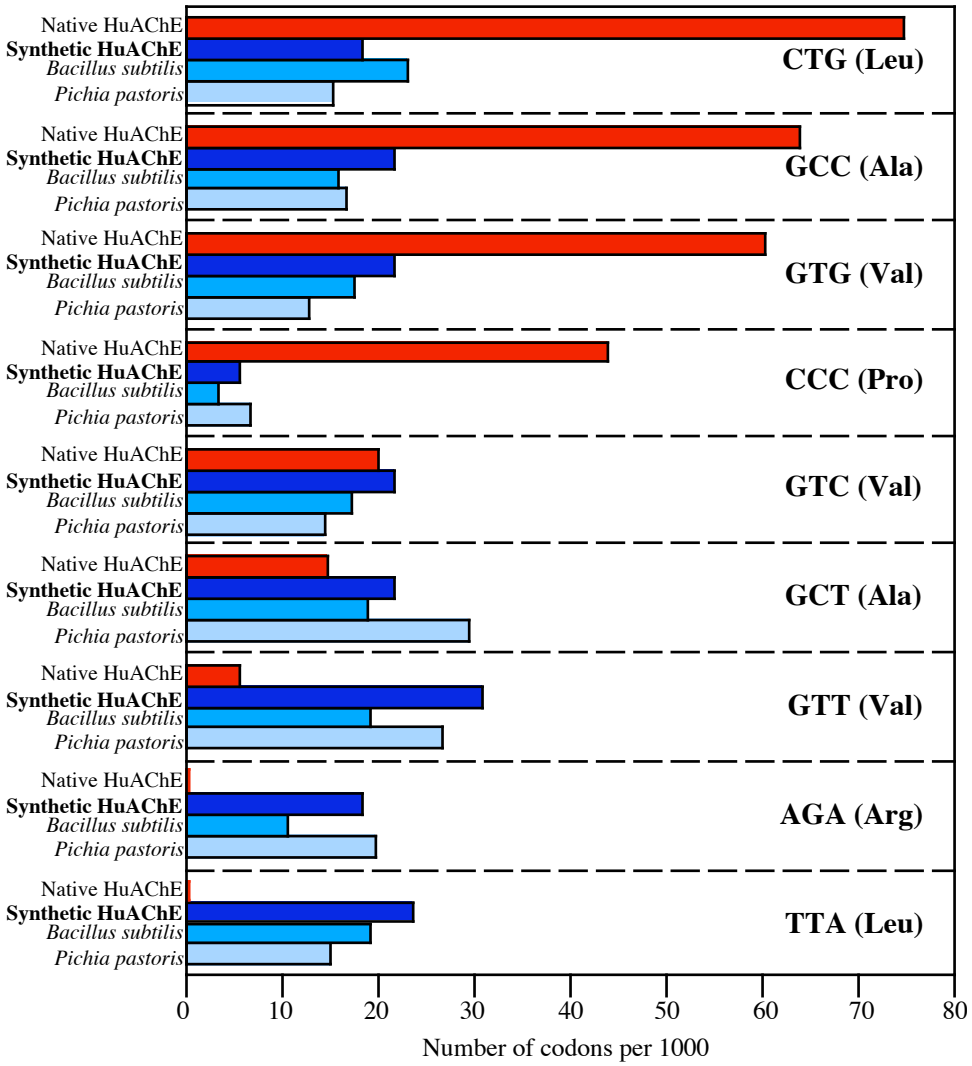

B.

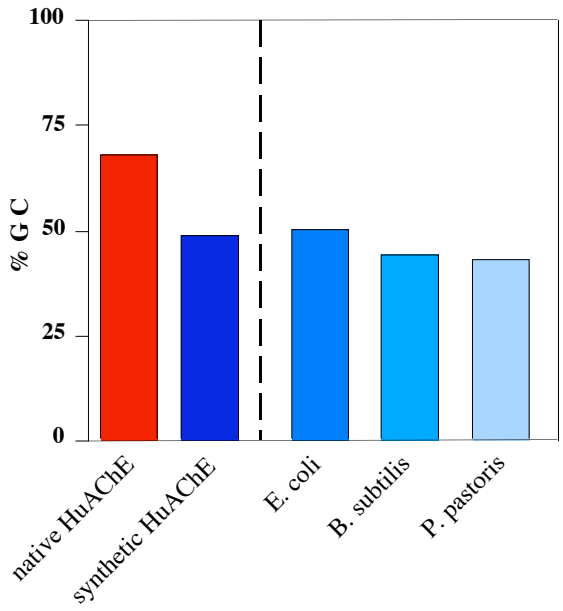

Figure 27: Representative codon usage (A) and GC content (B) of native rHuAChE, synthetic HuAChE and several microorganisms.

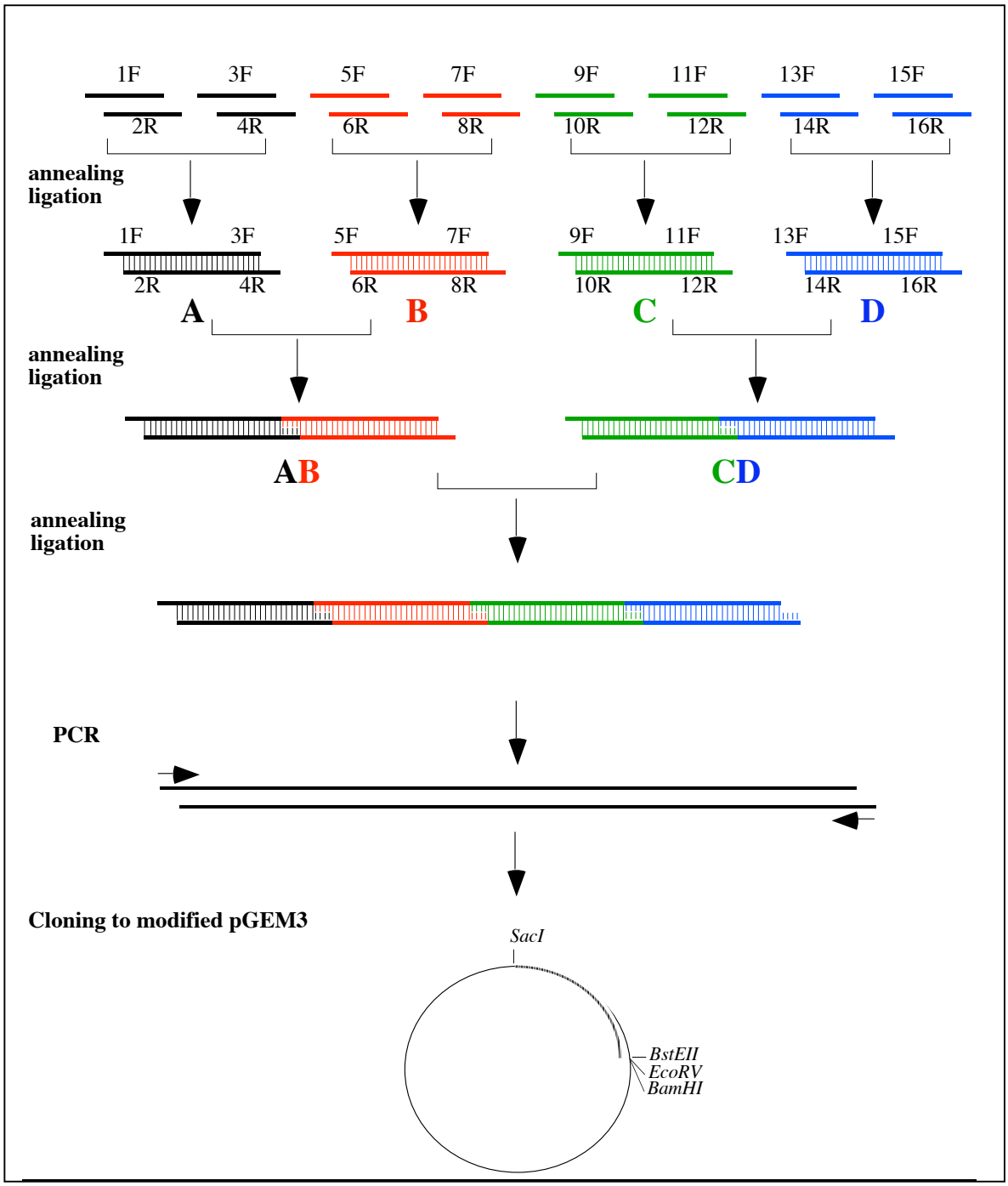

Figure 28: Schematic presentation of the assembly of the synthetic HuAChE gene. Synthetic oligonucleotides of the N-terminal, mid-gene, or C-terminal segments of the HuAChE coding regions were assembled in a stepwise manner which included rounds of annealing and ligation, PCR amplification of the combined gene segment, and cloning of the PCR product into the pGEM3 vector. In the case of the N-terminal portion of the gene, oligonucleotides corresponding to the ribosome binding site and signal peptide of the *B. brevis* cell wall protein (CWP) were included for assembly upstream to the sAChE gene.

Characterization of the Synthetic Human AChE Gene Product in an *in-vitro* Transcription-Translation System

To determine that the synthetic human AChE gene can indeed be translated into authentic AChE, the sAChE-containing pGEM3-based vector, which contains the T7 promoter upstream to the sAChE sequence, was subjected to radioactively labeled *in-vitro* transcription-translation (TnT system, Promega Inc.), followed by immunoprecipitation with polyclonal mouse anti-HuAChE antibodies. Immunoprecipitated protein was resolved by SDS-PAGE and visualized by fluorography. A single major protein product corresponding to full-length AChE was specifically precipitated by the anti-AChE antibodies (Fig. 29B), verifying that genuine human AChE enzyme was indeed generated.

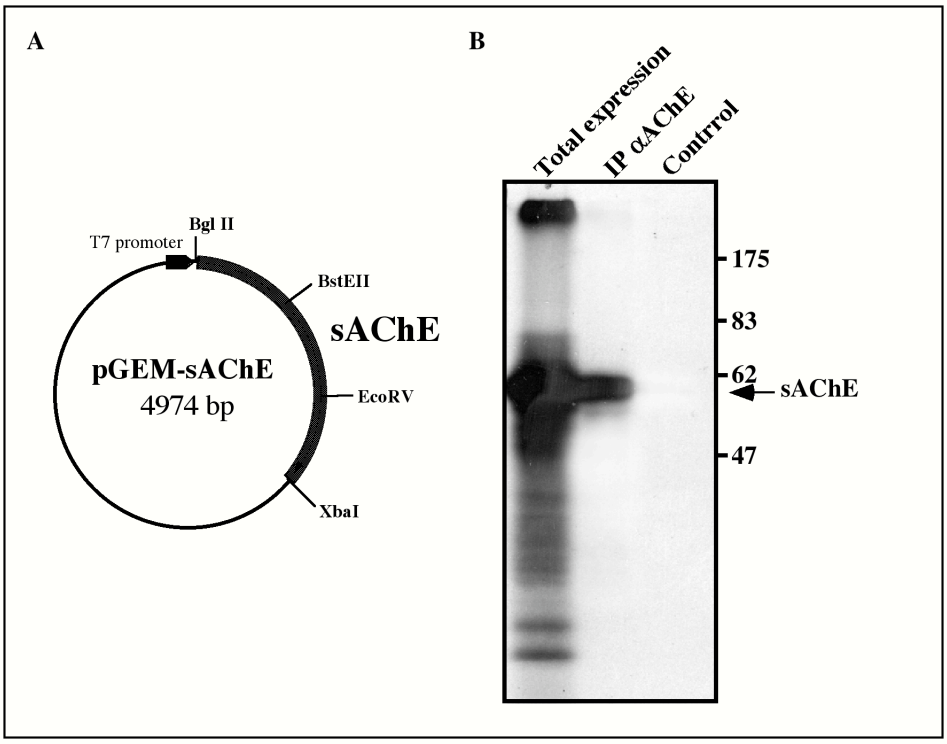

Figure 29: Description of the assembled synthetic AChE gene and characterization of its protein product in an *in-vitro* transcription/translation system. A. The three synthetic gene segments coding for the N-terminal, middle, and C-terminal regions of the human *ache* gene were assembled in tandem within the pGEM3 cloning vector, to generate the pGEM-sAChE plasmid, containing the full length synthetic *ache* gene, under control of the T7 promoter. B. The pGEM-sAChE plasmid was subjected to radioactively labeled *in-vitro* transcription-translation, followed by immunoprecipitation with polyclonal mouse anti-HuAChE antibodies, or with non-related control anti-GFP antibodies. Immunoprecipitated protein was resolved by SDS-PAGE and visualized by fluorography.

Expression of the Synthetic Human AChE Gene in *Bacillus brevis*

To allow expression of the synthetic AChE in *Bacillus* systems, the synthetic AChE coding region, including a *Bacillus*-oriented ribosome binding site and the *B. brevis* cell wall protein signal peptide (Tsuboi, *et al.*, 1986; Yamagata *et al.*, 1987), was cloned into the *E. coli-Bacillus* shuttle vector pXX_{MCS-5} (Gat *et al.*, 2003) downstream to three different promoters: (1) the α-amylase promoter of *Bacillus amyloliquefaciens*, P*amy*, (2) the *Bacillus anthracis* surface antigen protein promoter, $Psap_{long}$ and (3) the *Bacillus brevis* cell wall protein promoter, P*cwp*. The P*amy* promoter has been shown in the past to drive high levels of expression of recombinant protein in *B. subtilis* and *B. anthracis* (over 100 μg/ml, Cohen *et al.*, 2000). The P*sap* promoter controls expression of the S-layer proteins, which are often the most abundant proteins in bacterial cells, and is considered to be among the strongest known in nature. Indeed expression of heterologous genes under control of the P*sap* promoter, resulted in an 8-fold increase in production levels as compared to P*amy* promoter-driven expression of the same genes (Gat *et al.*, 2003). The P*cwp* promoter controls expression of the cell wall proteins in *B. brevis* (Adachi *et al.*, 1991), and can be regarded as the *B. brevis* counterpart to the *B. anthracis* P*sap* promoter.

The synthetic HuAChE gene, together with the *B. brevis* cell-wall protein ribosomal binding site (RBS) and signal peptide (SP) were excised from the pGEM3-sAChE vector, and used to replace the GFP coding region and RBS in the $pGuv_{amy}$ and $pGuv_{sapL}$ vectors (Gat *et al.*, 2003). The resulting constructs, $psAChE_{amy}$ and $psAChE_{sapL}$, contain the sAChE coding sequence under control of P*amy* and P*sap* promoters, respectively (Fig. 30). For the generation of P*cwp*-controlled sAChE, P*cwp* specific primers were utilized for PCR amplification of the P*cwp* region (Adachi *et al.*, 1991), using *B. brevis* chromosomal DNA as template. The resulting PCR product was verified by sequencing, and was used to replace the Pamy promoter of $psAChE_{amy}$ to generate $psAChE_{cwp}$ (Fig. 30).

For expression of the synthetic rHuAChE gene, we chose the *B. brevis choshinensis* strain (Takagi *et al.*, 1993), which has been shown in the past to sustain high levels of expression and secretion of recombinant proteins from various sources (e.g. Ebisu *et al.*, 1996; Nagahama *et al.*, 1996; Takimura *et al.*, 1997). Competent cells were prepared by a calcium

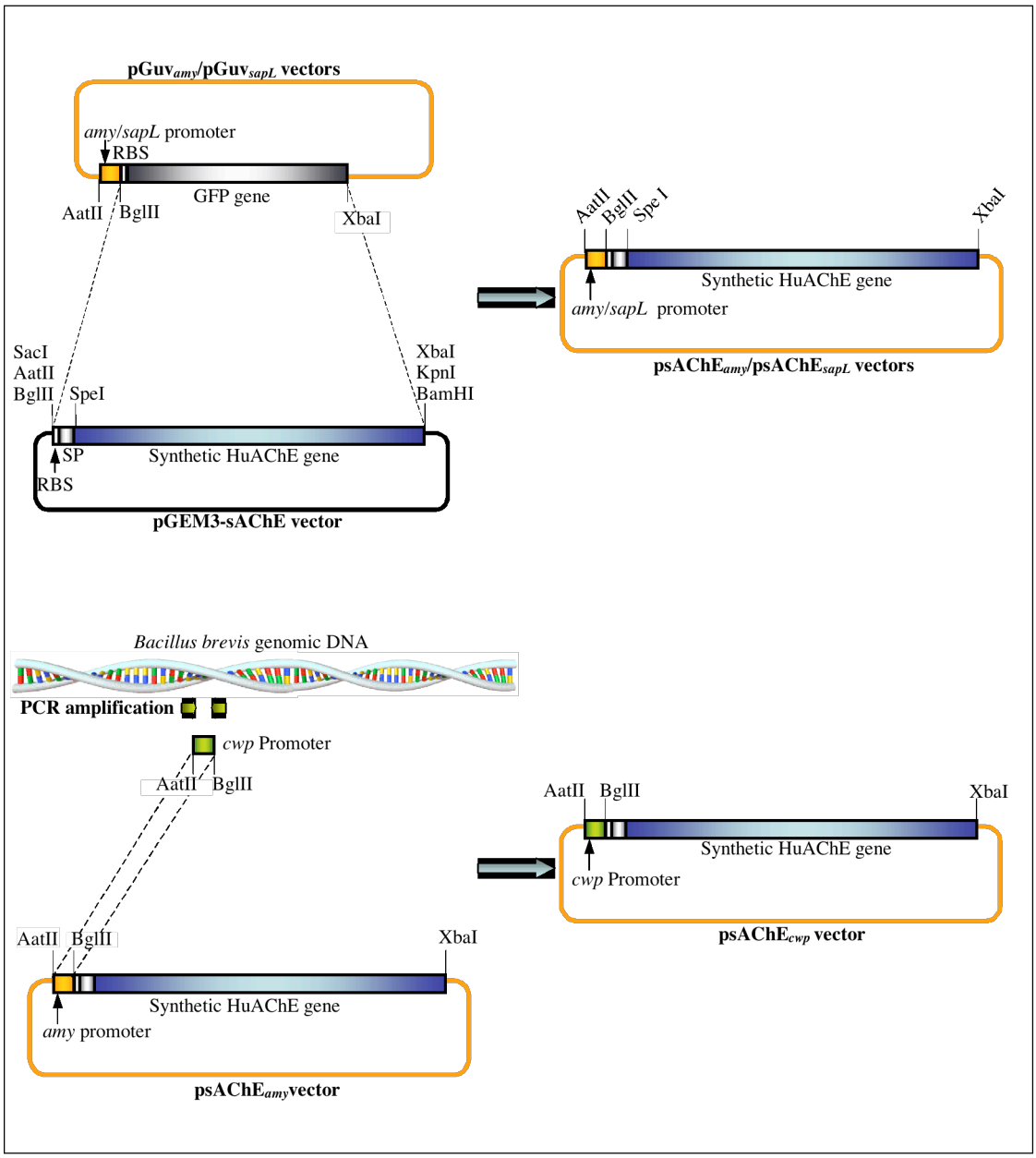

Figure 30: **Description of the construction of the three *Bacillus*-oriented synthetic AChE expression vectors.** SP - Signal Peptide, RBS - Ribosomal Binding Site, GFP - Green Fluorescent Protein,

chloride method adapted for these cells (Okamoto *et al.*, 1997), and plasmid DNA was introduced by electroporation, following meticulous calibration of the settings for optimal cell transformation. The three *Bacillus*-oriented sAChE expression vectors were introduced into *B. brevis* cells, which were then selected for neomycin resistance (Fig. 31). Several neomycin resistant clones were examined for the presence of the expression plasmid by PCR analysis, utilizing internal primers for the synthetic AChE gene. In all cases, the transformed clones were shown to contain the AChE gene.

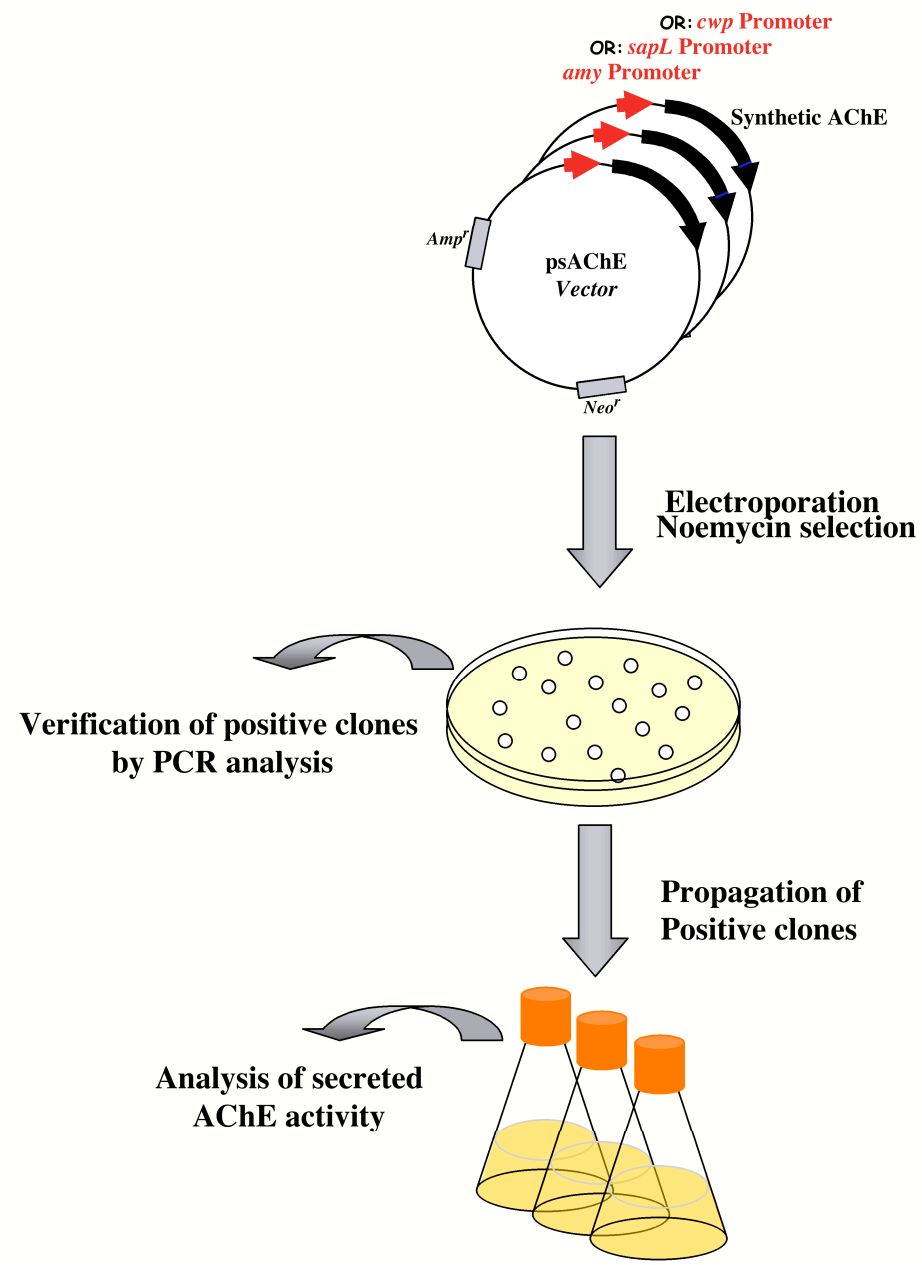

Figure 31: **Schematic presentation of the generation and initial analyses of human AChE transformed *B. brevis* cells.**

Careful inspection of cell clones expressing each of the different constructs failed to detect AChE activity in the growth medium at both the logarithmic and stationary phase. We therefore examined whether AChE activity can be detected within the bacterial cell. Indeed, Western immunoblotting analysis (Fig. 32) allowed us to determine the presence of intracellular AChE at logarithmic phase (8 hours culture), and to a lower extent at stationary phase (16 hours). However, densitometric analysis of intracellular AChE revealed that the

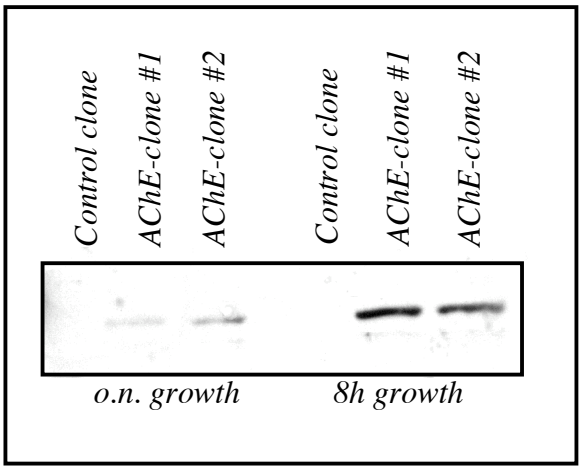

Figure 32: **Western blot analysis of intracellular recombinant human AChE in *B. brevis* cells.** *B. brevis* cells stably transformed with the psAChE$_{amy}$ AChE expression vector or control vector were propagated . Samples (1 ml) were removed at 8 hours and 16 hours, intracellular protein was extracted, and then subjected to Western blot analysis using anti-HuAChE polyclonal antibodies (Shafferman *et al.*, 1992a). Similar results were obtained for cells transformed with the psAChE$_{sapL}$, expression vectors (not shown).

quantities of enzyme are very low, 1 μg/liter cell culture. This unexpectedly low level of enzyme expression (as compared to GFP production), may stem from an inefficiency of regulatory elements within the expression vector. To address this issue, we constructed control plasmids in which the AChE coding region was substituted by that of the green fluorescence protein (GFP) gene. *B. brevis choshinensis* cells were transformed with the pGuv$_{amy}$ expression vector, and several neomycin resistant clones were examined for GFP expression. High level GFP expression was evident by UV illumination (Fig. 33A). Indeed, Western blot analysis followed by densitometric quantitation of the intracellular GFP (Fig. 33B), allowed us to determine that the expressed protein reached a level 10,000-fold higher than AChE (10 mg/liter cell culture). Thus, the expression vehicles used in these studies, are fully capable of supporting high-level expression of heterologous proteins in the *B. brevis choshinensis* cells. The low level of AChE gene product in the bacterial cells, may therefore be an outcome of low transcription/translation levels, or conversely, from an instability of either the message RNA or the protein product.

To determine whether the low level of AChE gene product in the bacterial cells is due to low transcription levels or to an instability of the sHuAChE message RNA, transformed cells (10^9 cells) expressing heterologous rHuAChE or rGFP were harvested at log-phase growth, and total RNA was isolated and subjected to Northern blot analysis (Fig. 34). Detection of the

rHuAChE and rGFP mRNAs was carried out with equal amounts of ^{33}P-ATP labeled 100-bp probes complementary to the 3'-end of the corresponding transcripts. Following fluorography, the ~1850 base-long band corresponding to the AChE transcript and the ~1200 base-long band corresponding to the GFP transcript displayed very similar intensities, attesting to the nearly equal amounts of the two heterologous RNAs within the respective cells at steady-state. The finding that the intracellular level of rGFP protein is 10,000-fold higher than that of intracellular rHuAChE protein, even though transcript levels of the corresponding RNAs are similar, suggests that the limitation in rHuAChE production is a result of either inefficient translation or instability of the translated protein product.

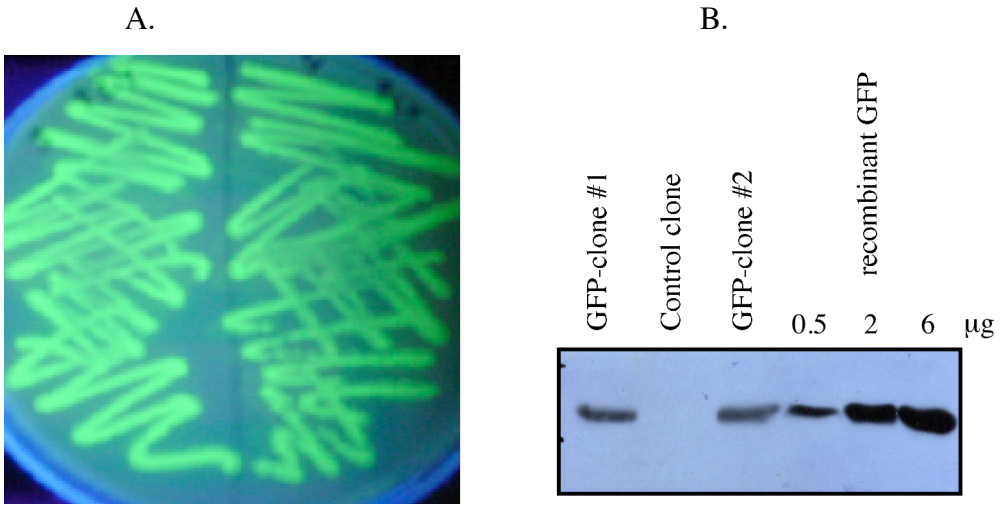

Figure 33: **Expression of GFP in *B. brevis* cells.** (A) *B. brevis* cells stably transformed with the pGuv$_{amy}$ GFP expression vector were streaked unto LB agar plates and inspected by UV light (366 nm). (B) *B. brevis* cells stably transformed with the pGuv$_{amy}$ GFP expression vector or control vector were propagated. Samples (1 ml) were removed, intracellular protein was extracted, and then subjected to Western blot analysis using anti-GFP polyclonal antibodies (Clontech Inc.). Recombinant GFP (Upstate biotechnology Inc.) loaded on the same gel at different quantities served as a standard curve for densitometric quantitation. Similar results were obtained for cells transformed with the pGuv$_{sapL}$ expression vectors (not shown).

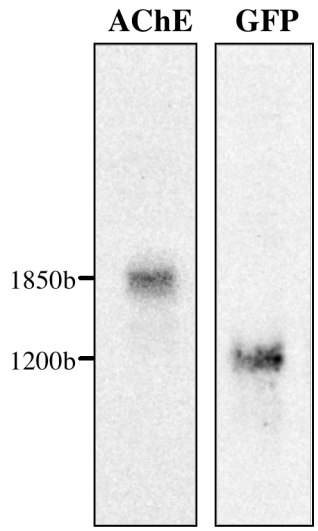

Figure 34: **Northern blot analyses of rAChE and rGFP mRNAs expressed in transformed *B. brevis* cells.** Equal amounts of total RNA isolated from *B. brevis* cells transformed with the *E. coli-Bacillus* shuttle vector pXX_{MCS-5} carrying the rHuAChE gene (left) or rGFP gene (right) were denatured with glyoxal/DMSO, resolved on agarose gels and subjected to Northern blot analyses. Detection of the respective mRNAs was achieved by hybridization to ^{33}P-ATP labeled 100-bp probes complementary to the 3'-end of the corresponding transcripts, followed by fluorography.

To address this issue, comparative pulse-chase experiments were performed to determine the relative stability of the sAChE and rGFP protein products. To this end, equal amounts of sAChE- and rGFP-transformed cell clones were subjected to metabolic labeling for 30 minutes with [^{35}S] methionine/cysteine and then chased by adding non-labeled methionine/cysteine at excess. At various chase periods, culture media was collected and washed cells were lysed by sonication. Recombinant GFP and AChE proteins were immunoprecipitated from cleared cell lysates with rabbit anti-GFP antibodies (Clontech Inc.) and mouse anti-AChE antibodies (Shafferman *et al.*, 1992a), respectively, and then adsorbed with Protein G. Immunoprecipitates were analyzed by reducing SDS-PAGE followed by fluorography, and fluorograms were quantified by densitometry.

SDS-PAGE analysis of the immunoprecipitates allowed us to determine that the rAChE protein product was much less stable than rGFP. Thus, while levels of intracellular rGFP displayed no more than a 25% reduction within the 30-minute chase period, intracellular levels of rAChE could barely be detected at 30 minutes (Fig. 35A). Indeed, densitometric analysis allowed to quantify the relative amounts of intracellular GFP and AChE at the various time points (Fig. 35B), and to determine half live values of 52 minutes and 4.5 minutes for GFP and AChE, respectively.

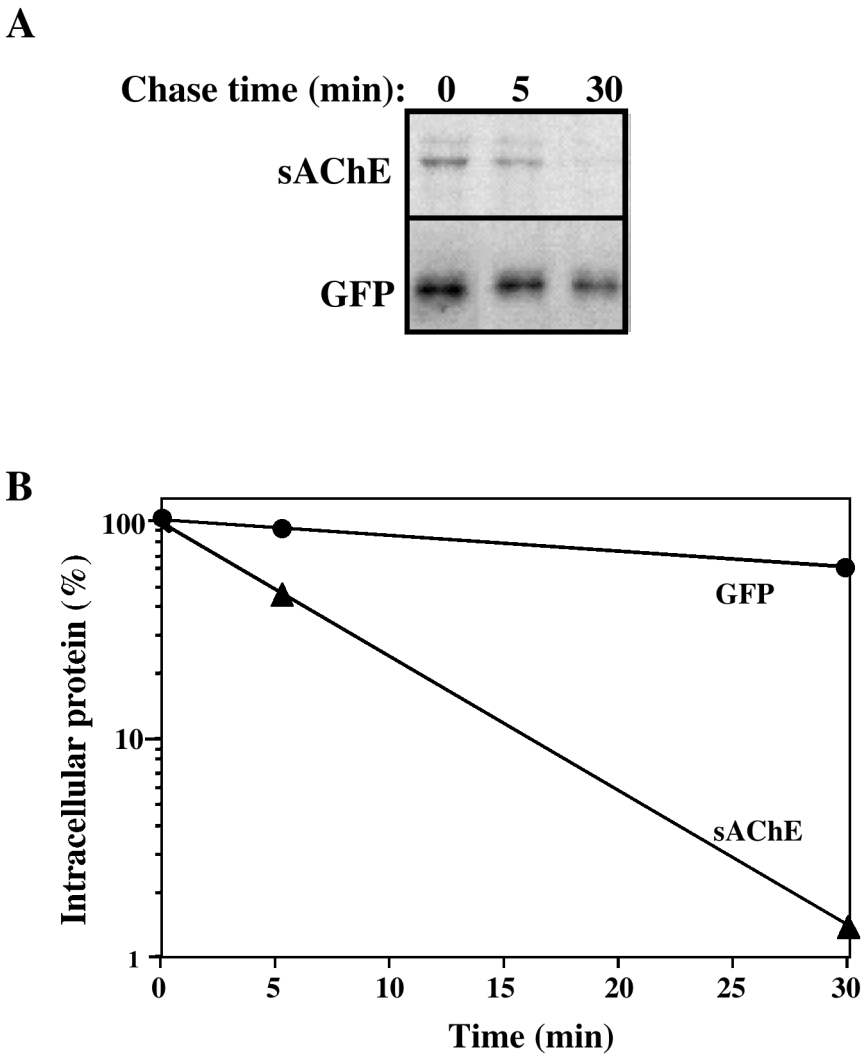

Figure 35: Pulse-chase analysis of intracellular AChE and GFP in transformed *B. brevis* cell clones. AChE- and rGFP-transformed cell clones were subjected to metabolic labeling with [^{35}S] methionine/cysteine and then chased by adding non-labeled methionine/cysteine at excess. Cleared cell lysates prepared from recombinant GFP and AChE expressor cells harvested at various chase periods, were incubated with rabbit anti-GFP antibodies or mouse anti-AChE antibodies, and then adsorbed with Protein G. (A) Analysis of immunoprecipitates by reducing SDS-PAGE followed by fluorography. (B) Protein band intensities were determined by densitometry of the fluorograms and the relative intracellular protein levels were plotted against chase time points.

Taken together, these results clearly indicate that the low yield of recombinant AChE in transformed *B. brevis* cells stems from a marked intracellular instability of the protein product. Seemingly, some features of the rHuAChE molecule predestine the newly synthesized protein product to rapid degradation within the *Bacillus* cells.

To overcome this problem, modified *Bacillus* cells displaying attenuated proteolytic performance should be examined for their ability to sustain rHuAChE production. One should however keep in mind that protease-deficient bacterial cells are often impaired in their ability to propagate and therefore do not always sustain high level production of recombinant proteins. The effective expression of functional human AChE may therefore require exploitation of specialized expression systems of eukaryotic origin to provide a cellular environment that supports proper folding of eukaryotic proteins. We therefore initiated studies with a yeast-derived expression system to evaluate its ability to support cost-effective high-level production of recombinant HuAChE.

Expression of the Synthetic Human AChE Gene in *Pichia pastoris*

GC content and codon usage may play an important role in determining heterologous gene expression in *Pichia pastoris*. Comparison between the human AChE gene and the genome of *P. pastoris* (Nakamura *et al.*, 2000) demonstrates a substantial disparity in GC contents and codon usage (for examples see Fig. 27). However, the synthetic gene (sAChE) coding for the authentic human AChE that we have constructed for expression in various microorganisms (see above), was designed to suit expression of HuAChE in *Pichia pastoris* as well. This synthetic HuAChE coding gene is characterized by an overall GC content of 51.7%, as opposed to 65.2% in the original ΔC-HuAChE gene and by a codon usage that conforms to that of *P. pastoris,* to a much greater extent (Fig. 27).

To facilitate expression of human AChE in *P. pastoris* cells, both the synthetic and non-modified human AChE coding regions were cloned into the specialized *P. pastoris* expression vector, pPICZα, which includes the methanol-controlled AOX1 inducible promoter and the secretion signal sequence of the *Saccharomyces cerevisiae* MATα factor. These commonly used genetic elements have been shown in the past to promote high levels of expression and extracellular secretion of various heterologous proteins in *Pichia pastoris* (Cereghino and Cregg, 2000; Daly and Hern, 2005). Cloning was achieved by PCR amplification of the open reading frames of the synthetic and non-modified AChE genes, utilizing primers especially designed to include appropriate restriction sites for the in-frame insertion, downstream to the α-factor signal sequence and Kex2/STE13 cleavage sequence, Glu-Lys-Arg-Glu-Ala-Glu-Ala. AChE coding sequences, as well as sequences spanning the *Saccharomyces cerevisiae* MATα factor/AChE junction, were verified by DNA sequencing.

The *Pichia*- HuAChE expression vectors were introduced into two *Pichia* strains: KM71H, and GS115. The KM71H strain carries a mutation at the *aox1* locus, one of the two alcohol oxidase coding genes, resulting in a slow growth phenotype on methanol medium (Mut^S phenotype). The GS115 host strain has a wild-type *AOX1*, and thus can utilize methanol for fast growth (Mut^+ phenotype). AChE constructs were used to transform both the Mut^+ and the Mut^S strain, since previous studies (Macauley-Patrick *et al.*, 2005; Cos *et al.*, 2005) have shown that one of the two phenotypes may favor better expression of a given heterologous protein, and that there is no rule by which one may predict beforehand which would allow higher levels of expression of recombinant human AChE.

Competent yeast cells of both strains were prepared according to the manufacturer's instructions, and conditions for optimal electroporation yields were determined. The transformed yeast cells were selected on YPD plates containing 100μg/ml zeocin. Under these conditions (1500V; 50μF; 10msec; 5 μg linearized linear DNA) 100-300 Zeocin resistant yeast colonies were generated per transformation. Ten resistant colonies of KM71H-synHuAChE, and GS115-synHuAChE, picked at random, were examined for secreted AChE production following growth and 72h of induction and were found to exhibit significantly different levels of secreted AChE activity, ranging from 9 to 300mU/ml. These findings suggest that an extensive screening of individual transformant clones will be required for the identification of clones expressing rHuAChE at very high levels.

As an initial step preceding the screening procedure, we set out to determine the various parameters (e.g. composition and pH of growth medium, aeration, temperature), which may influence yeast cell growth and recombinant protein production. To this end, we first compared the levels of secreted active rHuAChE of a representative KM71H AChE producer clone when propagated and induced in 50 ml test tubes containing 5 ml of medium adjusted to pH 6.0 or 7.0. Following 144 hours of methanol induction (0.5%) secreted AChE levels were approximately 50 and 350 ng/ml, at pH 6.0 and 7.0, respectively (Fig. 36). Cell densities at the two different pH conditions were similar throughout the induction phase (for instance, 72 hours post-induction, OD_{550} values at pH 6.0 and pH 7.0 were 25.2 and 26, respectively), suggesting that the unequal secreted AChE levels is not due to differences in the growth rates of the two cell cultures. It therefore seems that the pH conditions affect either the production/secretion or the stability of the secreted rHuAChE product.

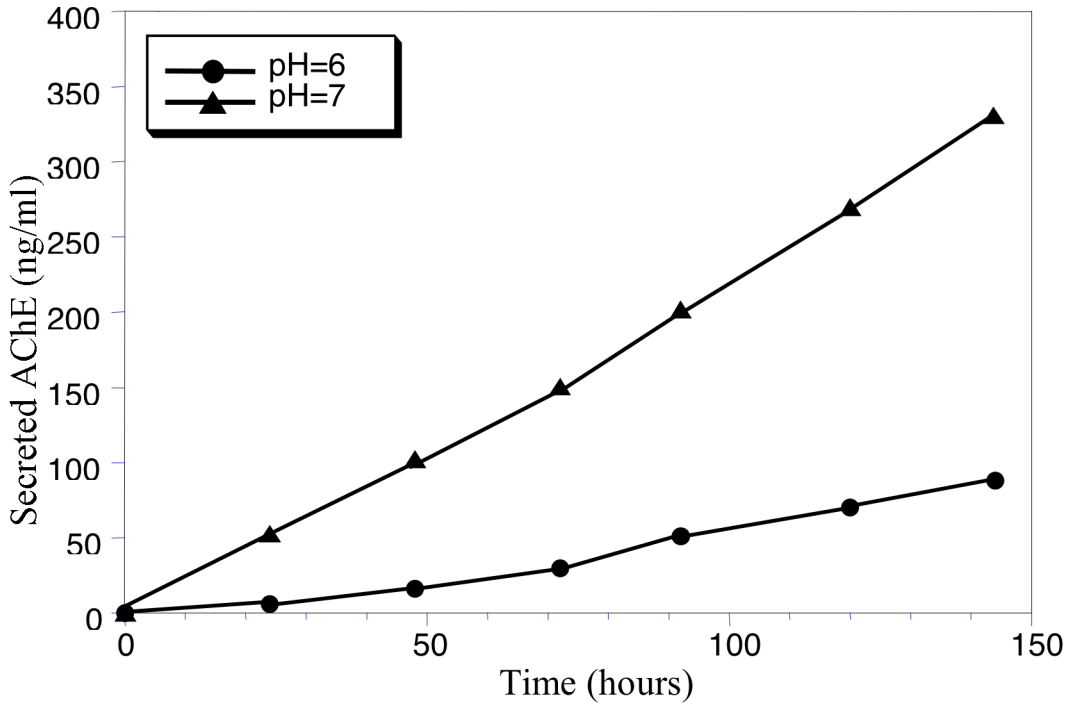

Figure 36: **AChE activity secreted by a KM71H produce cell clone at different pH conditions.** A KM71H AChE producer cell clone was propagated in growth medium for 48 hrs. Cells were then diluted in parallel into test tubes containing 5 ml of induction medium adjusted to pH 6.0 and to pH 7.0. Cells were incubated at 28^0C, 150 RPM and 0.5% methanol was added daily. AChE activity was determined in samples removed at the indicated time points.

To determine whether the pH indeed affects rHuAChE stability in the culture medium, purified rHuAChE was added in parallel to induction medium (BMMY medium) adjusted to pH 6.0 and to pH 7.0, and residual enzymatic activity was monitored at different time points following incubation at 28^0C. While incubation of HuAChE at pH 6.0 for 120 hours led to a loss of 30 % of initial activity, incubation of the purified enzyme at pH 7.0 for the same period of time led to a loss of only 7 % of initial activity (Fig. 37). Thus, the apparent difference in AChE levels observed under the different pH conditions may be attributed, at least in part, to a differential stability of the secreted enzyme product.

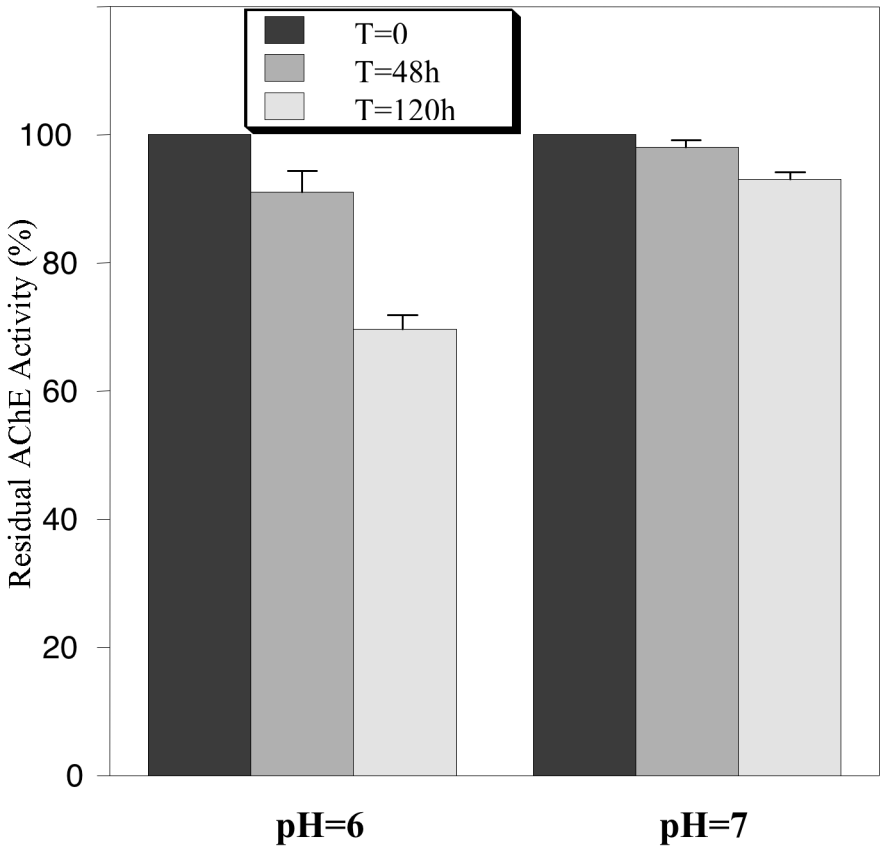

Figure 37: **Stability of purified AChE in induction medium at different pH conditions.** Purified rHuAChE (5 units) was added to 5 ml of induction medium adjusted to pH 6.0 and to pH 7.0 and incubated at 28^0C. Residual AChE activity was determined in samples removed at the indicated time points.

We next evaluated the influence of temperature on human AChE production levels in the *P. pastoris* system. To this end, the representative KM71H AChE producer clone was grown in propagation medium (BMGY medium) for 72 hours at 30^0C, cells were then washed and re-fed with induction medium (BMMY medium) and incubation was continued for an additional 96 hours at either 30^0C or 22^0C. Methanol (0.5%) was added during the induction phase at 24-hour intervals. Examination of AChE activity in medium samples removed at various time points during the induction phase, allowed us to determine that secreted enzyme levels were considerably higher when cells were induced at 30^0C (Fig. 38). Cell densities were similar following induction at the two different temperatures, indicating that elevating the temperature from 22^0C to 30^0C directly affects production and/or secretion rates of the recombinant product, rather than affecting cell growth rate.

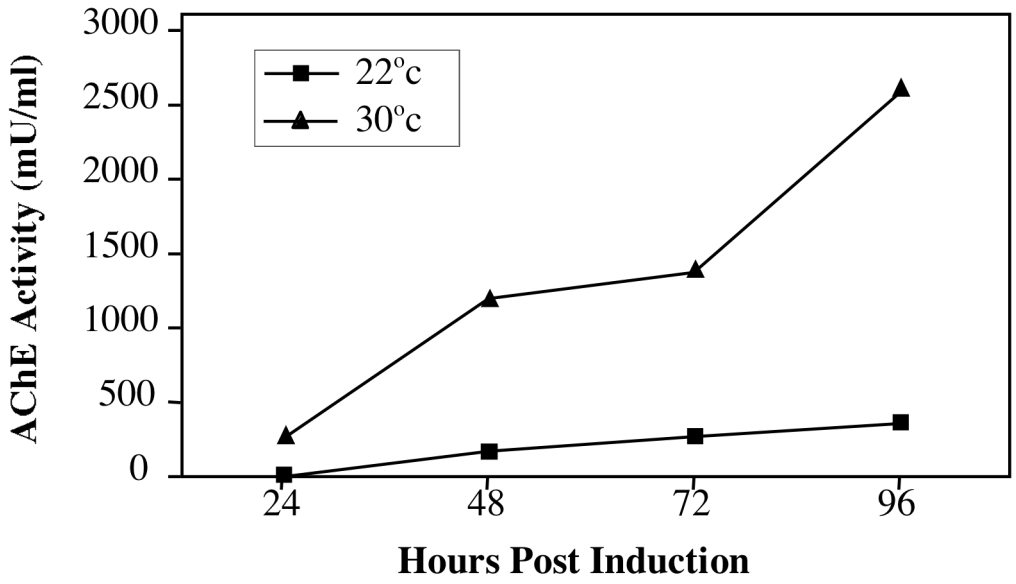

Figure 38: **AChE activity secreted by a KM71H producer cell clone at different temperature conditions.** A KM71H AChE producer cell clone was propagated in growth medium for 72 hours at 30^0C, cells were then transferred to induction medium for an additional 96 hours at either 30^0C or 22^0C. Methanol (0.5%) was added daily. AChE activity was determined in samples removed at the indicated time points.

The conditions determined for the efficient expression and secretion of bioactive rHuAChE in *P. pastoris* transformant cells will be implemented for the selection of individual transformed *P. pastoris* cells exhibiting exceedingly high levels of rHuAChE production, which may serve for cost-effective large-scale production of the recombinant enzyme.

VII. STEREOSELECTIVITY TOWARD VX IS DETERMINED BY INTERACTIONS WITH RESIDUES OF THE ACYL POCKET AND THE PERIPHERAL ANIONIC SITE OF AChE

INTRODUCTION

The catalytic efficiency of acetylcholinesterase and its high reactivity toward both covalent and noncovalent inhibitors are believed to originate from the unique architecture of the AChE active center (Kaplan *et al.*, 2001, 2004; Barak *et al.*, 2002;). Elements of this architecture, unraveled during over a decade by x-ray crystallography (Sussman *et al.*, 1991; Bourne *et al.*, 1995; Kryger *et al.*, 2000; Harel *et al.*, 2000), site directed mutagenesis and kinetic studies of the AChE mutants (Shafferman *et al.*, 1992a, b; Radic *et al.*, 1992, 1993; Vellom *et al.*, 1993; Ordentlich *et al.*, 1993, 1998a, b; Barak *et al.*, 1994; Ariel *et al.*, 1998), include a) the esteratic site containing the active site serine; b) the "oxyanion hole" consisting of residues Gly120(118*), Gly121(119) and Ala204(201); c) the "anionic subsite" or the choline binding subsite -Trp86(84) ; d) the hydrophobic site for the alkoxy leaving group of the substrate containing an "aromatic patch" that includes residues Trp86(84), Tyr337(330) and Phe338(331); e) the acyl pocket - Phe295(288) and Phe297(290) and f) the peripheral anionic site (PAS) localized at or near the rim of the active site gorge and consisting of residues Asp74(72), Tyr72(70), Tyr124(121), Trp286(279), Tyr341(334). Among the AChE ligands that have been used to probe the molecular environment of the active center, organophosphorus inhibitors such as dialkyl phosphates and methylphosphonates, are particularly suitable. Their unusually high reactivity toward the enzyme indicates efficient accommodation by the active center binding elements (Hosea *et al.*, 1995, 1996; Ordentlich *et al.*, 1996, 1999; Barak *et al.*, 2000). The high affinity toward OP inhibitors may result from their ground state tetrahedral geometry that mimics to some degree the spatial disposition of the intermediate ACh-AChE adduct (Hosea *et al.*, 1995; Ordentlich *et al.*, 1996). In the noncovalent OP-AChE complex, accommodation of the tetrahedral phosphoryl moiety includes polar interactions of the phosphyl oxygen with the oxyanion hole as well as that of His447 with the phosphate (or phosphonate) alkoxy oxygen. The alkyl moieties of the inhibitor are contained within the hydrophobic domains of the active center (acyl pocket and the hydrophobic patch), with the spatial differences between those sites presumably

* Numbers in parentheses refer to positions of analogous residues in TcAChE according to the recommended nomenclature (Massoulie *et al.*, 1992)

contributing to the inherent asymmetry of the AChE active center environment (Ordentlich *et al.*, 1999). The resulting stereoselectivity in particular with respect to methylphosphonofluoridates were utilized for in depth investigation of the hydrophobic and steric interactions with the structural elements of the active center (Ordentlich *et al.*, 1999). Early modeling studies attributed the 10^4-fold stereoselectivity of AChE toward the P^S-enantiomer of sarin mainly to the restrictive dimensions of the acyl pocket (Barak *et al.*, 1992). More recent studies with the diastereomers of soman suggest that a more complex array of interactions is affecting affinity and reactivity in the corresponding phosphylation reactions (Ordentlich *et al.*, 1999). In the case of phosphonofluoridates those interactions do not seem to include the leaving group and therefore interactions with the fluorine do not contribute to AChE stereoselectivity toward soman.

Interaction of the AChE active center with OP agents bearing positively charged leaving group is characterized by additional polar interaction that should affect the affinity as well as the stereoselectivity toward these inhibitors (Hosea *et al.,* 1996; Shafferman *et al.,* 1998; Kovarik *et al.,* 2003). Indeed, AChE inhibition studies with various charged and noncharged O-ethyl methylphosphonothioates demonstrated the contribution of such polar interactions to the reactivities of the respective inhibitors (Kabachnik *et al.,* 1970). All those reactions result in the same phosphonylation product (O-ethyl methylphosphono-AChE) the structure of which has been recently determined by x-ray crystallography, following AChE phosphonylation by VX (Millard *et al.,* 1999b). Also, AChE stereoselectivity toward certain O-alkyl S-[(trimethylamino)ethyl] methylphosphono-thioates was found to be much lower than that found for analogous phosphonofluoridates (Hosea *et al.,* 1996; Shafferman *et al.,* 1998). These studies indicated also that the thiocholine leaving group of these inhibitors is oriented toward the gorge entrance and that residue Asp74 is a primary determinant in AChE specificity for cationic organophosphorus agents (Hosea *et al.,* 1996). This finding is quite surprising in view of the x-ray structures of AChE in complex with noncovalent inhibitors like edrophonium (Harel *et al.,* 1993) or conjugated with covalent modifiers like TMTFA (Harel *et al.,* 1996) that show invariably that the ammonium cationic head points toward the anionic subsite residue Trp86 and being quite remote from Asp74.

In the present report we provide data regarding the origins of HuAChE stereoselectivity toward the enantiomers of VX determined by comparison with their noncharged isosteres as well as with the symmetrical diethyl phosphates echothiophate and its noncharged analogue. Our results indicate that in the case of VX stereoselectivity is a result of multiple interactions

involving several elements of the active center and the peripheral anionic site, including polar interactions with the charged leaving group.

METHODS

Enzymes and Reagents

Mutagenesis of AChE was performed by DNA cassette replacement into a series of HuAChE sequence variants, which conserve the wild-type coding specificity (Soreq *et al*., 1990) but carry new unique restriction sites (Shafferman *et al*., 1992a). Generation of mutants D74N, D74E, W86A, W86F, G122A, W286A, F295A, F297A, Y337A, F338A, and Y341A was described previously (Shafferman *et al*., 1992a, 1992b; Ordentlich *et al*., 1995, 1996, Barak *et al*., 1995). The D74E mutant was introduced by replacing the AccI-EspI DNA fragment of the pAChE-w4 variant (Shafferman *et al*., 1992a) with the respective synthetic DNA duplexes carrying the mutated GAG (Glu) codon.

Expression of recombinant HuAChE and its mutants in a human embryonal kidney-derived cell line (HEK-293) (Velan *et al*., 1991; Shafferman *et al*., 1992a, Kronman *et al*., 1992) and generation of all the mutants were described previously (Shafferman *et al*., 1992a, 1992b; Ordentlich *et al*. 1993; Barak *et al*., 1995). Stable recombinant cell clones expressing high levels of each of the mutants were established according to the procedure described previously (Kronman *et al*., 1992). Acetylthiocholine iodide (ATC) and 5,5-dithiobis(2-nitrobenzoic acid) (DTNB) were purchased from Sigma.

Organophosphate Inhibitors

The enantiomers of VX [*O*-ethyl S-(2-diisopropylaminoethyl) methylphosphonothioate] were synthesized by following a literature procedure (Hall *et al*., 1977). The final reaction step was modified by using *N,N*-diisopropylaziridinium chloride rather than *N,N*-diisopropylaminoethyl chloride that gave the pure enantiomers without further purification: ^{1}H NMR ($CDCl_3$) δ 1.00 (d, *J* = 6.5 Hz, 12H), 1.33 (t, *J* = 7.0 Hz, 3H), 2.78 (m, 2H), 2.99 (septet, *J* = 6.4 Hz), 4.11 (m, 2H); ^{31}P{^{1}H} NMR δ 51.14; $[\alpha]^{20}_{D}$ = 31.0° (*R*), -30.2° (*S*).

Enantiomers of nc-VX [O-ethyl S-(3-isopropyl-4-methylpentyl) methylphosphonothioate] were synthesized from the enantiomeric O-ethyl methylphosphonothioate sodium salt (Berman and Leonard, 1989) and 3-(2-bromoethyl)-2,4-dimethylpentane.

Kinetic Studies

HuAChE activity was assayed according to the method of Ellman *et al*. (1961) in the presence of 0.1 mg/ml BSA, 0.3 mM DTNB, 50 mM sodium phosphate buffer (pH 8.0), and

various concentrations of ATC at 27 °C and monitored with a Thermomax microplate reader (Molecular Devices).

Measurements of phosphorylation rates for VX and nc-VX were carried out with at least four different concentrations of VX and nc-VX (PX), and enzyme residual activity (E) at various times was monitored. The apparent bimolecular phosphorylation rate constants (k_i) determined under pseudo first-order conditions were computed from the plot of slopes of ln(E) versus time at different inhibitor concentrations. Rate constants under second-order conditions were determined from plots of ln{E/[I_o - (E_o - E)]} versus time (Ordentlich *et al.*, 1996). Both VX and nc-VX were stable in the reaction medium (phosphate buffer) within the time scale of the kinetic experiments. The half-life time ($t_{1/2}$) for hydrolysis of both inhibitors was more than 100 h as determined by $^{31}P\{^{1}H\}$ NMR. This estimation is in accordance with measurement of VX stability at pH 8 in an aqueous solution (Epstein *et al*., 1974).

Determination of the bimolecular rate constants for phosphorylation by echothiophate and nc-echothiophate was carried out following the double-reciprocal method of Hart and O'Brien (1973), as described previously (Ordentlich *et al*., 1996). Apart from bimolecular rate constants, this method allows for evaluation of the apparent dissociation constant for the enzyme inhibitor Michaelis complex (K_d) k_{-1}/k_1) and the phosphylation rate constant of the reaction (k_2).

Molecular Dynamics Simulations

Simulations of the HuAChE Michaelis complexes with VX^S and VX^R were performed using the AMBER 5.0 suite of programs with an all atom parameter set. Characterization and visual examination of the molecular structures were carried out using the molecular modeling package SYBYL 6.7 running on an SGI Octane workstation. The starting conformation of the enzyme was obtained from the X-ray structure of the HuAChE fasciculin complex model (Kryger *et al*., 2000; Protein Data Bank entry 1b41).

The rim of the active site gorge as well as the active center was solvated by adding a spherical cap of water (using the SOL option of AMBER). The cap waters were restrained by a soft half-harmonic potential to avoid evaporation without affecting the protein movement. The part of the complex included in the simulation (using the belly option in AMBER) was comprised of residues in the active center gorge and around the ligand as well as the ligand itself (150 residues were included, and the number varied slightly depending upon the definition of the belly region for the specific simulation experiments). Partial charges of the VX enantiomers were assigned the Del Re method implemented in SYBYL. Model

optimization and dynamics simulations were carried out according to a protocol described previously (Kaplan *et al.*, 2004).

RESULTS

Preparation of organophosphate inhibitors: Resolved O-ethyl methylphosphonothioic acids, which served as starting materials for both the VX and the nc-VX enantiomers (Fig. 39), were synthesized following the procedure of Berman and Leonard (1989). S- alkylation of the resolved enantiomers, using N,N-diisopropylaziridinium chloride, yielded pure VX enantiomers. This procedure was found more convenient than that using N,N-diisopropylaminoethyl chloride, as reported earlier (Hall *et al.,* 1977). Analogous preparation of the nc-VX enantiomers was carried out using 3-(2-bromoethyl)-2,4-dimethylpentane as the alkylating agent. The resulting nc-VX were obtained >95% enantiomerically pure as shown by ^{1}HNMR using the chiral reagent [R]-2,2,2-trifluoro-1-(9-anthryl)ethanol. O,O-diethyl S-(3,3-dimethylbutyl) phosphorothioate ("nc-echothiophate") was prepared from 3,3-dimethylbutyl bromide (Ordentlich *et al.,* 1993) and potassium salt of diethyl thiophosphoric acid.

Reactivity of HuAChE toward VX and nc-VX enantiomers: Reactivity of recombinant wild type HuAChE toward VX^S was 115-fold higher than toward the VX^R with the respective values of the bimolecular rate constants being $1.4x10^8$ $min^{-1}M^{-1}$ and $1.2x10^6$ $min^{-1}M^{-1}$. Such HuAChE stereoselectivity toward VX enantiomers is consistent with earlier reports on AChE reactivities toward VX (Hall *et al.,* 1977; Benschop and De Jong 1988) and toward other charged methylphosphonothiocholines (Hosea *et al.,* 1996; Berman and Leonard, 1989). In particular, AChE from bovine erythrocytes was reported to display a 200- fold stereoselectivity toward the VX^S enantiomer (Benschop and De Jong 1988).

The HuAChE enzyme displayed 60-fold stereoselectivity toward the noncharged nc-VX^S (Figure 39), with reactivity toward this enantiomer being about 12500-fold lower than that toward VX^S (Tables 7,8). The corresponding reactivity toward the nc-VX^R was exceedingly low (the value bimolecular rate constant k_i was $2x10^2$ $min^{-1}M^{-1}$) and the actual measurements of this constant, as well as of those for other HuAChE enzymes, was made possible only by the stability of the inhibitors in buffer solutions, and by the ability to produce sufficient amounts of recombinant enzyme proteins, using the remarkably efficient HEK 293 expression system (Shafferman *et al.,* 1992a; Kronman *et al.,* 1992).

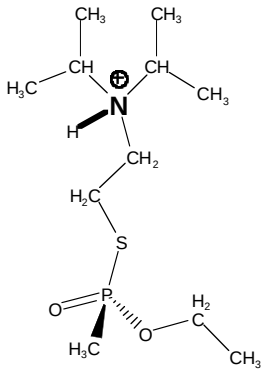

VX^S

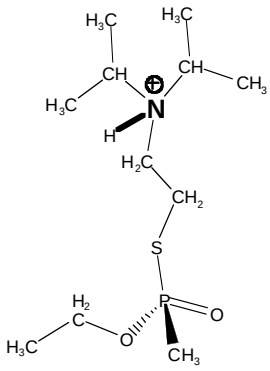

VX^R

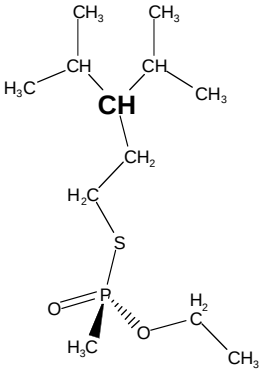

nc-VX^S

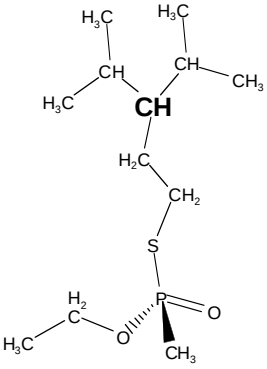

nc-VX^R

Figure 39: **Chemical formulae of VX enantiomers and their noncharged isosteres.** The protonated forms of both VX^S and VX^R are shown since the charged species are present under our experimental conditions (pK_a value for VX was recently reported to be 9.4, see Van der Schans, *et al.,* 2003)

Table 7: **Apparent bimolecular rate constants[a] (k_i) of phosphonylation of HuAChE enzymes by VX^S and VX^R.**

	VX^S		VX^R		
HuAChE	k_i ($x10^{-4}xM^{-1}xmin^{-1}$)	WT/ mutant	k_i ($x10^{-4}xM^{-1}xmin^{-1}$)	WT/ mutant	VX^S/VX^R
Wild Type	13700	1	118.0	1	115
F295A	1600	9	360.0	0.3	5
F297A	1560	9	22.5	5	70
F295A/F29	18	760	3.4	35	5
W86F	465	30	10.0	12	50
W86A	3	4500	0.1	980	30
D74N	107	130	48.0	2.5	2
D74E	5900	2	31.0	4	190
W286A	13000	1	85.0	1	170
Y341A	5100	3	13.0	9	370
Y337A	4000	3	30.0	4	130
F338A	2700	5	30.0	4	90
G122A	7	2000	0.3	400	25

[a]Values represent mean of triplicate determinations with standard deviation not exceeding 20%.

Table 8: **Apparent bimolecular rate constants[a] (k_i) of phosphonylation of HuAChE enzymes by nc-VX^S and nc-VX^R.**

	nc-VX^S		nc-VX^R		
HuAChE	k_i ($x10^{-4}$x $M^{-1}xmin^{-1}$)	WT/ mutant	k_i ($x10^{-4}$x $M^{-1}xmin^{-1}$)	WT/ mutant	VX^S/VX^R
Wild	1.1	1	0.02	1	60
F295	0.5	2	0.03	1	20
F297	3.4	0.3	0.02	1	170
F295	0.04	27	0.003	7	13
W86F	0.6	1.8	0.025	1	25
W86A	0.3	3.7	0.01	2	30
D74N	2.0	0.5	0.03	1	70
D74E	0.9	1	0.01	2	90
W286	1.5	0.7	0.015	1	100
Y341	2.5	3	0.02	1	23
Y337	63.0	0.03	0.07	0.3	900
F338	0.9	1	0.003	7	300
G122	0.02	60	0.0004	50	50

[a]Values represent mean of triplicate determinations with standard deviation not exceeding 20%.

Wild type HuAChE displayed a 850-fold higher reactivity toward the diethyl phosphate echothiophate than toward its noncharged isostere nc-echothiophate (see Table 9). Since for both phosphates disposition of the phosphyl ethoxy substituents with respect to the HuAChE active center should be similar, the different reactivities signify the contribution of interactions with the charged leaving group. Thus the large reactivity differences between the VX enantiomers and their corresponding noncharged isosteres (nc-VX) may have also resulted predominantly from accommodation of the diisopropylammonium group in the active center.

Table 9: **Apparent bimolecular rate constants[a] (k_i) of phosphonylation of HuAChE enzymes by Echothiophate and nc-Echothiophate**.

	Echothiophate			nc-Echothiophate		
HuAChE	k_i ($x10^{-4}$x $M^{-1}xmin^{-1}$)	k_2 (min^{-1})	K_i ($x10^{-6}M$)	k_i ($x10^{-4}xM^{-1}xmin^{-1}$)	k_2 (min^{-1})	K_i ($x10^{-6}M$)
Wild Type	154	3.7	2.4	0.18	0.6	325
F295A	6000	0.8	0.0013	1.46	0.95	65
F297A	58	4.4	7.6	0.2	0.3	146
F295A/F297	45	ND[b]	ND	0.02	ND	ND
W86F	17	0.7	4.2	0. 25	0.56	220
W86A	0.08	0.8	1020	0.02	0.8	4570
D74N	3.8	5.5	147	0.96	0.55	57
D74E	32	1.1	3.4	0.18	0.92	510
D74G	14	0.9	3.2	0.72	0.6	83
W286A	260	1.7	0.64	1.07	0.6	55
Y341A	40	1.2	3.0	0.4	0.97	244
Y337A	34	1.8	5.5	0.06	0.34	540
F338A	12	1.7	14.1		0.13	1500

[a] Values represent mean of triplicate determinations with standard deviation not exceeding 20%.
[b] Not determined

While interactions with the charged leaving group seem to consist the major contribution to the HuAChE affinity toward the two VX enantiomers, the question regarding the specific interactions contributing to the 115-fold stereoselectivity toward VX^S remains open. Since stereoselectivity has usually been associated with perturbations at the acyl pocket (Barak *et al.,* 1992; Ordentlich *et al.,* 1993, 1999), the lower reactivity of HuAChE toward VX^R may still be a result of inferior accommodation of the ethoxy substituent. Comparison of the bimolecular rate constant (k_i) for HuAChE phosphonylation by VX^R and by echothiophate shows quite similar values ($1.2x10^6$ $min^{-1}M^{-1}$ and $1.5x10^6$ $min^{-1}M^{-1}$ respectively), suggesting that such interactions of the ethoxy moiety may indeed determine the affinities of these two charged organophosphorus inhibitors. On the other hand, HuAChE reactivity toward nc-echothiophate was found to be only 6-fold lower than toward nc-VX^S, indicating that replacement of a methyl group by ethoxy group in the acyl pocket results roughly in a 6-fold decrease in binding affinity. This effect seems too low to account for the observed HuAChE stereoselectivity toward VX^S.

Therefore it was important to investigate the dependence of stereoselectivity toward VX enantiomers on interactions with the different components of the active center functional architecture. To this end, enzyme derivatives with modifications introduced by site directed mutagenesis at active center subsites involved in ligand accommodation such as the acyl pocket, anionic subsite, hydrophobic subsite, peripheral anionic site and the loop of the oxyanion hole, were introduced. Kinetic evaluation of the reactivity characteristics of these HuAChE enzymes toward the charged and non-charged VX as well as toward the symmetric phosphate echothiophate allowed for characterization of the main elements of the HuAChE chirality toward charged methylphosphonates.

Stereoselectivity of HuAChE enzymes carrying mutations at the acyl pocket: Replacements of the acyl pocket residues Phe295 or Phe297 by alanine had quite different effects on stereoselectivity toward the VX^S enantiomer. While the F295A enzyme was only 5-fold more reactive toward the VX^S than toward the VX^R enantiomer, the corresponding ratio for the F297A was 70-fold, resembling that of the wild type HuAChE (see Table 7). The decrease in stereoselectivity of the F295A enzyme resulted mainly from its lower reactivity toward VX^S (9-fold) rather than from increased reactivity toward VX^R (3-fold, see Table 7). Thus, while structural perturbation at position 295 of the acyl pocket affects stereoselectivity toward the VX^S enantiomer, the basis for the differential reactivity does not seem to involve steric exclusion from the acyl pocket. The notion that steric congestion at the acyl pocket does not determine HuAChE stereoselectivity toward VX^S is supported also by reactivities of the F297A enzyme toward the VX enantiomers. In this case the mutated enzyme is less reactive toward both VX^S (9-fold) and VX^R (5-fold), suggesting a suboptimal accommodation of the phosphonate in the active center irrespective of the substituent adjacent to the acyl pocket

Mutations at positions 295 and 297 in HuAChE had only a small effect on reactivity of the corresponding enzymes toward the nc-VX enantiomers (all effects were within factor 3, see Table 8). These findings seem to suggest that there is nearly no energetic penalty for accommodating the nc-VX^R ethoxy substituent in the HuAChE acyl pocket.

Replacement of the aromatic residue at position-295 resulted in a 40-fold reactivity increase toward the diethyl phosphate - echothiophate, relative to the wild type enzyme. Corresponding replacement at position-297 had practically no effect, suggesting that orientation of the ethoxy group with respect to the acyl pocket in the echothiophate-HuAChE

complex is somewhat different from that of the corresponding complex with the VX^R enantiomer. This different reactivity toward echothiophate may have to do with the other ethoxy substituent since similar effects, due to mutations at the acyl pocket, were reported for neutral diethyl phosphates like DEFP and paraoxone (Ordentlich *et al.,* 1996).

The double mutant F295A/F297A exhibits lower affinity toward both VX and nc-VX, with consistently larger effects for the P^S enantiomers (see Tables 7, 8). Interestingly, the reactivity decline toward VX^S is much more pronounced than that toward nc-VX^S (760-fold and 27-fold respectively), suggesting that the reactivity decrease does not seem to be a result of deficient accommodation of the methyl group. It appears also that the outcome of removing aromatic moieties from the acyl pocket, (e.g. enhanced mobility of the catalytic His447 see Kaplan *et al.,* 2001, 2004; Barak *et al.,* 2002) has larger effect on the presumably more rigidly oriented VX^S within the Michaelis complex as compared to the neutral nc-VX^S.

Stereoselectivity of HuAChE enzymes carrying mutations at the anionic subsite – choline binding site: Replacement of residue Typ86 by alanine had a dramatic effect on the reactivity toward both VX enantiomers, yet only a minor effect on stereoselectivity toward the VX^S (Table 7). The decrease of the W86A HuAChE reactivity toward the VX^S and VX^R enantiomers as compared to the wild type enzyme (the values of bimolecular rate constants decreased by 4500-fold and almost 1000-fold respectively, see Table 7) was compatible with what was observed in the past for other covalent or noncovalent charged ligands (Ordentlich *et al.,* 1993, 1995; Ariel *et al.,* 1998; Kabachnik *et al.,* 1970; Millard *et al.,* 1999b; Shafferman *et al.,* 1992b). The corresponding effects of the replacement of Trp86 by phenylalanine were much smaller and consistent with the well established role of the aromatic residue at position - 86 as the main interaction locus of the charged moieties of AChE ligands (Ordentlich *et al.,* 1995; Ariel *et al.,* 1998). Similarly, W86A was 1925-fold less reactive toward echothiophate than the wild type enzyme (Table 9). These effects are considerably higher than those reported for interaction of similar charged methylphosphonates, P^S-O-cycloheptyl methylphosphonylthiocholine, (40-fold) or the corresponding P^R- enantiomer (33-fold) with W86A mutant of the mouse AChE (Hosea *et al.,* 1996).

Mutations at the anionic subsite had only minor effects on HuAChE affinities toward the nc-VX enantiomers and the nc-echothiophate (Tables 8, 9), demonstrating again that the role of the aromatic moiety at position-86 consists mainly of accommodating the charged moieties of

substrates and other charged ligands. However, reactivity of the W86A HuAChE toward nc-VX^S was still 10-fold lower than that toward VX^S, suggesting participation of other elements in the active center in accommodation of the charged leaving group. Similarly, reactivity of this enzyme toward nc-echothiophate was 4-times lower than that toward echothiophate (Table 9).

Stereoselectivity of HuAChE enzymes carrying mutations at the hydrophobic subsite: Stereoselectivity toward VX^S as well as reactivity toward both VX enantiomers is only slightly affected by single replacements of elements of the hydrophobic pocket (aromatic patch, (Ariel *et al.,* 1998) residues Tyr337 and Phe338 (Table 7). The effects are small (~4-fold) and do not indicate disruption of major interactions with the active center environment. In view of this result it was rather surprising to find that replacement of this residue by alanine resulted in a 57-fold increase in affinity toward nc-VX^S, suggesting that the S-alkyl leaving group of nc-VX^S appears to interfere with the aromatic moiety of Tyr337 (Table 8). A small increase in affinity is observed also for the nc-VX^R and consequently the stereoselectivity of this enzyme toward nc-VX^S was ~900-fold. Such effect on stereoselectivity due to replacement of Tyr337 indicates that the leaving groups in VX and in nc-VX may point to somewhat different regions of the active site. Furthermore, the Y337A HuAChE was only 3-fold less reactive toward the nc-echothiophate than the wild type enzyme (Table 9), implying that the orientation of its leaving group, in the nc-echothiophate-Y337A complex, resembles more that of nc-VX^R than that of the VX^S (see Table 8). The findings indicate also that the positively charged leaving groups of either the VX enantiomers or echothiophate do not interact with the aromatic moiety of Tyr337 (Table 7, 9). In this respect the findings are consistent with our previously reported conclusion that residue Tyr337 is not a part of the anionic subsite participating in accommodation of the cationic head groups of AChE ligands (Ariel *et al.,* 1998), as suggested before (Harel *et al.,* 1996; Greenblatt *et al.,* 1999).

Stereoselectivity of HuAChE enzymes carrying mutations at the peripheral anionic site (PAS): Replacement of Asp74 by asparagine practically abolished stereoselectivity toward the VX^S enantiomer. The D74N HuAChE was 130-fold less reactive toward VX^S while its reactivity toward VX^R resembled that of the wild type enzyme (see Table 7). In contrast, substitution of the aspartate at position 74 by another acidic residue glutamate, yielded an

enzyme with nearly the same affinities toward both VX enantiomers as the wild type HuAChE. These results show that VX^S interacts with the acidic residue at position 74 of HuAChE, suggesting that in the case of VX enantiomers charged interactions of the leaving group are a major determinant of stereoselectivity. Thus, it is reasonable to expect that the charged leaving groups in the HuAChE Michaelis complexes of VX^S and VX^R assume somewhat different orientation, with the cationic head in the VX^S complex closer to the Asp74 carboxylate than in the corresponding VX^R complex.

Reactivity of the D74N HuAChE toward echothiophate was also 40-fold lower than that of the wild type enzyme (see Table 9), yet in this case the decrease may not result from loss of a specific electrostatic interaction of the cationic leaving group. This notion is suggested by the similar effects of replacing residue Asp74 by glutamic acid or by the noncharged residue glycine (5-fold and 10-fold respectively, see Table 9 and Shafferman *et al.,* 1998).

Replacement of Asp74 by asparagine had practically no effect on the reactivity toward nc-VX enantiomers (see Table 8). In addition, a minor (4-5-fold) increase was observed in the activity of D74N and D74G HuAChEs toward nc-echothiophate (Table 9). These findings are consistent with our previous observation that residue Asp74 contributes predominantly to binding of charged ligands in the HuAChE active center (Shafferman *et al.,* 1992b, 1998).

Replacement of other components of the PAS Tyr341 and Trp286 had only limited effect on reactivity toward VX enantiomers. The most pronounced effect was that due to substitution of position 341 by alanine on reactivity toward VX^R (9-fold). Also, these replacements had nearly no effect on affinities toward nc-VX enantiomers or nc-echothiophate (see Tables 7-9).

Stereoselectivity of HuAChE carrying mutation at position 122 next to the oxyanion hole: Residue Gly122 is adjacent to the oxyanion hole residues Gly120 and Gly121. Replacement of Gly122 by alanine was shown to introduce a methyl group into the space of the acyl pocket (Ordentlich *et al.,* 1998b, see also Harel *et al.,* 1996). As already reported, the reactivity of G122A toward phosphonates is affected to a larger extent than toward phosphates (Ordentlich *et al.,* 1998b), due to the size of the moiety in the immediate vicinity of the Ala122 methyl group (e.g. for DEFP reactivity of the G122A HuAChE was 95-fold lower than for the wild type HuAChE and for soman the corresponding ratio was 500 Ordentlich *et al.,* 1998b). In the case of VX^S the G122A HuAChE was 2000-fold less reactive, compared to the wild type enzyme while for VX^R the corresponding ratio is 400 (Table 7). Thus, G122A HuAChE displayed lower stereoselectivity, than the wild type

enzyme, toward the VX^S enantiomer (25-fold) probably due to impaired accommodation of the phosphonyl methyl group in the acyl pocket as a consequence of replacing the hydrogen by a methyl group in the G122A mutant. The G122A enzyme was also 260-fold less reactive toward echothiophate compared to the wild type HuAChE ($k_i = 6x10^3xM^{-1}xmin^{-1}$), suggesting that in the phosphate-G122A adduct the phosphate ethoxy group may be positioned in the acyl pocket more like that of VX^R (see Table 7) than like that of the homologous phosphate DEFP (Ordentlich *et al.,* 1998b). These observations may indicate that in the Michaelis complexes of both VX enantiomers or of echothiophate the methyl and the ethoxy moieties are located closer to Ala122 than in the corresponding complexes of DEFP or soman. Such proximity, which may be induced by the rigid orientation of the charged leaving group, suggests also that the corresponding phosphyl moieties are positioned closely to the oxyanion hole.

The reactivity of the G122A HuAChE toward the nc-VX^S enantiomer was 60-fold lower than that of the wild type enzyme (see Table 8). Such reactivity decrease is much smaller than could be expected from comparison to the corresponding ratios for both VX^S and soman (2000-fold and 500-fold respectively), again suggesting that accommodation of the nc-VX^S in HuAChE active center is quite different from that of the other phosphonates.

Molecular modeling of Michaelis complexes of HuAChE with VX enantiomers: The question of AChE stereoselectivity toward VX^S has already been addressed in the past by molecular dynamics simulations of the TcAChE-VX Michaelis complexes (Albaret *et al.,* 1997). In construction of the initial structures it was assumed that the cationic leaving group in both the VX^S and the VX^R complexes was oriented toward the peripheral anionic site and that the electrostatic interaction with Asp (72) contributes substantially to the accommodation of the charged diisopropylammonio moiety (Hosea *et al.,* 1996). Such assumption was consistent with the role played by residue Asp(72) in accommodating the charged groups of certain methylphosphonothiocholines in the Michaelis complexes with TcAChE (Hosea *et al.,* 1996). The simulations suggested that TcAChE stereoselectivity toward VX enantiomers resulted from impaired interaction of the VX^R with the oxyanion hole subsite (Albaret *et al.,* 1997). Our results, from kinetic studies with the wild type and the G122A enzymes, suggest however that in HuAChE both VX enantiomers appear to be well accommodated in the oxyanion hole. Furthermore, interactions with oxyanion hole seem to be crucial for HuAChE reactivity toward phosphate inhibitors and therefore a significant

misalignment of the P=O moiety with respect to this subsite could abolish the phosphylation process (Ordentlich *et al.*, 1998b). Thus it appeared interesting to examine the dynamic behavior of the HuAChE-VX complexes, especially in view of the finding, from kinetic studies, regarding the role of residue Asp74 in determining HuAChE stereoselectivity toward VX (Table 7).

In the present study molecular simulations of the HuAChE-VX complexes were performed assuming that proper orientation and proximity of the phosphorus atom to O^{γ}-Ser203 atom are essential for the phosphylation process and therefore should be kept throughout the simulation. In addition, interaction distances of the phosphyl oxygen from the oxyanion hole elements were maintained since polarization of the P=O bond was found to be of a crucial importance to subsequent chemical process. Therefore during optimization of the initial structures and the dynamic simulation runs the positioning of the VX P=O moieties was restrained with respect to the HuAChE active center. In the two diastereomeric initial structures of the VX-HuAChE Michaelis complexes the protonated diisopropylammonio group was juxtaposed with the anionic subsite Trp86 (see Table 10). Simulation experiments showed that for the VX^{R} complex there was no significant change in the positioning of the cationic head with respect to residues Trp86 and Asp74 (Fig. 40B). On the other hand, in the VX^{S} complex there is motion of the cationic head toward the gorge exit, shortening its distance from residue Asp74 (see Figs. 40A, 40C). Examination of the structures along the simulation trajectories suggested that orientation of the cationic leaving group was influenced by its interaction with the phosphonyl substituent pointing toward the acyl pocket. In the VX^{S} complex the phosphonyl methyl group is accommodated in the acyl pocket permitting the cationic leaving group to point toward the gorge entrance and to interact with both residues Trp86 and Asp74 (Fig. 40A). On the other hand, in the VX^{R} complex the ethoxy group is forced to point upward by the restricted space of the acyl pocket (see Fig. 40B). Such conformation of the ethoxy moiety interferes with the cationic leaving group inducing an alternative conformation where the diisopropylammonio group is displaced away from residue Asp74 (and toward residue Trp86), as compared to its orientation in the VX^{S} complex.

Table 10: Changes of relevant distances in the HuAChE Michaelis complexes of VX^S and VX^R following molecular dynamics simulation.

Distance	Initial Structures *(Å)*		Changes in Average simulated structures *(ΔÅ)*	
	VX^S	VX^R	VX^S	VX^R
$N_{G120} - O(=P)_{VX}$	2.97	2.98	0.12	0.22
$N_{G121} - O(=P)_{VX}$	2.88	3.18	-0.06	-0.21
$N_{A204} - O(=P)_{VX}$	3.40	3.10	0.27	0.10
$O^{\gamma}{}_{S203} - P_{VX}$	3.33	3.34	-0.03	0.16
$O^{\delta 1}{}_{D74} - N_{VX}$	7.30	7.69	-1.10	0.41
$C^{\delta 2}{}_{W86} - N_{VX}$	5.10	5.22	1.18	0.15

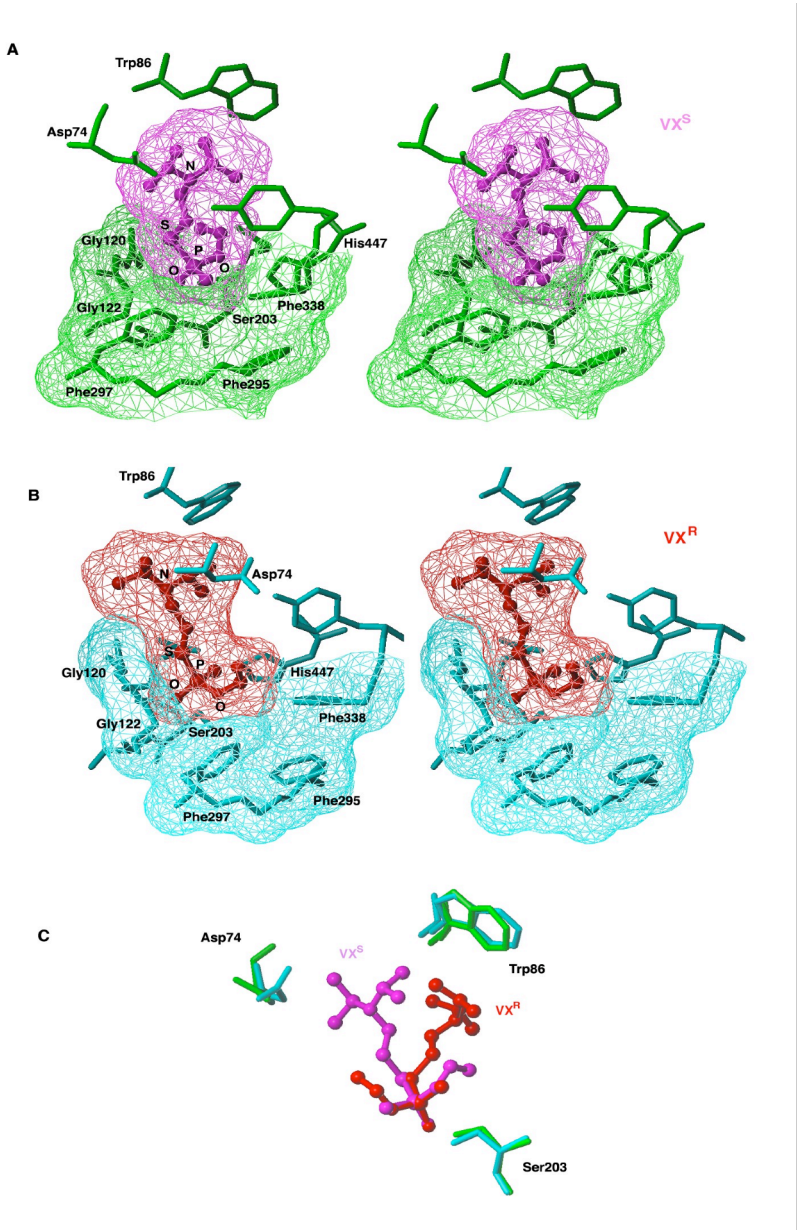

Figure 40: **Average structures from molecular dynamics simulations of Michaelis complexes of the VX^S and VX^R enantiomers with HuAChE.** Only amino acids adjacent to the inhibitor are shown and hydrogen atoms are omitted for clarity. Interatomic distances defining the relative orientation of the respective ligands are listed in Table 10. (A) Stereoview of the VX^S-HuAChE complex with the phosphonate depicted in magenta and the protein in green. The volumes of the VX^S and the molecular environment around the acyl pocket are shown as grid. (B) Stereoview of the VX^R-HuAChE complex with the phosphonate depicted in red and the protein in cyan. The volumes of the VX^R and the molecular environment around the acyl pocket are shown as grid. (C) Superposition of the VX^S-HuAChE and VX^R-HuAChE complex structures, using the Cα atoms of the residues shown and the respective phosphorus atoms as reference points. Note that the ammonio group of the VX^S complex (shown in magenta) is proximal to both Asp74 carboxylate and the indole moiety of Trp86, while that of the VX^R complex (shown in red) points exclusively in the direction of residue Trp86.

DISCUSSION

Early hypotheses (Jarv, 1984) and modeling experiments (Barak *et al.,* 1992) related the pronounced stereoselectivity of AChE toward methylphosphonofluoridates like sarin or soman to the structure of the acyl pocket. The main reason for this assessment was that the homologous enzyme butyrylcholinesterase (BChE), in which residues at positions corresponding to 295 and 297 are isoleucine and valine respectively (Harel *et al.,* 1992), was found to be more reactive than AChE toward bulky substrates like butyrylcholine (BCh) and organophosphorus inhibitors like diisopropyl phosphorofluoridate (DFP) as well as not stereoselective toward sarin (Ordentlich *et al.,* 1993, 1999; Vellom *et al.,* 1993; Hosea *et al.,* 1995; Boter *et al.,* 1971). Indeed, studies of HuAChE reactivity using site directed mutagenesis and enzyme kinetics suggested that the acyl pocket residues Phe295 and to a lesser extent Phe297 determine specificity toward acylating (substrates) and phosphylating agents (Ordentlich *et al.,* 1993, 1996) mainly by limiting the volume of the acyl pocket. A more recent examination of stereoselectivity in reactions of HuAChE active center mutants with diastereomers of soman, suggested that while the AChE acyl pocket is in fact the main determinant of the relative reactivity toward the P^S- and the P^R- diastereomers, the actual mechanism of stereoselectivity is only partially related to steric interference (Ordentlich *et al.,* 1999). Further inquiry into the consequences of structural modifications at the HuAChE acyl pocket led us to propose that residues Phe295 and Phe297 are also part of an aromatic system involved in "trapping" the catalytic His447 (Kaplan *et al.,* 2001; Barak *et al.,* 2002). Thus, modifications of the AChE acyl pocket may perturb the positioning of His447 and thereby impair the accommodation of tetrahedral species in the active center. Such modifications of the acyl pocket could be brought about either by accommodation of bulky groups, leading to a significant relocation of the side chains of both Phe295 and Phe297, or by replacement of these residues by aliphatic amino acids (Kaplan *et al.,* 2001, 2004; Barak *et al.,* 2002).

Structural characteristics of the acyl pocket seem also to play a role in determining HuAChE stereoselectivity toward VX^S, as demonstrated by the mere 5-fold stereoselectivity of the F295A and the F295A/F297A enzymes (see Table 7). For the latter, the 760-fold reactivity decrease toward the VX^S enantiomer was accompanied by only a 35-fold reactivity decline toward the VX^R. Apparently the overall effect of the double mutation at the acyl pocket, on reactivity toward VX^R, was smaller due to some compensating factor. Such compensation

could come from relief of steric pressure (due to removal of the bulky aromatic residues) on the ethoxy substituent in the acyl pocket. Yet, there is no evidence that accommodation of an ethoxy group results in perturbation of the acyl pocket. In fact, the lack of AChE stereoselectivity toward MEPQ (see Figure 41), where all the phosphorus substituents apart from the charged leaving group are identical to those of VX (Levy and Ashani, 1986), indicates that the acyl pocket accommodates equally well the methyl and the ethoxy substituents. Therefore, the different effects, due to modifications of the acyl pocket, on reactivity toward the VX^S and the VX^R enantiomers have to originate from interactions with other elements of the active center. Indeed, for both the VX^S and the VX^R enantiomers interactions of the charged leaving group appear to be another major determinant of HuAChE stereoselectivity. The findings that the D74N HuAChE was practically devoid of stereoselectivity toward VX^S and yet reactivity of this mutant toward VX^R was nearly equivalent to that of the wild type enzyme, indicated that the difference in HuAChE accommodation of the two VX enantiomers can be reduced to a single interaction of the charged phosphyl substituent with residue Asp74. Thus, while the diisopropylammonium moiety in Michaelis complexes of both VX^S and VX^R enantiomers interacts mainly with the anionic subsite residue Trp86, as demonstrated by the respective 980-fold and 4500-fold decreases in reactivity toward the W86A enzyme (Table 7), in the HuAChE-VX^S complex additional stabilization is provided by its interaction with the carboxylate of residue Asp74. In fact, interaction of the thiocholine leaving groups of certain O-alkyl S-[(trimethylamino)ethyl] methylphosphonothioates with residue Asp74 has already been suggested (Hosea *et al.,* 1996). However for these ligands both enantiomers interacted with Asp74 and their interaction with Trp86 was less pronounced.

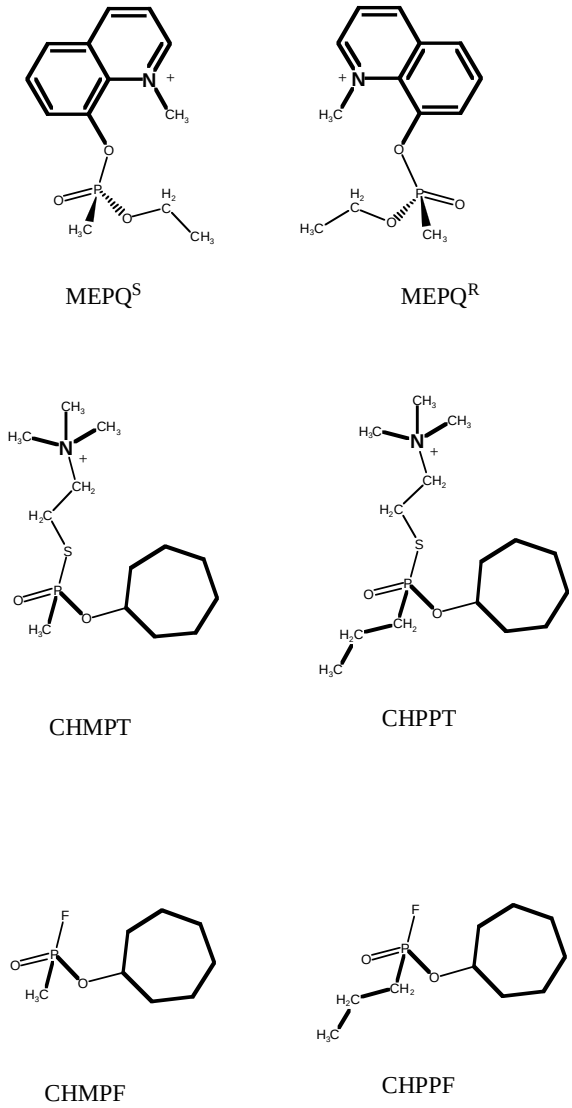

Figure 41: (A) Structural formulae of the MEPQ enantiomers which display nearly equivalent reactivity toward AChE (Levy and Ashani, 1986) while yielding the same adducts as the corresponding enantiomers of VX. (B) Formulae of O-cycloheptyl alkylphosphonate AChE inhibitors bearing thiocholine and fluorine as leaving groups (Berman, 1995). Note that while reactivities of the two methyl phosphonates CHMPT and CHMPF are similar, reactivity of CHPPT is much lower than that of CHPPF (see Berman, 1995 and text)

If stabilizing interaction of the diisopropylammonium moiety with Asp74 is possible in the VX^S Michaelis complex why is it absent in the corresponding VX^R complex. The reason for that is suggested by the molecular simulation experiments, which show the cationic moiety of VX^S to be located nearly 2 Å closer to the Asp74 carboxylate than the corresponding moiety of VX^R (see Table 10). Thus the respective locations of the VX cationic moieties seem to be determined by interactions with the phosphonyl ethoxy substituent. In the HuAChE-VX^S complex the ethoxy group, positioned in the hydrophobic pocket, allows for an apparently optimal juxtaposition of the diisopropylammonium group with respect to residues Trp86 and Asp74 (Fig. 9A). On the other hand, in the HuAChE-VX^R complex, the ethoxy group emerging from the acyl pocket, induces an alternative conformation of the leaving group, in which interaction with residue Asp74 is practically precluded (Fig. 40B). According to this molecular scenario opening of the acyl pocket, as in the F295A/F297A HuAChE, may relieve the steric crowding around the VX^R phosphorus, allowing for interaction of the cationic moiety in the corresponding Michaelis complex with the carboxylate of Asp74.

To our knowledge, the notion that *intramolecular* interactions of the phosphyl moiety may contribute to AChE stereoselectivity toward VX^S or any other organophosphate inhibitor was not considered before. Yet certain results reported in the past seem consistent with the suggestion that interactions of charged leaving groups with other bulky substituents affect the inhibition properties of the corresponding phosphates and phosphonates. One such example is the different accommodation, by AChE, of n-propylphosphonates bearing either fluorine or thiocholine as a leaving group (Berman, 1995), as compared to the respective methylphosphonates (see Fig. 41). While cycloheptyl n-propylphosphonofluoridate (CHPPF) was only ~2-fold less reactive than the corresponding methylphosphonofluoridate (CHMPF) the cycloheptyl n-propylphosphonothiocholine (CHPPT) was found to be 220-fold less reactive than the methylphosphonothiocholine (CHMPT). Since reactivities of the two cycloheptyl methylphosphonates were quite similar ($6.8x10^8$ $min^{-1}M^{-1}$ and $1.4x10^8$ $min^{-1}M^{-1}$ for CHMPF and CHMPT respectively), the 360-fold lower reactivity of CHPPT, relative to the corresponding fluoridate (CHPPF), may indicate mutual interference of the two bulky phosphyl substituents. The resemblance of the reactivity ratio between CHPPT and CHMPT (220-fold) and the stereoselectivity observed here toward the VX enantiomers (115-fold, see Table 7) may not be accidental, since the overall dimensions of propyl and ethoxy substituents are quite similar. Therefore the relative reactivity decline for both the VX^R and

the propylphosphonothiocholine may originate from similar interactions between the phosphonyl substituents.

The HuAChE reactivities toward echothiophate and its noncharged isostere nc-echothiophate is also consistent with the idea that the charged bulky leaving group affects the orientation of the ethoxy substituents within the active center. The value of the dissociation constant K_d for the HuAChE-echothiophate Michaelis complex is practically equivalent to that of the corresponding complex with DEFP (2.4×10^{-6} M and 1.9×10^{-6} M respectively, (Ordentlich *et al.,* 1996), despite the fact that in the latter there is no stabilization due to charge interactions. The fact that hydrophobic interactions due to the ethoxy moieties, which stabilize the DEFP complex, do not seem to contribute to accommodation of the echothiophate complex can be understood by assuming that these moieties are improperly oriented with respect to the active center of the enzyme, by interactions within the ligand. Furthermore, removal of the charged interaction, either through modification of the enzyme (aliphatic replacement at position 86 of HuAChE) or by utilizing the noncharged nc-echothiophate resulted in very low values of the respective bimolecular rate constants k_i (see Table 9). Thus, it appears that irrespective of charge, a large leaving group interferes with the hydrophobic stabilization of the HuAChE-diethyl phosphate complex.

The analysis presented above suggests that comparison of reactivities of the isosteric VX and nc-VX analogs toward HuAChE, in fact isolates the effect of charge on the relative affinity of the enzyme toward these methylphosphonothiolates. Without the charge interactions and in absence of significant contribution of the nc-VX hydrophobic substituents to accommodation in the active center, the reactivities of both nc-VX^S and nc-VX^R enantiomers were exceedingly low. Yet, HuAChE reactivity toward nc-VX^S was still 60-fold higher, as compared to that toward nc-VX^R, indicating presence of specific interactions underlying this HuAChE stereoselectivity. Although such interactions could not be fully characterized on the basis of the functional analysis described here, they appear to be different from those contributing to stereoselectivity toward VX^S. The largest effects observed are related to either introduction or removal of steric obstructions (e.g. effects due to replacement of Gly122 or Tyr337 respectively), rather to the effects related to perturbation at the acyl pocket (see Table 8).

The suggestion that interactions of the charged leaving group constitute the main determinant of HuAChE stereoselectivity toward VX^S may also provide an insight into the question regarding the wide range of AChE stereoselectivities toward different methylphosphonates.

Namely, the outstanding stereoselectivity toward the P^S- diastereomers of soman (e.g. $7.5x10^4$-fold for the P^SC^S over the P^RC^S diastereomer, Ordentlich *et al.*, 1999), seems to be in contrast to that observed here, and in previous studies, for the VX^S (Benschop and De Jong, 1988). The AChE stereoselectivity toward P^SC^S- and P^SC^R-soman diastereomers is also much higher than the stereoselectivity reported in the past for methylphosphonates carrying other leaving groups like p-nitrophenol (Benschop, *et al.,* 1985) or thiocholine (Hosea *et al.,* 1996*;* Berman and Leonard, 1989). These different stereoselectivities result predominantly from the exceedingly low reactivity of the P^R - diastereomers of methylphosphonofluoridates. For instance, while the AChE phosphonylation rate constant by VX^S ($1.37x10^8$ min^{-1} M^{-1} see Table 7) is similar to those measured for the P^SC^S- and P^SC^R diastereomers of soman ($1.5x10^8$ and $0.8x10^8$ $min^{-1}M^{-1}$ respectively; (Ordentlich, *et al.,* 1999), the corresponding constant for the VX^R ($1.18x10^6$ min^{-1} M^{-1}) is about 600-fold higher than those for the P^RC^S- or the P^RC^R-soman isomers ($2.0x10^3$ $min^{-1}M^{-1}$ for both cases). In fact, the reactivities of the P^R-soman diastereomers toward HuAChE resemble those of the nc-VX^S and nc-VX^R enantiomers, suggesting that hydrophobic interactions contribute little to the accommodation of the P^RC^S- or the P^RC^R-diastereomers of soman in the AChE active center.

In conclusion, it appears that HuAChE stereoselectivity toward methylphosphonates is determined by both the nature of the phosphonyl leaving group and the inherent asymmetry of the active center environment. The relative contribution of each of these elements seems to depend upon the nature of the specific inhibitor, with the active center asymmetry playing a dominant role in stereoselectivity toward P^S-soman while the positive charge of the leaving group being dominant in stereoselectivity toward VX^S as well as toward other P^S-methylphosphonothiocholines. In contrast to the notion regarding the acyl pocket as the main component of the AChE active center asymmetry, it appears now that other subsites and in particular the PAS contribute to stereoselectivity of HuAChE toward VX and other methylphosphonates.

VIII. KEY RESEARCH ACCOMPLISHMENTS

1. Determination of the *Macaca mulatta* AChE sequence, generation of recombinant rhesus AChE (rRhAChE) in the HEK-293 cell system and its purification.

2. Determination of the pharmacokinetic profiles of asialylated, partially sialylated and fully sialylated rRhAChE in its non-tetramerized or tetramerized form, in mice. These studies allowed us to determine that circulatory retention of rhesus AChE in mice is governed by the same set of post-translation-related rules as the bovine and human enzyme forms.

3. Demonstration that primate AChEs (human and rhesus) are specifically removed from the circulation of rhesus macaques via species-specific amino-acid-related epitopes located at the enzyme surface, in a manner which overrides the positive effect of enzyme subunit assembly on circulatory retention.

4. Demonstration that efficient conjugation of PEG to primate AChEs (human or rhesus) results in the generation of an enzyme species which resides in the circulation of rhesus macaques for very long periods of time (Mean residence time ~10, 000 mins.).

5. Demonstration that PEG-AChE has a circulatory residence time comparable or longer than that of native serum-derived BuChE.

6. Demonstration that PEGylation of AChE can overcome a quantitative deficiency in oligosaccharides side-chains, such as manifested by the monoglycosylated N350Q/N464Q rHuAChE mutant, resulting in the generation of circulatory long-lived molecules.

7. Demonstration that PEGylation of AChE can overcome inefficient glycan sialylation. Upon PEGylation, partially sialylated or totally asialylated HuAChEs manifest long-term circulatory residence.

8. Demonstration that PEGylation of AChE can overcome inefficient assembly into tetramers. Upon PEGylation, dimeric or monomeric HuAChEs manifest long-term circulatory residence.

9. Determination of the ability to extend by PEG-conjugation, the circulatory lifetime of AChE species exhibiting high-mannose type N-glycans or which are totally devoid of N-glycans.

10. A most important practical implication of the findings that PEGylation of AChE overrides post-translation-related suboptimal processing of the enzyme (points 6-9 above) is that one can consider production at large scale of recombinant human AChE in any production system (e.g. bacteria, yeast, plants, transgenic animals), since the enzyme generated in any production system can be readily converted into circulatory long-lived bioscavenger molecules by PEG-conjugation.

11. Planning and construction of a human *ache* gene with altered codons (lower GC contents), optimized for expression of human AChE in both the prokaryotic *Bacillus brevis* and eukaryotic *Pichia pastoris*-based expression systems.

12. Verification that the synthetic *ache* gene codes for an authentic human AChE protein by an *in-vitro* transcription-translation system.

13. Evaluation of human AChE production in *Bacillus brevis* bacterial cells utilizing the synthetic human *ache* gene under various transcription signals demonstrated that production of rHuAChE in *Bacillus brevis* cells should be avoided due to the rapid intracellular degradation of the newly synthesized rHuAChE product.

14. Demonstration that the *Pichia pastoris* yeast cell expression system can serve for the generation of bioactive rHuAChE, and establishment of the basic conditions for the effective production of the recombinant enzyme.

15. Generation of a series of hypolysine AChEs, to allow the evaluation of different enzyme forms which may serve for the generation of homogenous PEG-conjugated circulatory long-lived OP bioscavengers.

16. Demonstration that substitution of one or two lysine residues does not significantly alter the enzymatic activity or thermostability of human AChE.

17. Generation of a multilysine-mutated human AChE enzyme exhibiting undiminished enzymatic activity and stability, for evaluation of its pharmacokinetic properties following PEGylation.

18. Demonstration that homogenous PEGylated tetralysine mutant rHuAChE is retained in the circulation of mice for extended periods of time, similar to wild-type PEGylated rHuAChE.

19. Demonstration by *in-vitro* immunoprecipitation experiments, that PEG-conjugation of recombinant human AChE results in the generation of an enzyme form exhibiting significantly reduced antigenicity.

20. Demonstration that the PEG-conjugated enzyme (unlike non-modified recombinant human AChE) fails to elicit a significant antibody response even in a heterologous animal model.

21. Demonstration that HuAChE stereoselectivity toward VX enantiomers is practically abolished by replacement of the aromatic residues Phe295 and Phe297 of the acyl pocket as well as of the PAS residue Asp74, and that HuAChE interaction with the cationic moiety of is a major determinant of stereoselectivity toward VX enantiomers.

IX. REPORTABLE OUTCOME

List of publications related to the current contract

Cohen, O., Kronman, C., Chitlaru, T., Velan, B. and Shafferman, A. (2003) Uses of chemically modified cholinesterases for detoxification of organophosphorus compounds. Patent application no. 10/476,338 applied to the U.S patent office by the state of Israel represented by IIBR.

Kaplan, D., Barak, D., Ordentlich, A., Kronman, C., Velan, B., and A. Shafferman (2004). Is aromaticity essential for trapping the catalytic His447 in human acetylcholinesterase. *Biochemistry,* **43**: 3129-3136

Cohen, O., Kronman, C., Velan, B. and Shafferman, A. (2004). Amino-acid domains control the circulatory residence time of primate acetylcholinesterase in rhesus macaques. *Biochem. J.* **378**: 117-128

Shafferman, A., Chitlaru, T., Ordentlich, A., Velan, B. and Kronman, C. (2004). A complex Array of Post-Translation Modifications Determines the Circulatory Longevity of AChE in a Hierarchical Manner. In: *Cholinergic Mechanisms.* Eds. I. Silman, H. Soreq, L. Anglister, D. Michaelson and A. Fisher (Taylor & Francis Publication), 245-253.

Ordentlich, A., Barak, D., Ariel, N., Kronman, C., Kaplan, D., Velan, B. and Shafferman, A. (2004) Surprising findings from the functional analysis of Human AChE adducts of Alzheimer's disease drugs. In: *Cholinergic Mechanisms.* Eds. I. Silman, H. Soreq, L. Anglister, D. Michaelson and A. Fisher (Taylor & Francis Publication), 177-181.

Cohen, O., Kronman, C., Chitlaru, T., Ordentlich, A., Velan, B. and Shafferman, A. (2004) Generation of pharmacokinetically improved recombinant Human Acetylcholinesterase by polyethylene glycol modification. In: *Cholinergic Mechanisms.* Eds. I. Silman, H. Soreq, L. Anglister, D. Michaelson and A. Fisher (Taylor & Francis Publication), 519-521.

Kaplan, D., Ordentlich, A., Barak, D., Ariel, N., Kronman, C., Velan, B., and Shafferman, A. (2004) Attempts to engineer an enzyme-mimic of Butyrylcholinesterase by substitution of the six divergent aromatic amino acids in the active center of AChE. In: *Cholinergic Mechanisms.* Eds. I. Silman, H. Soreq, L. Anglister, D. Michaelson and A. Fisher (Taylor & Francis Publication), 601-605.

Elhanany, E., Ordentlich, A., Dgany, O., Kaplan, D., Segall, Y., Barak, R., Velan, B., and Shafferman A. (2004) MALDI-TOF/MS analysis of tabun-AChE conjugate: A tool for resolution of "aging" pathway. In: Eds. I. Silman, H. Soreq, L. Anglister, D. Michaelson and A. Fisher (Taylor & Francis Publication), 563-565.

Kronman, C., Chitlaru, T., Seliger, N., Lazar, S., Lazar, A., Zilberstein, L., Velan, B., and Shafferman, A. (2004). Some basic rules governing oligosaccharide-dependent circulatory residence of glycoproteins are revealed by MALDI-TOF/MS mapping of the multiple N-glycans associated with recombinant bovine acetylcholinesterase. In: *Cholinergic Mechanisms.* Eds. I. Silman, H. Soreq, L. Anglister, D. Michaelson and A. Fisher (Taylor & Francis Publication), 613-616.

Chitlaru, T., Kronman, C., Lazar, S., Seliger, N., Velan B. and Shafferman, A. (2004). Effect of post-translation modifications of human acetylcholinesterase on its circulatory residence. In: *Cholinergic Mechanisms*. Eds. I. Silman, H. Soreq, L. Anglister, D. Michaelson and A. Fisher (Taylor & Francis Publication), 511-514.

Ordentlich, A., Barak, D., Sod-Moriah, G., Kaplan, D., Mizrahi, D., Segall, Y., Kronman, C., Karton, Y., Lazar, A., Marcus, D., Velan, B. and Shafferman, A. (2004) Stereoselectivity toward VX is determined by interactions with residues of the acyl pocket as well as of the peripheral anionic site of AChE. *Biochemistry* 43, 11255-11265.

Shafferman, A., Barak, D., Kaplan, A., Ordentlich, N., Ariel, N. And Velan, B., (2004) The aromatic "trapping" of histidine 447 in catalysis of acetylcholinesterases In: Cholinesterases in the Second Millenium: *Biomolecular and Pathological Aspects*, 181-186

Shafferman, A. (2004) Circulatory residence of the AChE OP-bioscavenger is regulated by a hierarchy of amino-acid and post-translation specific signals. *Bioscience 2004 Medical Defense Review*

Kronman, C., Cohen, O. Velan, B. and Shafferman, A. (2005) Host-regulated disposition of mammalian AChEs. *Chemico-Biological Interactions*, **157-158**: 51-55

Ordentlich, A. Barak, D. Sod-Moriah, G. Kaplan, D. Mizrahi, D. Segall, Y. Kronman, C. Karton, Y. Lazar, A. Marcus, D. Velan, B. and Shafferman, A. (2005) The role of AChE active site gorge in determining stereoselectivity of charged and noncharged VX enantiomers. *Chemico-Biological Interactions*, **157-158**: 191-198.

Shafferman, A. Barak, D. Kaplan, D. Ordentlich, A. Kronman, C. and Velan, B. (2005) Functional requirements for the optimal catalytic configuration of the AChE active center. *Chemico-Biological Interactions*, **157-158**: 123-131.

Barak, D., Ordentlich, A., Kaplan, D., Kronman, C., Velan, B. and Shafferman, A. (2005) Lessons from functional analysis of AChE covalent and noncovalent inhibitors for design of AD therapeutic agents. *Chemico-Biological Interactions*, **157-158**: 219-226.

Cohen, O., Kronman, C., Raveh, L., Mazor, O., Ordentlich, A. and Shafferman, A. (2006) Comparison of polyethylene glycol-conjugated recombinant human acetylcholinesterase and serum human butyrylcholinesterase as bioscavengers of organophosphate compounds. *Molecular Pharmacology*, **70**: 1121-1131.

Kronman, C., Cohen, O., Raveh, L., Mazor, O., Ordentlich, A. and Shafferman, A. (2006) Polyethylene glycol-conjugated recombinant human acetylcholinesterase serves as an efficacious bioscavengers against soman intoxification. *Toxicology, in press*.

X. CONCLUSIONS

Enhancement of the circulatory life span of recombinant AChEs is of crucial importance for their employment as therapeutic bioscavengers of OP compounds. Extensive studies involving characterization and modulation of recombinant AChE post-translation processing, firmly established that improved post-translation-related maturation contributes in a marked manner to their circulatory longevity. In a different set of experiments we determined that chemical modification of AChEs by conjugation of PEG molecules can also give rise to bioactive enzyme forms which are retained in the circulation for even longer periods of time.

To define the possible interrelationship between PEG-conjugation and post-translation modifications of AChE enzyme forms with regard to circulatory residence, we examined the pharmacokinetic performance of well-defined AChE forms differing in their post-translation processing. This line of studies allowed us to determine that PEG-conjugation increased the circulatory retention of suboptimally processed AChE forms characterized by low glycan contents, inefficient sialylation or incomplete assembly into tetramers. Moreover, AChE species exhibiting altered glycan structures that do not conform with the classical complex-type of oligosaccharides typical of animal cell proteins or which were entirely devoid of glycan appendages, also displayed prolonged circulatory retention following PEG-conjugation. Most notably, the differently processed AChE forms displayed nearly equal circulatory residence time values subsequent to PEGylation. Taken together, these studies show that PEGylation of AChE overrides post-translation-related suboptimal processing and that the extent of circulatory retention of the chemically modified enzyme is determined solely by the appended PEG moieties.

During the course of the present research, we have documented a significant body of data regarding the factors contributing to AChE circulatory residence, all based on extensive studies carried out in the mouse animal model. We have now used the various AChE forms described above to profile their pharmacokinetic behavior in rhesus macaques (Cohen *et al.*, 2004). Although these pharmacokinetic studies were funded by sources other than USAMRMC, they have important implications to this contract. These studies in rhesus macaques allowed us to determine that: (1) Glycan sialylation, enzyme tetramerization and glycan loading determine circulatory retention of AChE in rhesus macaques, according to the hierarchical rules determined in the mouse animal system. (2) A mechanism for AChE removal, which was not previously detected in mice, facilitates AChE elimination from the circulation of rhesus macaques. (3) This mode of AChE removal is mediated through

interactions with primate-specific AChE amino-acid epitopes, and seems to reflect a system which has evolved to eliminate "self" or "self-like" acetylcholinesterase in macaques. Thus, amino-acid-epitopes serve as an additional element, which together with post-translation-related factors determine the circulatory fate of AChEs in non-human primates. (4) The controlled conjugation of PEG to primate (human or rhesus) AChEs, results in the generation of bioactive enzyme which resides in the circulation of macaques for extraordinarily long periods of time, demonstrating that AChE shielding by PEG-appendage protects the enzyme from the amino-acid-related elimination system.

The use of human AChE as a bioscavenger of OP compounds and the possible requirement in certain situations for repeated administration of this therapeutic agent, are a cause for concern regarding the possible development of unfavorable immunogenic responses to the bioscavenger. However, if indeed PEG conjugation decreases interactions between the modified enzyme and other proteins as suggested above, the PEGylated version of AChE might elicit a lesser immune response than the non-modified version of AChE. Indeed, immunological studies of the non-modified and PEGylated human AChE allowed us to determine that the chemical modification of the enzyme significantly decreased the antigenicity and immunogenicity of the enzyme. This result demonstrates that the conjugation of PEG to human AChE contributes to its therapeutic appropriateness not only by improving the pharmacokinetic performance of the enzyme, but also by reducing immunological responses to the administered recombinant protein.

A key implication of the findings that PEGylation of AChE overrides post-translation-related suboptimal processing of the enzyme, is that it is now possible to consider production at large scale of recombinant human AChE in low-cost microorganisms-based production systems, since the enzyme product produced in such systems can be readily converted into circulatory long-lived bioscavenger molecules by PEG-conjugation. We therefore generated a synthetic *ache* gene which has been adapted for efficient expression both in bacteria (*Bacillus brevis*) and yeast (*Pichia pastoris*), by lowering the GC contents of the coding sequences of the native human gene. We then demonstrated that this synthetic gene expresses authentic AChE *in vitro*. However, detailed analysis demonstrated that following introduction of the synthetic *ache* gene into *Bacillus brevis* cells the enzyme is produced in low yields due to a marked intracellular instability of the protein product. Seemingly, some features of the rHuAChE molecule predestine the newly synthesized protein product to rapid degradation within the *Bacillus* cells. On the other hand, we demonstrated that bioactive rHuAChE was produced in

the methylotrophic yeast *Pichia pastoris* following introduction of the synthetic *ache* gene, and further studies allowed us to establish the basic conditions for the effective production of the recombinant enzyme in this system.

The use of PEGylated AChE as a therapeutic agent would require that the enzyme product exhibit a high degree of homogeneity. This in turn, may require that some of the lysine residues which serve as targets for PEGylation be eliminated, to allow production of uniformly PEGylated enzyme. During the present study, we have established that substitution of one or two lysine residues of human AChE, does not significantly compromise enzymatic performance or thermostability of the enzyme. Encouraged by these results, we began the generation of multiple lysine mutants. To date, one such multilysine mutated rHuAChE, K23A/K332A/K348A, was subjected to thorough characterization and was found to yield an homogenous product upon PEGylation The PEGylated K23A/K332A/K348A rHuAChE demonstrated extended circulatory longevity in mice, in a manner similar to that of PEGylated wild-type rHuAChE. In addition, PEGylation of this multilysine mutant rHuAChE, was found to effectively reduce the antigenicity and immunogenicity of this enzyme form. Based on these findings, we intend to examine whether further reduction of lysine PEG target sites will also give rise to bioactive AChE forms which display extended circulatory longevity and reduced immunorecognition, following PEG conjugation.

Finally, we investigated the stereoselectivity of human AChE toward the P^S enantiomer of the lethal chemical warfare agent VX, by examining the reactivity of HuAChE and its mutant derivatives toward purified enantiomers of VX and its noncharged isostere O-ethyl S- (3-isopropyl-4-methyl-pentyl) methylphosphonothioate (nc-VX) as well as echothiophate and its noncharged analogue. Reactivity of the wild type HuAChE toward VX^S was 115-fold higher than that toward VX^R, with the corresponding bimolecular rate constants $1.4x10^8$ $min^{-1}M^{-1}$ and $1.2x10^6$ $min^{-1}M^{-1}$. HuAChE was also 12500-fold more reactive toward VX^S than toward nc-VX^S. Substitution of the cation binding subsite residue Trp86 by alanine resulted in a 3-orders of magnitude decrease in HuAChE reactivity toward both VX enantiomers, while this replacement had only a marginal effect on the reactivity toward the enantiomers of nc-VX and the noncharged echothiophate. These results attest to the critical role played by Trp86 in accommodating the charged moieties of both VX enantiomers. Marked decrease in stereoselectivity toward VX^S was observed following replacements of Phe295 at the acyl pocket (F295A and F295A/F297A). Replacement of the peripheral anionic site (PAS) residue Asp74 by asparagine (D74N) practically abolished stereoselectivity toward VX^S (130-fold decrease), while substitution which retains the negative charge at position 74

(D74E) had no effect. The results from kinetic studies and molecular simulations suggest that the differential reactivity toward the VX enantiomers is mainly a result of a different interaction of the charged leaving group with residue Asp74. Thus, the combined mutagenesis and kinetics studies with various derivatives of VX allowed us to resolve on a molecular basis, the unique stereoselectivity of AChE towards these types of CW agents.

XI. REFERENCES

Adachi, T., Sakakibara, T., Yamagata, H., Tsukagoshi, N. and Udaka, S. (1991) Analysis by deletion and site directed mutagenesis of promoters of the cell wall protein gene operon in *Bacillus brevis* 47. *Agric. Biol. Chem.* **55**:189-194

Albaret, C., Lacoutiere, S., Ashman, W.P., Groment, D. and Fortier, P-L. (1997) Molecular mechanic study of nerve agent O-ethyl S-[2-(diisopropylamino)ethyl]-methylphosphonothioate (VX) bound to the active site of *Torpedo californica* acetylcholinesterase. *Proteins* **28**:543-555

Anumula, K.R. and Dhume, S.T. (1998). High resolution and high sensitivity methods for oligosaccharide mapping and characterization by normal phase high performance liquid chromatography following derivatization with highly fluorescent anthranilic acid. *Glycobiology* **8**:685-694

Aoki, S., Kitagawa, M. and Okumura, K. (2001) Pharmacokinetic studies of Gln117 tissue-type plasminogen activators in rats. *J. Pharm. Biomed.* **26**:453-462

Ariel, N., Ordentlich, A., Barak, D., Bino, T., Velan, B. and Shafferman, A. (1998). The "aromatic patch" of three proximal residues in the human acetylcholinesterase active centre allows for versatile interaction modes with inhibitors. *Biochem. J.* **335:**95-102

Balasubramanian, A.S. and Bhanumathy, C.D. (1993) Noncholinergic functions of cholinesterases. *FASEB J.* **7**, 1354-1358

Barak, D., Ariel, N., Velan, B. and Shafferman, A. (1992), Molecular models for human AChE and its phosphonylation products. In: Multidisciplinary Approaches to Cholinesterase Functions. (Shafferman A. and Velan B. Eds), pp 195-199 Plenum Pub. Co. London.

Barak, D., Kronman, C., Ordentlich, A., Ariel, N., Bromberg, A., Marcus, D., Lazar, A., Velan, B. and Shafferman, A. (1994) Acetylcholinesterase peripheral anionic site degeneracy conferred by amino acid arrays sharing a common core. *J. Biol. Chem.* **264**:6296-6305

Barak, D., Ordentlich, A., Bromberg, A., Kronman, C, Marcus, D., Lazar, A., Ariel, N., Velan, B. and Shafferman, A. (1995) Allosteric modulation of acetylcholinesterase activity by peripheral ligands involves a conformational transition of the anionic subsite, *Biochemistry* **34**:15444-15452

Barak, D., Ordentlich, A., Kaplan, D., Barak, R., Mizrahi, D., Kronman, C., Segall, Y., Velan, B. and Shafferman, A. (2000) Evidence for P-N bond scission in phosphoroamidate nerve agent adducts of human acetylcholinesterase. *Biochemistry* **39**:1156-1161

Barak, D., Kaplan, D., Ordentlich, A., Ariel, N., Velan, B. and Shafferman, A. (2002) The aromatic "trapping" of the catalytic histidine is essential for efficient catalysis in acetylcholinesterase. *Biochemistry* **41**:8245-8252

Berman, H.A. and Leonard, K.J. (1989) Chiral reactions of acetylcholinesterase probed with enantiomeric methylphosphonothioates. Noncovalent determinants of enzyme chirality. *J. Biol. Chem.* **264**:3942-3956

Berman, H. (1995) Reaction of acetylcholinesterase with organophosphonates. in: *Enzymes of the Cholinesterase Family* (Quinn, D.M., Balasubramanian, A.S., Doctor, B.P. and Taylor, P. eds) pp177-182, Plenum Press, New York

Benschop, H.P., Konings, C.A.G., Van Gendern, J. and De Jong, L.P.A. (1985) Stabilization and gas chromatographic analysis of the four stereoisomers of 1,2,2-trimethylpropyl methylphosphonofluoridate (soman) in rat blood. *Anal. Biochem.* **151**:242-253

Benschop, H.P. and De Jong, L.P.A. (1988) Nerve agent stereoisomers: analysis, isolation and toxicology. *Acc. Chem. Res.* **21**:368-374

Bigge, J.C., Pate, T.P., Bruce, J.A., Goulding, P.N., Charles, S.M. and Parekh, R.B. (1995). Nonselective and efficient fluorescent labeling using 2-amino-benzamide and anthranilic acid. *Anal. Biochem.* **230**:229-238

Blum, P.J., Ory, J., Bauernfeind, J. and Kraska, J. (1992). Physiological consequences of DNAK and DNAJ overproduction in Escherichia coli. *J.Bacteriol.* **174**:7436-7444

Boter, H.L., De Jong, L.P.A. and Kienhuis, H. (1971) in Interaction of Chemical Agents with Cholinergic Mechanisms, Israel Ins. Biol. Res. 16th Annual Biology Conference, pp 9-26.

Bourne, Y., Taylor, P. and Marchot, P. (1995) Acetylcholinesterase inhibition by fasciculin: crystal structure of the complex. *Cell* **83**:503-512

Bourne, Y., Grassi, J., Bougis, P.E. and Marchot, P. (1999). Conformational flexibility of the acetylcholinesterase tetramer suggested by x-ray crystallography. *J. Biol. Chem.* **274**:30370-30376

Broomfield, C.A., Maxwell, D.M., Solana, R.P., Castro, C.A, Finger, A.V. and Lenz, D.E. (1991) Protection by butyrylcholinesterase against organophosphorus poisoning in nonhuman primates. *J. Pharmacol. Exp. Ther.* **259**:683-698

Carmona, G.N., Baum, I., Schindler, C.W., Goldberg, S.R., Jufer, R., Cone, E., Slaughter, C.E., Belendiuk, G.W. and Gorelick, D.A. (1996) Plasma butyrylcholinesterase activity and cocaine half-life differ significantly in rhesus and squirrel monkeys. *Life Science* **59**:939-943

Cascio, C., Comite, C., Ghiara, M., Lanza, G. and Ponchione, A. (1988) Use of serum cholinesterase in severe organophosphorus poisoning. Our experience. *Minerva Anestesiol.* **54**:337-338

Cereghino, J.L. and Cregg, J.M. (2000) Heterologous protein expression in the methylotrophic yeast *Pichia pastoris. FEMS Microbial. Rev.* **24**: 45-66

Chitlaru, T., Kronman, C., Zeevi, M., Kam, M., Harel, A., Ordentlich, A., Velan, B. and Shafferman, A., (1998) Modulation of circulatory residence of recombinant acetylcholinesterase through biochemical or genetic manipulation of sialylation levels. *Biochem. J.* **336**:647-658

Chitlaru, T., Kronman, C., Velan, B. and Shafferman, A. (2001) Effect of human acetylcholinesterase subunit assembly on its circulatory residence. *Biochem. J.* **354**:613-625

Chitlaru, T. ,Kronman, C., Velan, B. and Shafferman, A. (2002) Overloading and removal of N-glycosylation targets on human acetylcholinesterase: effects on glycan composition and circulatory residence time. *Biochem. J.* **363**:619-631

Cohen, S., Mendelson, I., Altboum, Z., Kobiler, D., Elhanani, E., Bino, T., Leitner, M., Inbar, I., Rosenberg, H., Gozes, Y., Barak, R., Fisher, M., Kronman, C., Velan, B. and Shafferman, A. (2000) Attenuated nontoxinogenic and nonencapsulated recombinant *Bacillus anthracis* spore vaccines protect against anthrax. *Infect. Immun.* **68**:4549-4558

Cohen, O., Kronman, C., Chitlaru, T., Ordentlich, A., Velan, B. and Shafferman, A. (2001) Chemical modifications of recombinant human acetylcholinesterase by polyethylene glycol generates an enzyme with exceptional circulatory longevity. *Biochem. J.* **357**:795-802

Cohen, O., Kronman, C., Velan, B. and Shafferman, A. (2004) Amino-acid domains control the circulatory residence time of primate acetylcholinesterases in rhesus macaques (*Macaca mulatta*). *Biochem. J.* **378**:117-128

Cos, O., Serano, A., Montesinos, J.L., Ferrer, P., Cregg, J.M. and Valero, F. (2005) Combined effect of the methanol utilization (Mut) phenotype and gene dosage on recombinant protein production in *Pichia pastoris* fed-batch cultures. *J. Biotechnocol.* **116**:321-335

Coyle, J.T., Price, D.L. and DeLong, M.R. (1983). Alzheimer's disease: A disorder of cortical cholinergic innervation. *Science* **219**:1184-1190

Daly, R. and Hern, M.T. (2005) Expression of heterologous proteins in *Pichia pastoris*: a useful experimental tool in protein engineering and production. *J. Mol. Recognit.* **18**:119-138

Doctor, B.P., Blick, D.W., Gentry, M.K., Maxwell, D.M., Miller, S.A., Murphy, M.R. and Wolfe, A.D. (1992). Acetylcholinesterase: a pretreatment drug for organophosphate poisoning. In: *Multidisciplinary Approaches to Cholinesterase Functions.* (Shafferman A. and Velan B. Eds),pp. 277-286, Plenum Pub. Co., London.

Dubaquie, Y., Mortensen, D.L., Intintoli, A., Hogue, D.A., Nakamura, G., Rancatore, P., Lester, P., Sadick, M.D., Filvaroff, E., Fiedler, P.J. and Lowman, H.B. Binding protein-3-selective insulin-like growth factor I variants: Engineering, biodistributions, and clearance. (2001) *Endocrinology* **142**:165-173

Ebisu, S., Tagaki, H., Kadowaki, K., Yamagata, H. and Udaka, S. (1996). The efficient production of human epidermal growth factor by *Bacillus brevis*. *Ann. NY Acad. Sci.* **782**:115-122.

Ellman, G.L., Courtney, K.D., Andres, V. and Featherstone, R.M. (1961) A new and rapid colorimetric determination of acetylcholinesterase activity. *Biochem. Pharmacol.* **7**, 88-95

Epstein, J., Callahan, J.J., and Bauer, E. (1974) The kinetics and mechanism of hydrolysis of phosphonothiolates in dilute aqueous solution. *Phosphorus,* **4**:157-163

Fischer, M., Ittah, A., Liefer, I. and Gorecki, M. (1993). Expression and reconstitution of biologically active human acetylcholinesterases from *E. coli. Cell. Mol. Neurobiol.* **13**:25-38

Gat, O., Inbar, I., Aloni-Greenstein, R., Zahavi, E., Kronman, C., Mendelson, I., Cohen, S., Velan, B. and Shafferman, A. (2003) Use of a promoter trap system in *Bacillus anthracis* and *Bacillus subtilis* for the development of recombinant protective antigen-based vaccines. *Infect. Immun.* **71**:801-813

Greenblatt, H.M., Kryger, G., Lewis, T., Silman, I. and Sussman, J.L. (1999) Structure of acetylcholinesterase complexed with (-)-galanthamine at 2.3 A resolution,. *FEBS Lett.* **463**:321-326

Grisaru, D., Sternfeld, M., Eldor, A., Glick, D. and Soreq, H. (1999) Structural roles of acetylcholinesterase variants in biology and pathology. *Eur. J Biochem.* **264**:672-86

Hall, C.R., Inch, T.D., Inns, R.H., Muir, A.W., Sellers, D.J., and Smith, A.P. (1977) Differences between some biological properties of enantiomers of alkyl S-alkyl methylphosphonothioates. *J. Pharm. Pharmacol.* **27**:574-576

Harel, M., Sussman, J.L., Krejci, E., Bon, S., Chanal, P., Massoulie, J. and Silman, I. (1992) Conversion of acetylcholinesterase to butyrylcholinesterase: modeling and mutagenesis. *Proc. Natl. Acad. Sci. USA.* **89**:10827-10831

Harel, M., Schalk, I., Ehret-Sabatier, L., Bouet, F., Goeldner, M., Hirth, C., Axelsen P.H., Silman, I. and Sussman, J.L. (1993) Quaternary ligand binding to aromatic residues in the active-site gorge of acetylcholinesterase. *Proc. Natl. Acad. Sci. U S A.* **90**:9031-9035

Harel, M., Quinn, D.M., Nair, H.K., Silman, I. and Sussman, J.L. (1996) The x-ray structure of a transition state analog complex reveals the molecular origins of the catalytic power and substrate specificity of acetylcholinesterase. *J. Am. Chem. Soc.* **118**:2340-2346

Harel, M., Kryger, G., Rosenberry, T.L., Mallender, W.D., Lewis, T., Fletcher, R.J., Guss, J.M., Silman, I. And Sussman, J.L. (2000) Three-dimensional structures of *Drosophila melanogaster* acetylcholinesterase and of its complexes with two potent inhibitors. *Protein Sci.* **9**:1063-1072

Hart, G.J. and O'Brien, R.D. (1973) Recording spectrophotometric method for determination of dissociation and phosphorylation constants for inhibition of acetylcholinesterase by organophosphates in the presence of substrate. *Biochemistry*, **12**:2940-2945

Hosea, N.A., Berman, H.A. and Taylor, P. (1995) Specificity and orientation of trigonal carboxyl esters and tetrahedral alkylphosphonyl esters in cholinesterases. *Biochemistry* **34**:11528-11536

Hosea, N.A., Radic, Z., Tsigelny, I., Berman, H.A., Quinn, D.M. and Taylor, P. (1996) Aspartate 74 as a primary determinant in acetylcholinesterase governing specificity to cationic organophosphonates. *Biochemistry* **35**:10995-11004

Jarv, J. (1984) Stereochemical aspects of cholinesterase catalysis. *Bioorg. Chem.***12**:259-278

Jenkins, T., Balinsky, D. and Patient, D.W. (1967) Cholinesterase in plasma: first reported absence in Bantu; half-life determination. *Science* **156**:1748-1750

Kabachnik, M.I., Brestkin, A.P., Godovkin, N.N., Michelson, M.J., Rozengart, E.V. and Rozengart, V.I. (1970) Hydrophobic areas on the active surface of cholinesterases. *Pharmacol. Rev.* **22**:355-388

Kaplan, D., Ordentlich, A., Barak, D., Ariel, N., Kronman, C., Velan, B. and Shafferman, A. (2001) Does "butyrylization" of acetylcholinesterase through substitution of the six divergent aromatic amino acids in the active center gorge generate an enzyme mimic of butyrylcholinesterase. *Biochemistry* **40**:7433-7445

Kaplan, D., Barak, D., Ordentlich, A., Kronman, C., Velan, B. and Shafferman, A. (2004) Is aromaticity essential for trapping the catalytic histidine 447 in human acetylcholinesterase. *Biochemistry* **43**:3129-3136

Keyt, B.A., Paoni, N.F., Refino, C.J., Berleau, L., Nguyen, H., Chow, A., Lai, J., Pena, L., Pater, C., Ogez, J., Etheverry, T., Botstein, D. and Bennett, W.F. (1994) A faster-acting and more potent form of tissue plasminogen activator. *Proc. Natl. Acad. Sci.* **91**:3670-3674

Kovarik, Z., Radic, Z., Berman, H.A., Simeon-Rudolf, V., Reiner, E. and Taylor, P. (2003) Acetylcholinesterase active centre and gorge conformations analyzed by combinatorial mutations and enantiomeric phosphonates. *Biochem. J.* **373**:33-40

Kronman, C., Velan, B., Gozes, Y., Leitner, M., Flashner, Y., Lazar, A., Marcus, D., Sery, T., Grosfeld, H., Cohen, S. and Shafferman, A. (1992) Production and secretion of high levels of recombinant human acetylcholinesterase in cultured cell lines: microheterogeneity of the catalytic subunit. *Gene* **121**:295-304

Kronman, C., Velan, B., Marcus, D., Ordentlich, A., Reuveny, S. and Shafferman, A. (1995) Involvement of oligomerization, N-glycosylation and sialylation in the clearance of cholinesterases from the circulation. *Biochem J.* **311**:959-967

Kronman, C., Chitlaru,T., Elhanany, E., Velan, B. and Shafferman, A. (2000) Hierarchy of post-translation modifications involved in the circulatory longevity of glycoproteins: demonstration of concerted contributions of glycan sialylation and subunit assembly to the pharmacokinetic behavior of bovine acetylcholinesterase. *J. Biol. Chem.* **275**:29488-29502

Kryger, G., Giles, K., Harel, M., Toker, L., Velan, B., Lazar, A., Kronman, C., Barak, D., Ariel, N., Shafferman, A., Silman, I. and Sussman, J.L. (1998). 3D structure at 2.7 Å resolution of native and E202Q mutant human acetylcholinesterases complexed with fasciculin-II. In: Structure and Function of Cholinesterases and Related Proteins . (Eds. Doctor, B.P., Quinn, D.M., Rotundo, R.L. and Taylor, P.) Plenum Publishing Corp. 323-326

Kryger, G., Harel, M., Giles, K., Toker, L., Velan, B., Lazar, A., Kronman, C., Barak, D., Ariel, N., Shafferman, A., Silman, I. and Sussman, J.L. (2000) Structures of recombinant native and E202Q mutant human acetylcholinesterase complexed with the snake-venom toxin fasciculin-II. *Acta Crystallogr.* **56**:1385-1394.

Kuster, B., Wheeler, S.F., Hunter, A.P., Dwek, R.A. and Harvey, D.J. (1997). Sequencing of N linked oligosaccharides directly from protein gels: in-gel deglycosylation followed by matrix assisted laser desorption/ionization mass spectrometry and normal phase high-performance liquid chromatography. *Anal. Biochem.* **250**:82-101

Laub, P.B. and Gallo, J.M. (1996) NCOMP - a Windows-based computer program for noncompartmental analysis of pharmacokinetic data. *J. Pharm. Sci.* **85**:393-395

Lazar, A., Reuveny, S., Kronman, C., Velan, B. and Shafferman, A. (1993) Evaluation of anchorage-dependent cell propagation systems for production of human acetylcholinesterase by recombinant 293 cells. *Cytotechnology* **13**:115-123

Lee, S.J., Kim, D.M., Bae, K.H., Byun, S.M. and Chung, J.H. (2000). Enhancement of secretion and extracellular stability of staphylokinase in Bacillus *subtilis* by wprA gene disruption. *Appl. Environ. Microbiol.* **66**:467-480

Levy, D. and Ashani, Y. (1986). Synthesis and *in vitro* properties of a powerful quaternary methylphosphonate inhibitor of acetylcholinesterase. A new marker in blood-brain barrier research, *Biochem. Pharmacol.* **35**:1079-1085

Li, B., Stribley, J.A., Ticu, A., Xie, W., Schopfer, L.M., Hammond, P., Brimijoin, S., Hinrichs, S.H. and Lockridge, O. (2000) Abundant tissue butyrylcholinesterase and its possible function in the acetylcholinesterase knockout mouse. *J. Neurochem.* **75**:1320-1331

Lockridge, O., Blong, R. M., Masson, P., Froment, M. T., Millard, C.B. and Broomfield, C.A. *(*1997). A single amino acid substitution Gly117His confers phosphotriesterase (organophosphorus acid anhydride hydrolase) activity on human butyrycholinesterase. *Biochemistry* **36:**786-795

Macauley-Patrick, S., Fazenda, M.L., McNeil, B. and Harvey, L.M. (2005). Heterologous protein production using the *Pichia pastoris* expression system. *Yeast*, **22**:249-270

Makrides, S.C. (1996). Strategies for achieving high-level expression of genes in *E. coli*. *Microbiol. Rev.* **60**:512-538

Massoulie, J., Sussman, J.L., Doctor, B.P., Soreq, H., Velan, B., Cygler, M., Rotundo, R., Shafferman, A., Silman, I. and Taylor, P. (1992) Recommendations for nomenclature in cholinesterases, in *Multidisciplinary Approaches to Cholinesterase Functions* (Shafferman, A. and Velan, B. Eds.) pp. 285-288, Plenum Press, NY.

Massoulie, J., Anselmet, A., Bon, S., Krecji, E., Legay, C., Morel, N. and Simon S. (1999) The polymorphism of acetylcholinesterase: post-translational processing, quaternary associations and localization. *Chemico-Biol. Interact.* **119-120:**29-42

Maxwell, D.M., Castro, C.A., De La Hoz, D.M., Gentry, M.K., Gold, M.B., Solana, R.P., Wolfe, A.D. and Doctor, B.P. (1992) Protection of rhesus monkeys against soman and prevention of performance decrement from submicrogram amounts of glycoproteins. *Toxicol. Appl. Pharmacol.* **115**:44-49

Mendelson, I., Kronman, C., Ariel, N., Shafferman, A. and Velan, B. (1998) Bovine acetylcholinesterase: cloning, expression and characterization. *Biochem. J.* **334**:251-259

Millard, C.B., Lockridge, O. and Broomfield, C.A. (1995) Design and expression of organophosphorus acid anhydride hydrolase activity in human butyrylcholinesterase. *Biochemistry* **34**:15925-15933

Millard, C.B., Kryger, G., Ordentlich, A., Harel, M., Raves, M.L., Greenblat, H., Segall, Y., Barak, D., Shafferman, A., Silman, I. and Sussman, J.L. (1999a). Crystal structure of aged phosphonylated acetylcholinesterase: nerve agent reaction products at the atomic level. *Biochemistry* **38**:7032-7039

Millard, C.B., Koellner, G., Ordentlich, A., Shafferman, A., Silman, I. and Sussman, J.L. (1999b) Reaction products of acetylcholinesterase and VX reveal a mobile histidine in the catalytic triad. *J. Am. Chem. Soc.* **121**:9883-9884

Monfardini, C. and Veronese, F.M. (1998) Stabilization of substances in circulation. *Bioconjug. Chem.* **9**:418-450

Nagahama, M., Michiue, K. and Sakurai J. (1996) Production and purification of *Clostridium perfringens* alpha-toxin using a protein-hyperproducing strain, *Bacillus brevis* 47. *FEMS Microbiol. Lett.*, **145**:239-243

Nagao, M., Inoue, K., Moon, S.K., Masuda, S., Takagi, H., Udaka, S. and Sasaki, R. (1997). Secretory production of erythropoietin and the extracellular domain of the erythropoietin receptor by Bacillus brevis: affinity, purification and characterization. *Biosci. Biotech. Biochem.* **61**:670-674

Nakamura, Y., Gojobori, T. and Ikemura, T. (2000). Codon usage tabulated from the international DNA sequence databases: status for the year 2000. *Nucl. Acids Res.* **28**:292-297

Odom, O.W., Kudlicki , W., Kramer, G. and Hardesty, B. (1997). An effect of polyethylene glycol 8000 on protein mobility in sodium dodecyl sulfate–polyacrylamide gel electrophoresis and a method for eliminating this effect. *Anal. Biochem* **245**:249–252

Okamoto, A., Kosugi, A., Koizumi, Y., Yanagida, F. and Udaka, S. (1997) High efficiency transformation of *Bacillus brevis* by electroporation. *Biosci. Biotech. Biochem.* **61**:203-203

Okafo, G., Burrow, L., Carr, S.A., Roberts, G.D. Johnson, W. and Camilleri, P. (1996). A coordinated high-performance liquid chromatogaphic, capillary electrophoresis, and mass spectrometric approach for the analysis of oligosaccharide mixtures derivatized with 2-aminoacridone. *Anal. Chem.* **68**:4424-4430

Okafo, G., Langridge, A., North, S., Organ, A., West, A., Morris, M. and Camilleri, P. (1997). High-performance liquid chromatographic analysis of complex N-linked glycans derivatized with 2-aminoacridone. *Anal. Chem.* **69:**4985-4993

Ordentlich, A., Barak, D., Kronman, C., Flashner, Y., Leitner, M., Segall, Y., Ariel N., Cohen, S., Velan, B. and Shafferman, A. (1993). Dissection of the human acetylcholinesterase active center - determinants of substrate specificity: Identification of residues constituting the anionic site, the hydrophobic site, and the acyl pocket. *J. Biol. Chem.* **268**:17083-17095

Ordentlich, A., Barak, D., Kronman, C., Ariel, N., Segall, Y., Velan, B. and Shafferman, A. (1995) Contribution of aromatic moieties of tyrosine 133 and of the anionic subsite tryptophan 86 to catalytic efficiency and allosteric modulation of acetylcholinesterase. *J. Biol. Chem.* **270**:2082-2091

Ordentlich, A., Barak, D., Kronman, C., Ariel, N., Segall, Y., Velan, B. and Shafferman, A. (1996). The architecture of human acetylcholinesterase active center probed by interactions with selected organophosphate inhibitors. *J. Biol. Chem.* **271**:11953-11962

Ordentlich, A., Barak, D., Ariel, N., Segall, Y., Velan, B. and Shafferman, A. (1998a). Exploring the active center of human acetylcholinesterase with stereomers of an organophosphorus inhibitor with two chiral centers. *J. Biol. Chem.* **273**:19509-19517

Ordentlich, A., Barak, D., Kronman, C., Ariel, N., Segall, Y., Velan, B. and Shafferman, A. (1998b) Functional characteristics of the oxyanion hole in human acetylcholinesterase. *J. Biol. Chem.* **273**:19509-19517

Ordentlich, A., Barak, D., Kronman, C., Benschop, H.P., De Jong, L.P.A., Ariel, N., Barak, R., Segall, Y., Velan, B. and Shafferman, A. (1999) Exploring the active center of human acetylcholinesterase with stereomers of an organophosphorus inhibitor with two chiral centers. *Biochemistry* **38***:*3055-3066.

Pugsley, A.P. (1993) The complete general secretory pathway in gram-negative bacteria. *Microbiol. Rev.* **57**:50-108

Radic, Z., Gibney, G., Kawamoto, S., MacPhee-Quigley, K., Bongiorno, C., and Taylor, P. (1992). Expression of recombinant acetylcholinesterase in Baculovirus system: kinetic properties of glutamate 199 mutants. *Biochemistry* **31**:9760-9767

Radic, Z., Pickering, N.A., Vellom, D.C., Camp, C. and Taylor, P. (1993). Three distinct domains in the cholinesterase molecule confer selectivity for acetyl- and butyrylcholinesterase inhibitors. *Biochemistry* **32**:12074-12084

Raveh, L., Ashani, Y., Levi, D., De La Hoz, D., Wolfe, A.D. and Doctor, B.P. (1989). Acetylcholinesterase prophylaxis against organophosphate poisoning: Quantitative correlation between protection and blood-enzyme level in mice. *Biochem. Pharmacol.* **38,** 529-534

Raveh, L., Grunwald, J., Marcus, D., Papier, Y., Cohen, E. and Ashani, Y. (1993) Human butyrylcholinesterase as a general prophylactic antidote for nerve agent toxicity. *Biochem. Pharmacol.* **45**:37-41

Raves, M.L., Harel, M., Pang, Y-P., Silman, I., Kozikowski, A.P. and Sussman J.L. (1997). Structure of acetylcholinesterase complexed with the nootropic alkaloid, (-)-huperzine A. *Nature Struc. Biol.* **4:**57-63

Rosenberg, Y., Luo, C., Ashani, Y., Doctor, B.P., Fischer, R., Wolfe, G. and Saxena, A. (2002) Pharmacokinetics and immunologic consequences of exposing macaques to purified homologous butyrylcholinesterase. *Life Sci.* **72**:125-134

Romanos, M.A., Hughes, F.J., Comerford, S.A. and Scorer, C.A. (1995) Production of a phosphorylated GST::HPV-6 E7 fusion protein using a yeast expression vector and glutathione S-transferase fusions. *Gene.* **152**:137-138

Rowland, M. and Tozer, T. N. (1989). *Clinical Pharmacokinetics: Concepts and Applications*, Lea & Febiger, Philadelphia, USA

Sagiya, Y., Yamagata, H. and Udaka, S. (1994). Direct high-level secretion into culture medium of tuna growth hormone in biologically active form by Bacillus brevis. *Appl. Microbiol. Biotechnol.* **42**:358-363

Saxena, A., Raveh, L., Ashani, Y. and Doctor, B.P. (1997) Structure of glycan moieties responsible for extended circulatory lifetime of fetal bovine serum acetylcholinesterase and equine serum acetylcholinesterase. *Biochemistry* **36**:7481-7489

Saxena, A., Ashani, Y., Raveh, L., Stevenson, D., Patel, T. and Doctor, B.P. (1998) Role of oligosaccharides in the pharmacokinetics of tissue-derived and genetically engineered cholinesterases. *Mol. Pharmacol.* **53**, 112-122

Shafferman, A., Kronman, C., Flashner, Y., Leitner, M., Grosfeld, H., Ordentlich, A., Gozes, Y., Cohen, S., Ariel, N., Barak, D., Harel, M., Silman, I., Sussman J.L. and Velan, B. (1992a) Mutagenesis of human acetylcholinesterase. Identification of residues involved in catalytic activity and in polypeptide folding. *J. Biol. Chem.* **267**:17640-17648.

Shafferman, A., Velan, B., Ordentlich, A ., Kronman, C., Grosfeld, H., Leitner, M., Flashner, Y., Cohen, S., Barak, D. and Ariel, N. (1992b) Mutagenesis of human acetylcholinesterase. Identification of residues involved in catalytic activity and in polypeptide folding. *EMBO J.* **11**:3561-3568.

Shafferman, A., Ordentlich, A., Barak, D., Kronman, C., Ariel, N., Leitner, M., Segall, Y., Bromberg, A., Reuveny, S., Marcus, D., Bino, T., Lazar, A., Cohen , S. and Velan, B. (1995). Molecular aspects of catalysis and of allosteric regulation of acetylcholinesterases. In: Enzymes of the Cholinesterase Family (Eds. Balasubarmanian, A.S., Doctor, B.P., Taylor, P., Quinn, D.M.) Plenum Publishing Corp. 189-196

Shafferman, A., Ordentlich, A., Barak, D., Stein, D., Ariel, N. and Velan, B. (1996). Aging of phosphylated human acetylcholinesterase: catalytic processes mediated by aromatic and polar residues of the active center. *Biochem. J.* **318:**833-840

Shafferman, A., Ordentlich, A., Barak, D., Kronman, C., Ariel, N., and Velan, B. (1998) Contribution of the active center functional architecture to AChE reactivity toward substrates and inhibitors, in Structure and Function of Cholinesterases and Related Proteins (Doctor, B.P., Taylor, P., Quinn, D.M., Rotundo, R.L. and Gentry, M. Eds.). pp 203-209 Plenum Publishing Co. New York.

Shiga, Y., Maki, M., Ohta, T., Tokishita, S., Okamoto, A., Tsukagoshi, N., Udaka, S., Konishi, A., Kodama, Y., Ejima, D., Matsui, H. and Yamagata, H. (2000). Efficient production of N terminally truncated biologically active human interleukin-6 by Bacillus brevis. *Biosci. Biotechnol. Biochem.* **64**:665-669

Simon, S., Krejci, E. and Massoulie J. (1998) A four-to-one association between peptide motifs: four C-terminal domains from cholinesterase assemble with one proline-rich attachment domain (PRAD) in the secretory pathway. *EMBO. J.* **17**:6178-6187

Simonen, M. and Palva, I. (1993). Protein secretion in *Bacillus* species. *Microbiol. Rev* **57**:109-137

Sloma, A., Rudolph, C.F., Rufo, Jr., G.A., Sullivan, B.J., Theriault, K.A., Ally, D. and Pero, J. (1990). Gene encoding a novel extracellular metalloprotease in Bacillus subtilis. *J. Bacteriol.* **172**:1024-1029

Soreq, H., Ben-Aziz, R., Prody, C.A., Seidman, S., Gnatt, A., Neville, A., Lieman-Hurwitz, J., Lev-Lehman, E., Ginzberg, D., Lapidot-Lifson, Y. and Zakut, H. (1990). Molecular cloning and construction of the coding region for human acetylcholinesterase reveals a G+C-rich attenuating structure. *Proc. Natl. Acad. Sci. USA* **87**:9688-9692

Soreq, H. and Seidman, S. (2001) Acetylcholinesterase - New roles for an old actor. *Nat. Rev. Neurosci.* **2**:294-302

Sreekrishna, K., Tschopp, J.F., Thill, G.P., Brierly, R.A. and Barr, K.A. (1998). Expression of human serum albumin in *Pichia pastoris*. US Patent 5707828.

Sussman, J.L, Harel M., Frolow F., Oefner C. Goldman A. and Silman I. (1991). Atomic resolution of acetylcholinesterase from *Torpedo californica*: A prototypic acetylcholine binding protein. *Science* **253**:872-879

Tagaki, H., Kadowaki, K. and Udaka, S. (1989). Screening and characterization of protein hyperproducing bacteria without detectable exoprotease activity. *Agric. Biol. Chem.* **53**:2279 2280

Takagi, H., Shida, O., Kadowaki, K., Komagata, K. and Udaka, S. *(*1993) Characterization of *Bacillus brevis* with descriptions of *Bacillus migulanius* sp. nov. *Bacillus choshinensis* sp. nov., *Bacillus parabrevis* sp. nov., and *Bacillus galactophilus* sp. nov. *Int. J. Syst. Bacteriol.* **43**:221-231.

Takao, M., Morioka, T., Yamagata, N., Tsukagoshi, N. and Udaka, S. (1989). Production of swine pepsinogen by protein-producing Bacillus brevis carrying swine pepsinogen cDNA. *Appl. Microbiol. Biotechnol.* **30**:75-80

Takimura, Y., Kato, M., Ohta, T., Yamagata, H. and Udaka, S. (1997) Secretion of human interleukin-2 in biologically active form by *Bacillus brevis* directly into culture medium. *Biosci. Biotechnol. Biochem.* **61**:1858-1861.

Taylor P. (1990). In: "*Pharmacological Basis of Therapeutics*" (Gilman A.G., Goodman L.S., Rall T. and Murad F. Eds.); MacMillan New York, pp 131-149

Taylor, P. and Radic, Z. (1994). The cholinesterases: from genes to proteins. *Pharmac. Toxicol.* **34**:281-320

Tsuboi, A., Uchihi, R., Tabata,R., Takahashi,Y., Hashiba,H., Sasaki,T., Yamagata,H., Tsukagoshi,N. and Udaka,S. (1986) Characterization of the genes coding for two major cell wall proteins from protein-producing Bacillus brevis 47: complete nucleotide sequence of the outer wall protein gene. *J. Bacteriol.* **168**:365-373

Tsukagoshi, N.S., Iritani, S., Sasaki, T., Takemura, T., Ihara, H., Idota, Y., Yamagata, H. and Udaka, S. (1985). Efficient synthesis and secretion of a thermophilic a-amylase by protein producing Bacillus brevis 47 carrying the *Bacillus stearothermophilus* amylase gene. *J. Bacteriol.* **164**:1182-1187

Udaka, S., Tsukagoshi, N. and Yamagata, H. (1989). Bacillus brevis, a host bacterium for efficient extracellular production of useful proteins. In G.E. Russel (ed.), Biotechnology and genetic engineering reviews. Intercept, Andover, England, 113-146

Van der Schans, M.J., Lander, B.J., van der Wiel, H., Langenberg, J.P. and Benschop, H.P. (2003) Toxicokinetics of the nerve agent (+/-)-VX in anesthetized and atropinized hairless guinea pigs and marmosets after intravenous and percutaneous administration. *Toxicol. Appl. Pharmacol.* **191**:48-62.

van Vlijmen, B.J., van Dijk, K.W., vant Hof, H.B., van Gorp, P.J.J., van der Zee, A., van der Boom, H., Breuer, M.L., Hofker, M.H. and Havekes, L.M. (1996) In the absence of endogenous mouse apolipoprotein E, apolipoprotein E*2(arg-158->cys) transgenic mice develop more severe hyperlipoproteinemia than apolipoprotein E*3-Leiden transgenic mice. *J. Biol. Chem.* **271**:30595-30602

Velan, B., Grosfeld, H., Kronman, C., Leitner, M., Gozes, Y., Lazar, A., Flashner Y., Marcus, D., Cohen, S., and Shafferman, A. (1991). The effect of elimination intersubunit disulfide bonds on the activity, assembly and secretion of recombinant human acetylcholinesterase. *J. Biol. Chem.* **266**:23977-23984

Velan, B., Kronman, C., Ordentlich, A., Flashner, Y., Leitner, M., Cohen, S. and Shafferman, A. (1993) N-glycosylation of human acetylcholinesterase: effects on activity, stability and biosynthesis. *Biochem. J.* **296**:649-656

Vellom, D.C., Radic, Z., Li, Y., Pickering, N.A., Camp, S. and Taylor, P. (1993) Amino acid residues controlling acetylcholinesterase and butyrylcholinesterase specificity. *Biochemistry* **32**:12-17

Wall, J.G. and Pluckthun, A. (1995). Effects of overexpressing folding modulators on the in vivo folding of heterologous proteins in Escherichia coli. *Curr. Opin. Biotechnol.* **6**:507-516

Wang, Y, Liang, Z.H., Zhang, Y.S., Yao, S.Y., Xu, Y.G., Tang, Y.H., Zhu, S.Q., Cui, D.F. and Feng, Y.M. (2001). Human insulin from a precursor overexpressed in the methylotrophic yeast *Pichia pastoris* and a simple procedure for purifying the expression product. *Biotechnol Bioeng*. **73**:74-79.

Waterham, H.R., Digan, M.E., Koutz, P.J., Lair, S.V. and Cregg, J.M. (1997). Isolation of the *Pichia pastoris* glyceraldehydes-3-phosphate dehydrogenase gene and regulation of its promoter. *Gene* **1**86:37-44.

Wolfe, A.D., Rush, R.S., Doctor, B.P. and Jones, D. (1987). Acetylcholinesterase prophylaxis against organophosphate toxicity. *Fundam. Appl. Toxicol*. **9:**266-270

Wu, X. C., Lee, W., Tran, L. and Wong, S. L. (1991). Engineering a *Bacillus subtilis* expression secretion system with a strain deficient in six extracellular proteases. *J. Bacteriol*. **173**:4952 4958

Yamagata, H., Adachi,T., Tsuboi, A., Takao, M., Sasaki, T., Tsukagoshi, N. and Udaka, S. (1987) Cloning and characterization of the 5' region of the cell wall protein gene operon in Bacillus brevis 47. *J. Bacteriol*. **169**:1239-1245

Yamagata, H., Nakahama, K., Suzuki, Y., Kakinuma, A., Tsukogoshi, N. and Udaka, S. (1989). Use of *Bacillus brevis* for efficient synthesis and secretion of human epidermal growth factor. *Proc. Natl. Acad. Sci. USA* **86**:3589-3593

Yasukawa, T., Kaneii-Ishii, C., Mackawa, T., Fujimoto, J., Yamamoto, T. and Ishii, S. (1995). Increase of solubility of foreign proteins in Escherichia coli by coproduction of the bacterial thioredoxin. *J. Biol. Chem.* **270**:25328-25331

Yates, C.M., Simpson, J., Moloney, A.F.J., Gordon, A. and Reid, A.H. (1980). Alzheimer like cholinergic deficiency in Down Syndrome. *Lancet*, **2**:979-980

Ye, R., Kim, J.H., Kim, B.G., Szarka, S., Sihota, E. and Wong, S.L. (1999). High-level secretory production of intact, biologically active staphylokinase from *Bacillus subtilis*. *Biotechnol. Bioeng*. **5**:87-96

XII. PERSONNEL RECEIVING PAY*

BARAK DOV

COHEN OFER

HOLTZMAN TZVI

LAZAR ARIE

LAZAR SHIRLEY

KAPLAN DANA

KRONMAN CHANOCH

MAZOR OHAD

ORDENTLICH ARIE

PAS REPHAEL

SEGALL YOFFI

SELIGER NEHAMA

SOD-MORIA GALIT

STEIN DANA

ZILBERSTEIN LEA

* Partial or Full Salary